Technical Report Documentation Page

Report No.	2. Government Accession No.	3. Recipient's Catalog No.
FHWA/TX-95+1244-10		

Title and Subtitle	5. Report Date
ANALYSIS OF JOINTED CONCRETE PAVEMENT	December 1994
	6. Performing Organization Code

Author(s)	8. Performing Organization Report No.
Stefan F. Gräter and B. Frank McCullough	Research Report 1244-10

Performing Organization Name and Address	10. Work Unit No. (TRAIS)
Center for Transportation Research The University of Texas at Austin 3208 Red River, Suite 200 Austin, Texas 78705-2650	11. Contract or Grant No. Research Study 0-1244
	13. Type of Report and Period Covered
2. Sponsoring Agency Name and Address Texas Department of Transportation Research and Technology Transfer Office P. O. Box 5051 Austin, Texas 78763-5051	Interim
	14. Sponsoring Agency Code

5. Supplementary Notes

Study conducted in cooperation with the U.S. Department of Transportation, Federal Highway Administration. Research study title: "Evaluation of the Performance of Texas Pavements Made with Different Coarse Aggregates"

6. Abstract

This report describes the behavior of jointed concrete pavement based on field performance and current analysis and design technology. Distress data from a rigid pavement database and existing analysis programs developed at the Center for Transportation Research at The University of Texas at Austin served as the basis for the analytical procedure. Since environmentally induced cracking in jointed concrete pavement is of considerable importance to the performance of the pavement during its service life, we developed an analysis program, termed JRCP-6, that is capable of modeling the mechanisms that lead to cracking. Specifically, this program simulates the behavior of concrete pavement subjected to changing temperatures and moisture conditions 1 year after construction. Special attention is given to modeling behavior of the pavement after cracking has occurred. In addition, calibration of the model and an explanation of program operation are presented, as well as initiatives for the incorporation of vehicular loading and distress prediction methodologies into the analysis.

17. Key Words	18. Distribution Statement
Jointed concrete pavement, JRCP-6 computer program, early-age modeling, failure prediction models	No restrictions. This document is available to the public through the National Technical Information Service, Springfield, Virginia 22161.

19. Security Classif. (of this report)	20. Security Classif. (of this page)	21. No. of Pages	22. Price
Unclassified	Unclassified	104	

Form DOT F 1700.7 (8-72) Reproduction of completed page authorized

ANALYSIS OF JOINTED CONCRETE PAVEMENT

by

Stefan F. Gräter

B. Frank McCullough

Research Report Number 1244-10

Research Project 0-1244
Evaluation of the Performance of Texas Pavements Made with Different Aggregates

conducted for the

Texas Department of Transportation

in cooperation with the

U.S. Department of Transportation
Federal Highway Administration

by the

CENTER FOR TRANSPORTATION RESEARCH
Bureau of Engineering Research
THE UNIVERSITY OF TEXAS AT AUSTIN

December 1994

IMPLEMENTATION STATEMENT

This report investigates and implements improvements to the analysis of jointed concrete pavement using research undertaken for Projects 1244 and 1169. A rigorous analysis of early-age reaction of the pavement to the environment has been combined with a simple vehicular loading analysis to predict critical distresses in an analysis procedure presented in program JRCP-6. Applications for the program include the analysis of jointed concrete pavement for a site-specific or individual case, or evaluation of the effect of input variables, such as coarse aggregate type, on the performance of jointed concrete pavement in general. While the report includes limited calibration and analysis logic checks, a more intensive investigation is recommended. Finally, the analysis procedure developed in this report may be used for future development of a design program or design procedure for jointed concrete pavement. An example of a design problem is presented for future development.

Prepared in cooperation with the Texas Department of Transportation and the U.S. Department of Transportation, Federal Highway Administration.

DISCLAIMERS

B. Frank McCullough, P.E. (Texas No. 19914)
Research Supervisor

TABLE OF CONTENTS

IMPLEMENTATION STATEMENT iii
SUMMARY ix

CHAPTER 1. INTRODUCTION 1
BACKGROUND 1
OBJECTIVE 1
SCOPE 3

CHAPTER 2. PERFORMANCE CONCEPTS 5
DESCRIPTION OF JOINTED CONCRETE PAVEMENT 5
General 5
Types of jointed concrete pavement 5
BEHAVIOR OF JOINTED CONCRETE PAVEMENT 7
Early-age behavior 7
In-service or long-term behavior 10
DISTRESS TYPES 10
Observed JCP distress types 10
Distress related to analysis and design 12
CONCEPTS FOR MODELING 13
Slab-subbase interaction 13
Reinforcement 15
Joints 16

CHAPTER 3. THEORETICAL MODELING 19
MATERIAL CHARACTERIZATION 19
Concrete 19
Structural steel 20
Subbase and subgrade 20
TEMPERATURE AND MOISTURE 20
GEOMETRY 21
BOUNDARY CONDITIONS 21
VARIABILITY 22
TRAFFIC LOADING 24

CHAPTER 4. EXISTING ANALYSIS AND DESIGN PROCEDURES 25
MATERIAL CHARACTERIZATION 25
JRCP ANALYSIS PROGRAMS 26
DESIGN AND PERFORMANCE PREDICTION MODELS 27

CTR JCP DATABASE 28

CHAPTER 5. IMPROVED EARLY-AGE MODELING 29
EARLY-AGE BEHAVIOR 29
Geometric models 29
Solution methods 40
JRCP-6 45

CHAPTER 6. VEHICULAR LOADING AND DISTRESS PREDICTION 49
TRAFFIC LOADING 49
DISTRESS PREDICTION 49
Transverse cracking 50
Spalling 55
Faulting 56
Corner breaks 57
D-cracking 59
Summary 59

CHAPTER 7. JRCP-6: APPLICATIONS AND SENSITIVITY ANALYSIS 61
APPLICATIONS 61
INPUT AND OUTPUT 61
SENSITIVITY ANALYSIS 65
MODEL1 66
MODEL2 67
EXAMPLE PROBLEMS 69
CALIBRATION 69
Design data 69
Material characteristics 70
Crack spacing distribution 70
Modeling results 71
Summary 72

CHAPTER 8. DESIGN 73
INTRODUCTION 73
THICKNESS 73
REINFORCEMENT 74
JOINTS 74
Load transfer 75
Joint width 77
JRCP-6 DESIGN APPLICATION 78

Input 78
Results 78

CHAPTER 9. SUMMARY, CONCLUSIONS, AND RECOMMENDATIONS 81
SUMMARY 81
CONCLUSIONS 81
RECOMMENDATIONS 82

REFERENCES 83
APPENDIX A: EXAMPLE PROBLEMS: INPUT AND OUTPUT SCREENS 87

SUMMARY

This report describes the behavior of jointed concrete pavement based on field performance and current analysis and design technology. Distress data from a rigid pavement database and existing analysis programs developed at the Center for Transportation Research at The University of Texas at Austin served as the basis for the analytical procedure. Since environmentally induced cracking in jointed concrete pavement is of considerable importance to the performance of the pavement during its service life, we developed an analysis program, termed JRCP-6, that is capable of modeling the mechanisms that lead to cracking. Specifically, this program simulates the behavior of concrete pavement subjected to changing temperatures and moisture conditions 1 year after construction. Special attention is given to modeling behavior of the pavement after cracking has occurred. In addition, calibration of the model and an explanation of program operation are presented, as well as initiatives for the incorporation of vehicular loading and distress prediction methodologies into the analysis.

CHAPTER 1. INTRODUCTION

BACKGROUND

The earliest recorded construction of portland cement concrete (PCC) pavement arguably occurred early in the 20th century. Regardless of the exact date of construction of the first PCC pavement, road builders must have rapidly realized the effect of uncontrolled cracking on pavement performance when large sections of concrete slabs were constructed. Numerous road tests, wherein engineers experimented with designs to curb rapid deterioration, were subsequently built in the early part of the century. The Pittsburgh Road Test in California and the Arlington Road Test in Virginia paved the way, so to speak, for more extensive road tests. Among the more important full-scale road tests involving PCC pavements were the Maryland Road Test and the AASHO Road Test conducted in 1941 and 1961, respectively. Today, half a century later, pavement engineers still apply the principles developed in these experiments. Concrete pavements are, accordingly, either constructed as small jointed slabs, which do not crack at early ages, or as large slabs reinforced with steel bars or mesh to control cracking. Sufficient subgrade support and efficient load transfer at joints have also remained basic design process principles.

Recent nation-wide surveys of in-service concrete pavements (Ref 1) have revealed that most pavements have performed better than expected. These pavements have provided safe, comfortable roadways capable of accommodating traffic volumes that exceed original design specifications. Because it is a durable material, concrete, when properly used in pavements, can provide satisfactory, long-lasting, maintenance-free service. However, continued research of the theory and behavior of rigid pavements is required to minimize lingering distresses and failures.

OBJECTIVE

Pavement engineering involves analysis and design of pavement structures. Definition of these two terms, for the purpose of further discussion in this study, is made as follows and is illustrated in Figure 1.1. Definitions for analysis and design are as follows:

1. Analysis: The process where design parameters, describing a predetermined pavement geometry and environment, are used as inputs in a model to predict pavement behavior, distress, and performance.
2. Design: The process that uses the type of structure, environment, desired behavior, distress and performance as input in a model to determine the required design parameters to achieve the performance goal.

It should be kept in mind that, during the analysis and design procedures, the main objective is the long-term performance of the pavement. One of the main concerns of the designer is to predict maintenance and rehabilitation over the life-cycle (or total cost) of the pavement. This study mainly focuses on the development of an analysis model for this purpose; it also proposes a methodology for use in the analysis and development of design models.

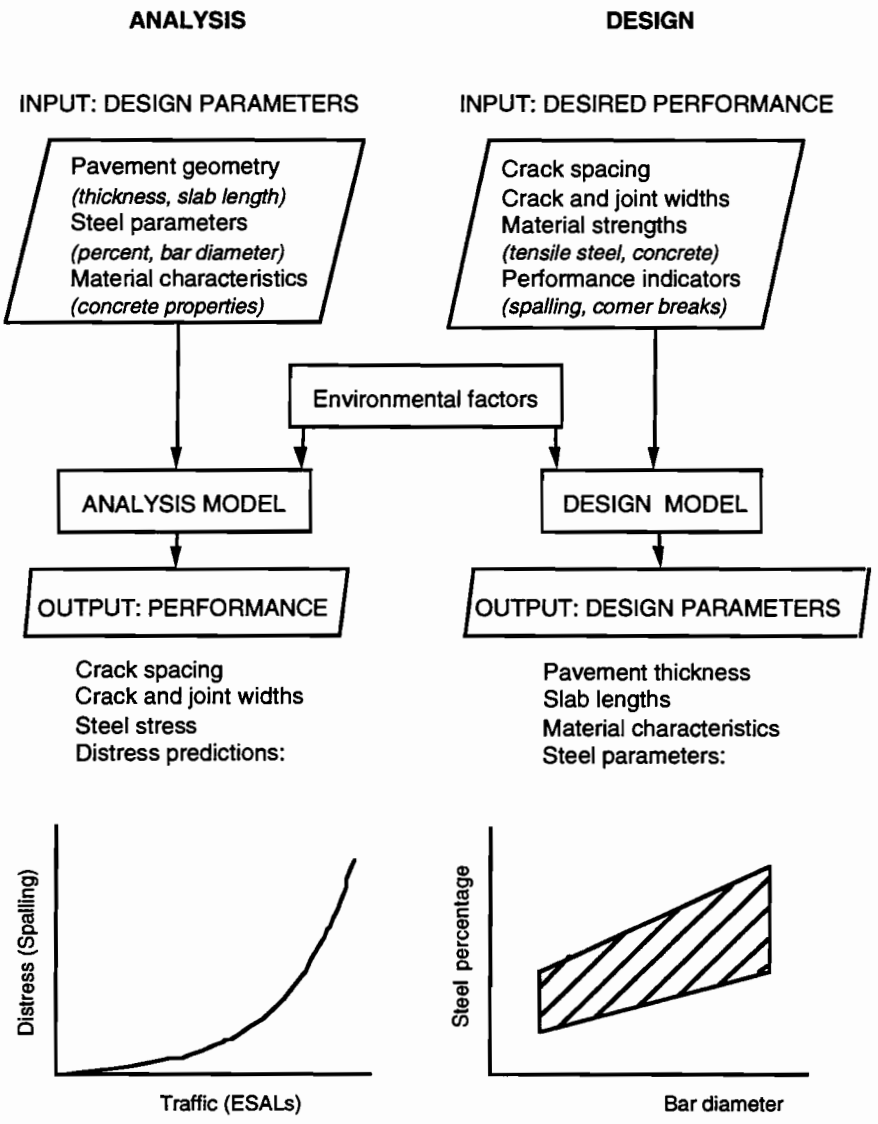

Figure 1.1 Definition of analysis and design

Concrete pavement behavior can be divided into three categories: (1) the reaction of the pavement to concrete drying shrinkage and changing pavement temperature over time; (2) the effect of differential moisture and temperature conditions through the depth of the slab (commonly called warping and curling); and (3) the response of the pavement to vehicular loading. While these three categories of behavior occur continuously and simultaneously during the life of the pavement, they are generally modeled separately during analysis.

The primary objective of this report is to identify the most important aspects of jointed concrete pavement (JCP) behavior, and to develop new analysis techniques. Objectives of the research include the following:

1. To develop detailed mechanistic models capable of determining the effects of the environment on the early-age and in-service behavior of jointed concrete pavement. Such modeling is based on work completed for jointed reinforced concrete pavement (Ref 2) and for continuously reinforced concrete pavement (Refs 3, 4).
2. To present a simplified analysis of vehicular loading of jointed concrete pavement based on existing technology (Ref 5).
3. To develop distress prediction principles based on analyses of environmental and traffic loading and on the Texas rigid pavement database.

SCOPE

This study describes the conceptual modeling of jointed concrete pavement, providing at the same time a general description of performance aspects during the service life. Common distresses and reactions to environmental and traffic loading conditions are discussed in Chapter 2. An overview of general modeling concepts in Chapter 3 leads to a presentation in Chapter 4 of existing modeling and design procedures used in the U.S. and, specifically, current analysis models for jointed reinforced concrete pavement in Texas. Chapter 5 focuses on improved analysis techniques for early-age behavior of the pavement related to environmental effects, culminating in the development of the computer program JRCP-6. Chapter 6 includes additions to the environmental analysis in the form of traffic loading analysis and distress prediction models to complete the development of JRCP-6. Sample applications and sensitivity analyses using JRCP-6 are presented in Chapter 7. The discussion in Chapter 8 of design techniques using JRCP-6 and existing distress data completes the report.

CHAPTER 2. PERFORMANCE CONCEPTS

This chapter describes the concept, mechanisms of behavior, and distress manifestations of jointed concrete pavement (JCP).

DESCRIPTION OF JOINTED CONCRETE PAVEMENT

Jointed concrete pavement, generally, consists of PCC slabs laid next to each other in the longitudinal direction (direction of traffic flow) on a prepared roadbed surface to form a pavement system classified as rigid pavement. Adjoining slabs of PCC are usually tied together by transverse steel (e.g., tie bars) in order to form an uniform whole in the transverse direction and to allow for load transfer. Concrete pavement is classified as prestressed concrete pavement (PCP), continuously reinforced concrete pavement (CRCP), or jointed concrete pavement (JCP). PCP is a special type of JCP, wherein compressive stress is induced into the slab to offset the weaker tensile strength properties of the concrete, resulting in a thinner pavement and longer joint spacing. CRCP consists of long slabs reinforced continuously in the longitudinal direction by large percentages of steel (0.5 to 0.7 percent) to control crack widths. Analysis and design of CRCP, PCP, and JCP require different procedures and are handled separately. This study only covers JCP analysis and design.

General

Jointed concrete pavement (JCP) includes any concrete pavement that is designed and constructed with slabs separated by transverse joints. The extremities of the slabs at these joints are not restricted to move longitudinally, and, in fact, transverse joints act as movement-absorbing devices allowing slabs to expand and contract as temperature and moisture conditions change with time. Movement, therefore, reduces stresses induced in the slab by climatic factors; however, much of the distress reductions occur at transverse joints. Transverse joint design and analysis, therefore, form an important part of any type of JCP analytical procedures. Substantial time is spent on modeling concrete behavior at the joints, as well as behavior leading to formation of transverse cracks.

Types of jointed concrete pavement

JCP is classified as plain (PJCP) or reinforced (JRCP) concrete pavement. These somewhat similar classification types are discussed below.

PJCP is typically constructed of short lengths of unreinforced concrete slabs; these slabs are sufficiently short and thick to ensure that no intermediate cracking will occur as a result of environment stress or traffic-induced stress. Slab lengths, typically 3 to 5 meters (10 to 15 ft) long, are separated by transverse joints. Experience has shown that PJCP performs better when the transverse joints have dowel bars as the load transferring devices between adjacent slabs. Problems are, however, found to be concentrated at the joints, as it is here that the largest stress concentrations occur. Concrete is also known to fail as a result of fatigue (Ref 6); this is the cause

of most transverse cracking in properly designed PJCP. When slabs do crack transversely, a situation results where serious deterioration can occur owing to a lack of load transfer at the crack.

The problem of unanticipated cracking can be addressed by design and construction of JRCP. Longer slabs (9 to 30 m or 30 to 100 ft) reinforced with 0.1 to 0.3 percent steel reduce the number of transverse joints, which in turn reduces the number of possible problem areas while achieving a better ride (owing to the absence of joints). When cracks do occur in the slab, they are held together by longitudinal steel, which increases load transfer and reduces secondary distresses associated with cracks. This is the only reason that reinforcing steel is used in JRCP. The enhancement in the structural load carrying capacity of the pavement is not taken into account in the analytical models.

It is argued that the most important mechanism leading to transverse cracking is contraction of concrete as result of temperature fluctuations and drying shrinkage; this process is critical during the curing stages of pavement life, when no traffic loading occurs. During the curing period, the PCC is weak and susceptible to failure. During the rest of the serviceable life of the pavement, cracking may continue owing to a combination of fatigue as a result of continued longitudinal shrinkage, warping and curling, and vehicular loading stresses. The amount of additional transverse cracking caused by these factors is considered secondary compared with the initial cracking process during curing during the first year of operation, as is illustrated in Figure 2.1. The figure shows reduction of crack spacing over time for CRCP from actual data (Ref 3), while a hypothetical line is introduced for JCP. It can be seen that primary crack spacing develops abruptly, while secondary cracking increases crack spacing marginally during pavement life. Consequently, most of the effort in this study was spent establishing crack spacing after 1 year of service (including the curing period of 28 days).

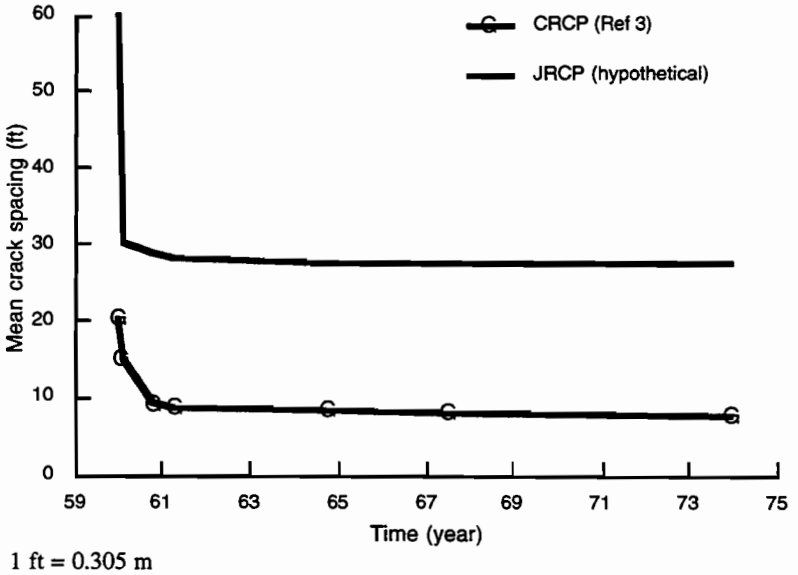

Figure 2.1 Crack spacing development over time for PCC pavement

BEHAVIOR OF JOINTED CONCRETE PAVEMENT

Analysis of any physical system requires prior knowledge of actual responses of the system to external factors. Basic assumptions can then be made in order to bring together mathematical models and observed field behavior. The behavior of JCP, as evidenced from previously constructed pavement, provides the background by which an analysis system can be broken down into simplified subsystems, which, when assembled collectively, form the whole pavement model.

Early-age behavior

It is known that PCC properties change with time after the initial setting period. Hydration of calcium alluminates, commonly preceded by a 2- to 6-hour dormant period after mixing, eventually leads to solidification of the cement paste and aggregate mix. During this process, the temperature of the PCC is raised significantly owing to strong chemical reactions, following a pattern illustrated in Figure 2.2 (Ref 7). Actual values of PCC temperature are dependent on ambient air temperature, concrete mix temperature at pouring, and the chemical composition of the portland cement and additives. At some stage during early setting, PCC changes from a plastic to a solid capable of withstanding stresses applied to it and generating internal stresses owing to differential shrinkage. Suh et al. (Ref 8) investigated the determination of concrete temperature at this transformation stage — a temperature called the setting temperature. The setting temperature plays a significant role in PCC behavior to varying pavement temperatures, as it forms the base temperature from which the concrete expands or contracts. High setting temperatures result in large temperature differentials during cold periods, causing high stresses, large movements, and high probabilities of cracking. Recent research (Ref 8) has, therefore, suggested controlling setting temperatures; this is reflected in Texas Department of Transportation specifications (Ref 9).

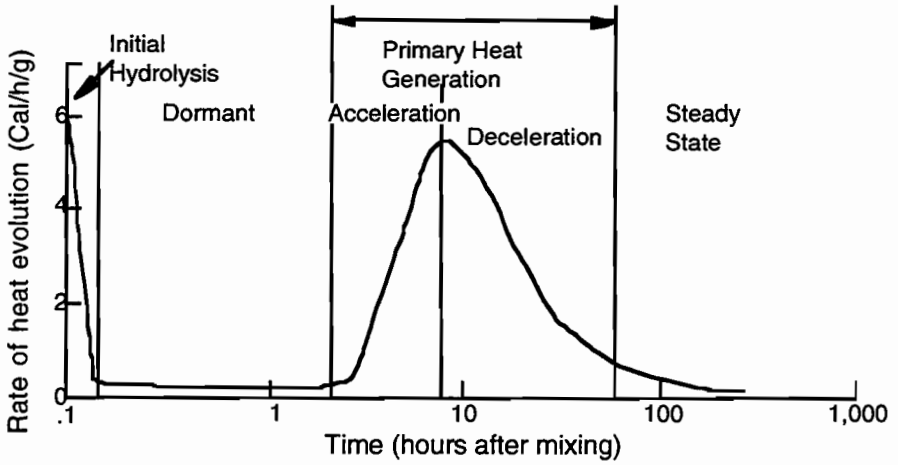

Figure 2.2 Typical pattern of heat generation during hydration of tricalcium silicate (Ref 7)

Once the concrete has reached setting temperature, properties such as modulus of elasticity, tensile strength, and drying shrinkage start to develop. Models describing concrete property development with age have been developed by various researchers (Refs 4, 10). Dossey and McCullough (Ref 11) summarize the equations in a search for models to characterize concrete properties as influenced by coarse aggregate type. Models typically take one of the following two forms:

$$f(t) = f(28) * \frac{t}{A + Bt} \tag{2.1}$$

$$f(t) = f(28) * A(2 - e^{-Bt} - e^{-\alpha}) \tag{2.2}$$

where:

f(t)	=	concrete property at time t
f(28)	=	concrete property at 28 days
t	=	time in days
A,B,C	=	coefficients of curvature specific to a given coarse aggregate

Property development typically takes the form illustrated in Figure 2.3.

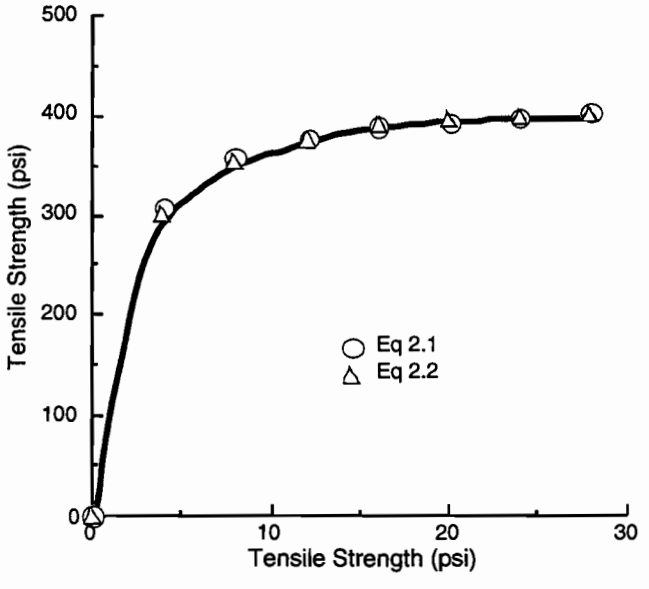

1 psi = 6.9 kPa

Figure 2.3 Typical concrete property development over time

Once the PCC slab has reached the setting point, and once physical properties common to the solid phase start developing, behavior is strongly influenced by the environment. The concrete continuously dries and shrinks, while pavement temperatures follow cyclic daily temperature fluctuations connected with ambient temperatures, as shown in Figure 2.4. The result is a concrete slab that shrinks, but is inhibited by reinforcement, if present, and friction from the subbase, causing tensile stresses to develop in the concrete. Concrete tensile stress and steel compressive stress reach maximum daily values at the minimum pavement temperature, which normally occurs around sunrise. Accurate pavement temperature prediction is a complex process requiring estimates for solar radiation and percent cloud cover among other variables. A rough estimate can, however, be predicted from the ambient air temperature, as has been determined by Jiminez et al. (Ref 12).

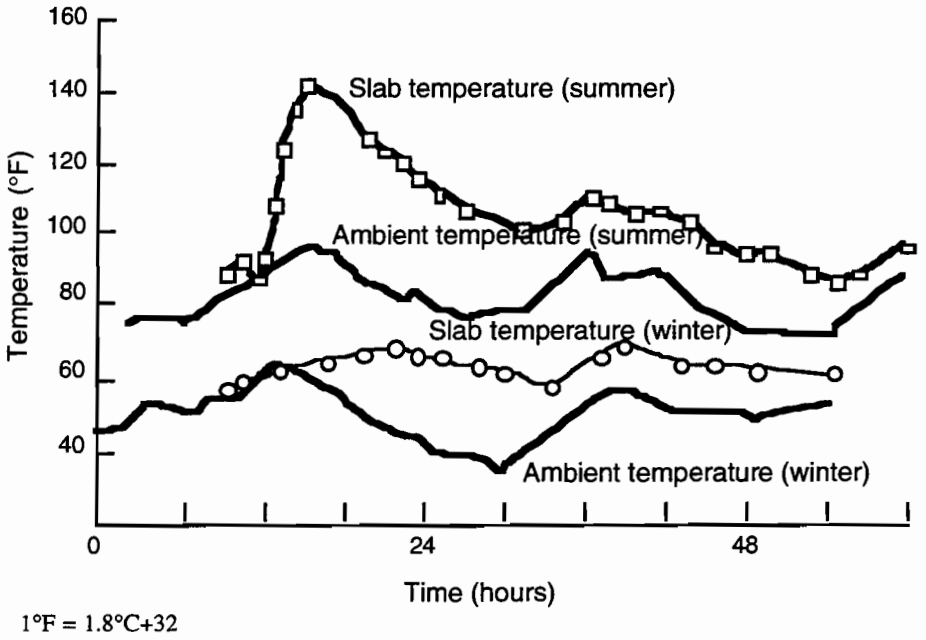

Figure 2.4 Early age concrete slab temperature fluctuations over time (Ref 7)

The slab, therefore, goes through daily stress cycles owing to the environment, while continuously changing mechanical properties. If at any time during the cycles, concrete stress exceeds concrete strength, the slab cracks. The process continues for the rest of the pavement life, but is less dynamic after the initial 28 days because most properties (excluding drying shrinkage), reach their design values at approximately 28 days. It is during this 28-day period, when the pavement is usually subjected to environmental effects only, that most transverse cracking occurs. The period of 24 hours after pouring and 28 days of curing are critical in determining proper crack spacing, reinforcement, and joint width. The temperature differential plays a large role in generating tensile stresses in the PCC slab, as will be discussed in Chapter 6.

In-service or long-term behavior

Cyclic stress and displacement due to the environment continue throughout the pavement's life. Additionally, the pavement is subjected to traffic loading, which adds a dynamic element. With every passing wheel load, the slab is subjected to loading at the joint, at the interior of the slab (between cracks or joints), and at transverse cracks. Slabs loaded at the interior act as plates on elastic foundations. Critical maximum tensile stresses occur directly below the load at the bottom of the slab. These stresses are assumed to remain constant for any wheel position a considerable distance from joints, cracks, or edges of the slab. When a condition occurs where there is no load transfer at cracks or joints (no dowel, reinforcing, or aggregate interlock), or when the wheel load is applied to the edge of the pavement, an edge loading condition exists. Critical maximum tensile stresses remain at the bottom of the slab directly under the wheel load, but are considerably larger owing to the lack of structural support provided by slab continuity. Furthermore, the critical stresses occur along an axis parallel to the free edge. In cases where load transfer is present at the discontinuity, a situation somewhere between the interior and edge loading cases occurs. Analysis of these cases are complex and usually require finite element approximations for modeling the problem. For the purpose of this study, free edges are assumed at all discontinuities. Stresses from vehicular loading may be added to the stresses from environmental loading by the principle of superposition. These combined stresses can then be used for further distress prediction procedures. All other known long-term structural behaviors, such as warping and curling, are not considered in this study. Although these mechanisms are considered secondary, they lend themselves to additional research and model development.

DISTRESS TYPES

Distress is the limiting response of pavement behavior. Once immediate response of pavements reach distress levels, performance starts to decline rapidly and the pavement requires attention in the form of maintenance or rehabilitation in order to sustain acceptable levels of serviceability. Prediction of distress development with time is, therefore, important when designing pavements. Maintenance and rehabilitation measures form part of the design strategy and economic analysis and rely totally on the designers ability to predict distress development. This section first discusses common distresses found in JCP, and then relates them to behavior.

Observed JCP distress types

Distresses in concrete pavement mostly occur as unwanted cracks, which develop into more serious distresses as time and traffic accumulates. It is recognized that surface roughness is a distress, usually caused by swelling clays or settlement of the subgrade. (This is not discussed in this report, as this distress is not a result of the structural behavior of the pavement.) Preventative measures against roughness are found in standard design procedures and specifications. Common distresses in jointed concrete pavement are categorized below:

Distresses occurring during the initial construction period:

(1) Transverse cracks: initially occur owing to concrete shrinkage as a result of temperature drops and drying shrinkage only.

(2) Spalling: delaminations occur during the curing stages of the PCC.

(3) Longitudinal cracks: same mechanisms as for transverse cracks except that the stresses are perpendicular (transverse direction). In some cases, reflection cracking owing to longitudinal cracks in cement-treated bases occur.

(4) Horizontal and vertical plastic shrinkage cracking: PCC dries out too quickly on the exposed surfaces.

Distresses occurring as a result of cyclic traffic and environmental loading:

(1) Transverse cracks: secondary development of transverse cracking occurs owing to combined environmental and traffic-induced stress. Occurrence of intermediate transverse cracks in PJCP leads to problems, such as faulting and pumping, owing to the lack of load transfer.

(2) Longitudinal cracking: secondary cracking leads to the same problems as transverse cracking when there is a lack of load transfer. Additional mechanisms that lead to these cracks during pavement life are reflection cracking and differential settlement.

(3) Corner breaks: the corner of a slab cracks from longitudinal joint or edge of the pavement to a transverse joint owing to vehicular loading.

(4) Spalling: delaminations that have occurred in the initial construction period develop to the stage where chunks of concrete debond from the rest of the slab at joints and cracks.

(5) D-cracking: D-shaped cracks at joints most probably related to coarse aggregate type.

(6) Surface defects: polishing and loss of aggregates as a result of vehicle tires.

(7) Joint sealant failure: joints become unsealed as result of sealant aging and or large joint movements.

Severe or tertiary distresses:

(1) Faulting: differential settlement or movement of adjoining slabs. Most common where slabs are undoweled or at cracks where no load transfer owing to reinforcement or aggregate interlock is present.

(2) Lane separation and differential settlement: occurs where adjoining slabs are not tied longitudinally by transverse steel or tie bars.

(3) Punchouts: a tertiary distress occurring after substantial cracking and spalling and when blocks of concrete between cracks are dislodged.

(4) Pumping: a distress at joints and cracks caused by vehicular loading. Fine material from the subbase is transported inside the subbase or from the subbase through the crack to the surface, resulting in non-uniform slab support.

This study focuses on transverse crack development, spalling, faulting, corner breaks, and D-cracking. These are the most common distresses reported in Texas and which are summarized in the JCP database, a part of the rigid pavement database, maintained by the Center for Transportation Research.

Distress related to analysis and design

Distress during analysis and design can be minimized in one of the following three ways:

Material specifications:

(1) D-cracking mechanisms are not well-identified. Some speculate that it develops as a result of freezing and thawing of coarse aggregates in concrete (Ref 13). Others have ascribed D-cracking to compression of waste material that gathers in joints and cracks (Ref 15), where compression occurs as a result of thermal expansion of the concrete slab. Lastly, chemical reaction between coarse aggregate and other PCC components (such as alkali-aggregate reaction) was also listed as being a possible cause. D-cracking is a common distress that may lead to more severe distress types, but which can be controlled by using coarse aggregate types known to be resistant to D-cracking.

(2) Surface defects: coarse aggregate type that is resistant to the abrasive action of vehicle tires.

(3) Joint sealant failure: a ductile and aging resistant sealer is specified.

(4) Plastic shrinkage cracking: reduced by correct mix design and curing procedures.

Construction procedures:

(1) Transverse cracks: correct procedures for construction of doweled and sawn transverse joints improve pavement behavior. Dowels need to be correctly aligned and sawcuts need to be undertaken at the optimum time and depth.

(2) Spalling: prevention of delaminations by correct curing conditions and construction time (minimizing hydration heat).

(3) Longitudinal cracks: same mitigation strategies as for transverse cracks.

(4) Lane separation: prevention is achieved by tied longitudinal joints.

(5) Pumping can be prevented by adequate load transfer at joints and correct subbase types.

Mathematical modeling:

(1) Transverse cracking distress has been discussed in the early-age behavior sections. This report concentrates on the modeling of the processes leading to transverse cracking.

(2) Spalling has been the subject of intensive investigation in another section of project 1244; for example, a complete explanation may be found in Report 1244-11 (Ref 14). A summary discussion of the findings will be presented here. During the formation of cracks or joints, the concrete at the discontinuity undergoes a change in stress

distribution as result of the changing boundary conditions. At the same time, a change in the moisture condition at the crack occurs, the severity of which is dependent on the age of the concrete. This initial combination of stress and moisture has been found to be critical in the formation of delaminations, where delaminations occur in a horizontal plane 25 to 50 mm (1 to 2 in) below the concrete surface at cracks or joints, increasing the chances that further spalling will occur. Of course, if a potential spalling situation is present, gradual development of spalling occurs with time. Development is dependent on traffic loading and environmental conditions. Spalling will develop into potholes or punchouts, if left unattended, since the roughness induces increased dynamic loading and, consequently, increases the rate of deterioration of the pavement. The minimization of spalling potential is, therefore, essential during design, as spalling decreases pavement serviceability and performance.

(3) Corner breaks are cracks that occur across the corner of a slab. When a slab is subjected to a wheel load at a corner, tensile stresses result at the top of the slab. This loading condition can result in high stresses, depending on load transfer at joints. In any case, corner breaks are assumed to be a result of wheel loading. Failure can occur as result of one load or as result of fatigue owing to repetitive loading.

(4) Faulting is identified when adjoining slabs are not equal in elevation at the joint. The resulting drop off or protrusion severely affects the driver's comfort level and, therefore, reduces serviceability. Additionally, the fault increases dynamic wheel loading at the joint, increasing stress and the possibility of development of further distress types. The differential settlement of slabs are usually a result of the pumping action of wheel loads. When a wheel load passes a transverse joint, fines from the subbase are transported by air or water present in the subbase from the downstream slab. Cumulative transportation of fines across the joint results in a cavity at one end and excess material at the other end. Adjoining slabs are consequently no longer aligned vertically. The preventative strategy to be taken is to ensure that adequate load transfer exists at all discontinuities.

(5) Punchouts are prevented by preventing primary distresses that lead to the development of this type of distress (e.g., transverse and longitudinal cracking and spalling).

CONCEPTS FOR MODELING

This section discusses the subsystems specific to JCP modeling; the possibilities for modeling are also investigated. The subsystems are slab-subbase frictional interaction, concrete-reinforcement interaction, and behavior at joints.

Slab-subbase interaction

The subbase is defined as the pavement layer on which the concrete slab rests. The subbase interacts with the concrete slab by supporting it vertically and spreading the load from the slab to layers below the concrete. For a concrete slab to function properly, subbase support needs to be uniform and homogeneous. The nature of vehicular interaction with the pavement system, however, causes a pumping of air or water present in the subbase with every passing wheel. Pumping results in fine material in the subbase being displaced; such displacement can be the

cause of a number of distresses, including faulting and corner breaks. An extensive study on the performance of jointed concrete pavements by Smith et al. (Ref 1) lists subbase types having a significant effect on performance. That survey found that subbases designed to be permeable performed better, in some areas, based on cracking, spalling, and faulting distresses. Caution is needed, however, in areas where bad drainage is combined with the use of an impermeable subbase. Typical subbases include the following:

(1) Cement-treated subbase (impermeable)
(2) Lean concrete subbase (impermeable)
(3) Asphalt concrete subbase (impermeable)
(4) Plain aggregate subbase (permeable)

Another aspect of slab-subbase interaction is the friction between the two layers. When concrete contracts or expands horizontally, a friction force at the interface between concrete and subbase layers partially restricts movement and causes stresses in the concrete and steel. Wimsatt and McCullough (Ref 16) investigated the forces involved in this process using field testing slabs. They concluded that the friction force is proportional to subbase type only, and is not influenced by the slab weight or friction coefficient, as is the accepted approach in classical physics and which had been proposed by various other researchers. A summary of research performed on the slab-subbase friction can be found in a report by Ioannides and Salsilli-Murua (Ref 17). Various calibrations on programs using the methods developed by Wimsatt and McCullough (Refs 8, 18) have verified the accuracy of the assumptions and, accordingly, will be used in this study. Figure 2.5 illustrates the concept.

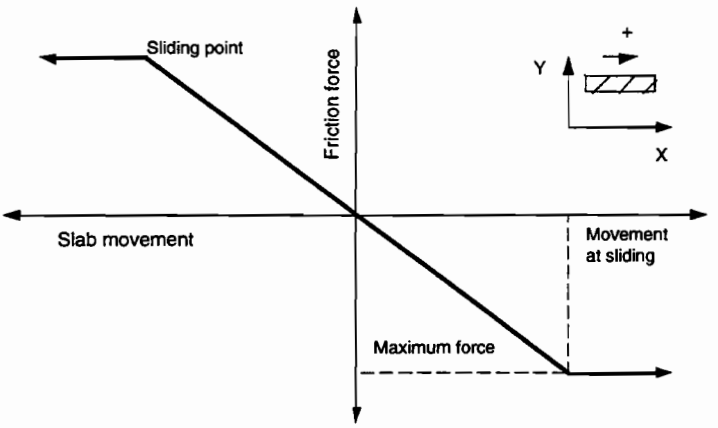

Figure 2.5 Slab-subbase friction model used in this study

Friction forces increase linearly in a direction opposite to the direction of slab movement up to a maximum point. At this point, called the sliding point, the slab continues to slide across the subbase, though the force remains constant at a maximum value. All slab-subbase interactions can, therefore, be characterized by this single sliding point (the behavior is symmetrical in the opposite direction). Typical values for different subbases are included in Table 2.1.

Table 2.1 Typical values for slab-subbase friction interactions from push off tests (Ref 4)

Subbase type	Maximum friction (psi)*	Movement at sliding (in.)**
Asphalt concrete	3.0, 3.4	0.020, 0.024
Asphalt stabilized	1.6, 2.2	0.030, 0.038
Cement stabilized	15.4	0.001
Lime-treated clay	1.6, 1.7	0.011, 0.012
Untreated clay	0.6, 1.1	0.030, 0.052

*1 psi = 6.9 kPa
**1 in. = 25.4 mm

Reinforcement

The purpose of reinforcement in concrete pavement is primarily to control cracking and behavior of the pavement at the crack. Steel, by bonding to the concrete, inhibits excessive horizontal movement, keeping cracks tightly closed. It provides an efficient load transferring mechanism, assisting the aggregate interlock mechanisms. This is accomplished by transferring load from one side of the crack to the other by pure shear, and by keeping the crack closed, ensuring that aggregates touch at the crack. Steel can, however, be detrimental to pavement behavior if not properly designed and constructed. Small-sized rebars can invoke large bearing stresses, while the steel-concrete interface may be an ideal plane for delaminations that can lead to spalling.

Reinforced concrete is a composite material consisting of steel and concrete which, though they have different material characteristics, act as one material as a result of full bond between the materials. When concrete contracts as a result of drying shrinkage, steel inhibits the contraction, causing stresses to build up in both materials. Similarly, when the concrete is subjected to temperature changes, the difference in thermal coefficient of the two materials results in stress build up. Tensile stresses in the concrete caused by drying shrinkage and temperatures below the setting temperature of concrete are critical, as these may be high enough to cause cracking. The higher the percentage of steel (in terms of cross sectional area) present in the pavement, the higher the stresses can be and the higher the risk of cracking. It therefore becomes an optimization process for the designer when designing steel reinforcement. The more steel put in, the better the load transfer; smaller crack widths are a result of smaller crack spacing.

An essential aspect to consider when modeling reinforced concrete pavement is the bond between steel and concrete. When fully bonded, the concrete and steel displacements are exactly the same. However, when bond slip occurs, as happens at cracks, relative movement occurs. Compatibility between concrete and steel is invalid and only equilibrium of forces apply.

Joints

The nomenclature for types of joints in JCP is quite varied. For the purpose of this study, distinction will be made between transverse and longitudinal joints, and between contraction and expansion joints. A summary of the following discussion is found in Table 2.2:

Longitudinal joints are defined as joints between individually paved lanes of concrete in the direction of the roadway (Figure 2.6). Deformed tie bars are typically used to connect adjoining slabs in the transverse direction (Figure 2.7). During ensuing analyses, unit widths of slabs are considered, with the concrete assumed to be homogeneous in the transverse direction.

Table 2.2 Summary of joint types and functions

Direction of joint	**Longitudinal**		**Transverse**	
Type / Function	Free	Tied	Free	Tied
Contraction	X	X	X	(X)
Expansion	X		X	

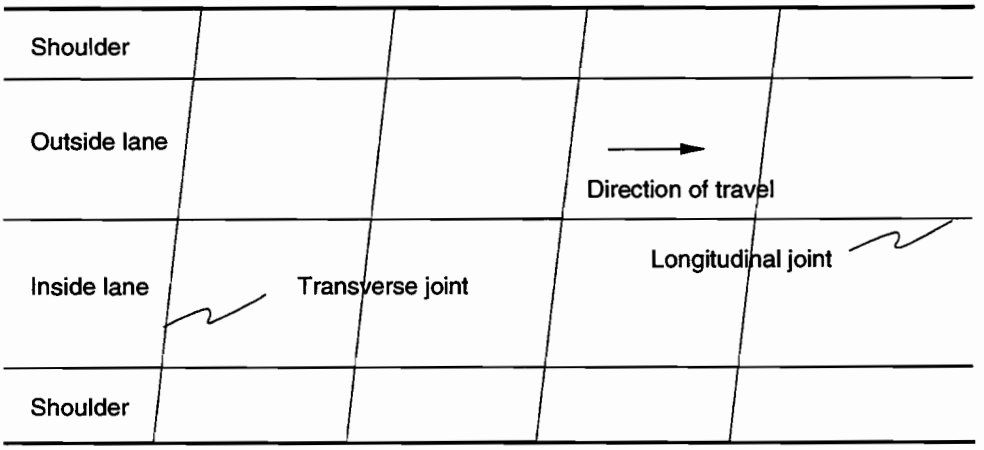

Figure 2.6 Typical JCP layout

Transverse joints act as expansion- and contraction-absorbing devices and as load transferring mechanisms in jointed concrete pavement. They are constructed at a specified spacing and are used in combinations of free and tied joints, resulting in a series of equal length slabs forming a strip of longitudinal pavement. Expansion joints are usually doweled, allowing free movement in the longitudinal direction. Contraction joints are sawed to promote cracking at specific distances, tied by longitudinal reinforcement, and are referred to in the literature as controlled cracks. Transverse joints may be skewed, as shown in Figure 2.6, or may be perpendicular to the direction of traffic flow; skewed joints are constructed to enhance ride quality by preventing both sets of wheels on vehicle axles to hit the joints at the same time. For analysis purposes, joints are considered perpendicular. A typical transverse expansion joint is illustrated in Figure 2.8. Dowel bars and subbase support act as primary load transferring devices. Design and analysis of JCP assume friction-free transverse joints. It is assumed that concrete slab movement is unrestricted in the direction running parallel to traffic flow. Restriction of movement can cause large stresses and may result in excessive cracking in the slab and around the joint. These joints must to be constructed carefully, ensuring correct alignment of dowel bars and non-bonding of concrete to dowel bars on at least one side of the joint to permit free movement of the slab.

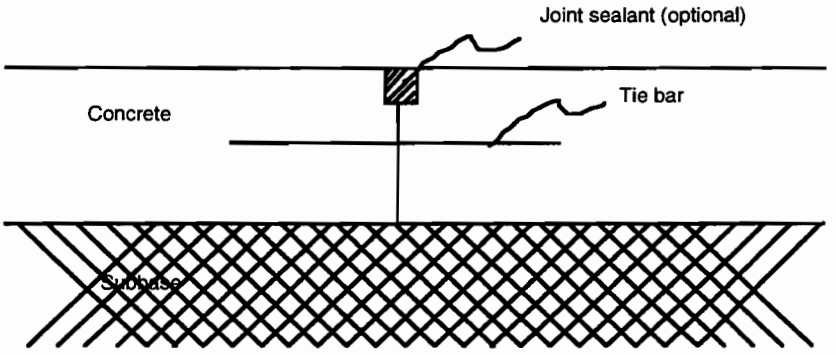

Figure 2.7 Typical longitudinal construction joint

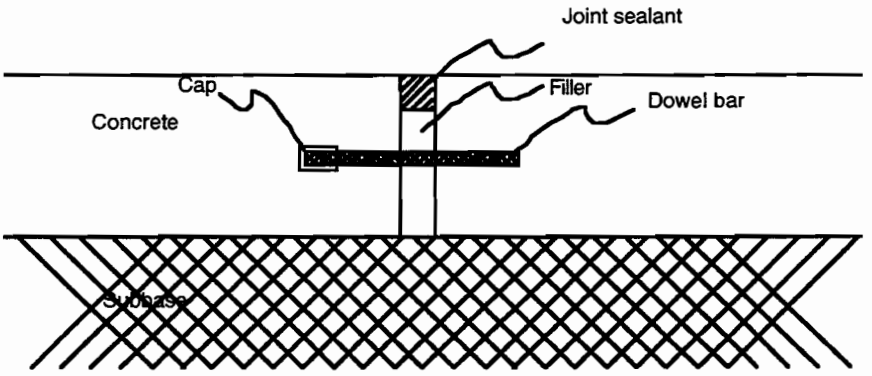

Figure 2.8 Typical transverse expansion joint

Analysis of the stresses around the dowel bar assumes transfer of load from one slab to the other occurs through the dowel bars and subbase or subgrade. The amount each component carries is an estimate or empirically derived value. Furthermore, it is accepted that dowel bars share transfer of load proportionally to the deflection of the slab at the joint. No play is assumed to exist between dowel bars and the surrounding concrete.

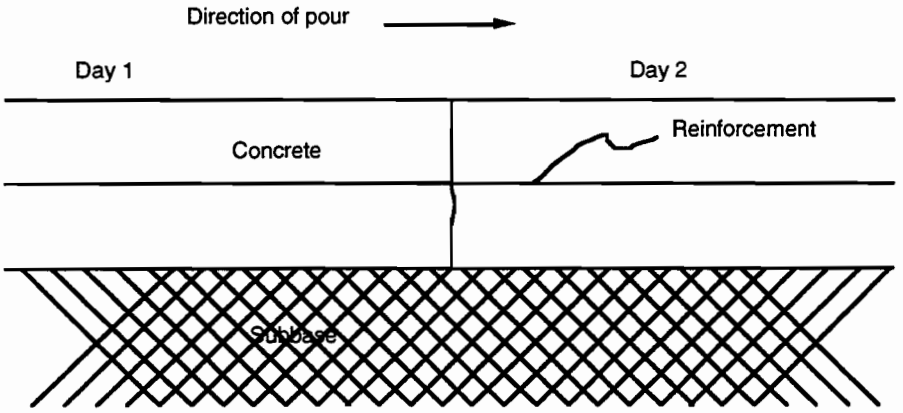

Figure 2.9 Typical transverse construction joint

Transverse construction joints are located where concrete pouring stops for an extended period of time and where the resulting joint is not located at a transverse joint, as shown in Figure 2.9. These joints are also referred to as butt joints, where construction simply resumes again when concrete is poured. Sometimes measures are taken to ensure bonding of old and new concrete, for example, roughening the old surface. In any case, construction joints are not considered during analysis. The slab is regarded as fully bonded and homogeneous across construction joints.

CHAPTER 3. THEORETICAL MODELING

MATERIAL CHARACTERIZATION

Analysis and design of physical systems require simulation of actual behavior by mathematical modeling. Mathematical models are usually developed based on observed behavior of the systems to be modeled. To make models easier to use, the developer often has to make simplifying assumptions that are not applicable to all possible ranges of behavior, but which are accurate within certain operating boundaries. An example is the linear elastic behavior of steel, where structural steel may be assumed to have linear elasticity below a certain stress level. Consequently, behavior of structural steel systems can be successfully modeled by linear elasticity as long as the steel does not reach the critical stress level (i.e., the plastic stage). Similarly mathematical models based on field and lab behavior are applicable only to the operating conditions under which the observations were taken. Materials are characterized by parameters required to use the selected models. These parameters are usually derived from laboratory tests simulating field conditions. In light of the discussion above, materials characterization should be determined by testing under the anticipated operating conditions in the field. The most important conditions are the state of stress, the state of strain and temperature, and moisture. In the following paragraphs, parameters are identified for selected mathematical models, with laboratory tests specified to measure these parameters.

Concrete

Concrete is modeled as a linear elastic material. Material behavior is described by a constant modulus of elasticity (E_c), Poisson's ratio (μ), drying shrinkage (Z), thermal coefficient of expansion (α_c), and tensile strength (f_t). The first four parameters are required to compute concrete stress levels, which are compared with the fifth property, tensile strength. Tensile strength is important because portland cement concrete (PCC) is weak in tension and almost exclusively fails in tension in pavement applications. For early-age analysis, all the properties required vary with time; therefore, such variation must be taken into account in the modeling process. Models discussed in Chapter 2 can be used to fit curves to concrete properties from the respective 28-day values. Alternately, test values for discrete points in time (1, 3, 7, 14, and 28 days) may be used directly, and parameters required for days in between the tested values can be determined by straight line interpolation.

Modulus of elasticity test methods are described in ASTM C-469 (Ref 19). The value is calculated from longitudinal deformations under continuous compressive loading, though tensile loading would be preferable, if feasible. Drying shrinkage is measured using the method described in ASTM C-157 (Ref 19). Modifications to this method have been made during research conducted in Projects 422 and 1244 at the Center for Transportation Research (Refs 11, 20). Thermal coefficient of expansion, which has been described by Dumas et al. (Ref 21), is

measured using ASTM C-531 (Ref 19). Tensile strength can be measured using the indirect tensile strength test described in ASTM C-496 (Ref 19).

By assuming linear elastic properties for PCC, all non-linear and plastic behavior of concrete, including creep, can be ignored. Creep effects may not be negligible when concrete is under constant stress over time. Concrete has been found to deform in ways other than elastic deformation, but the effect of creep is noticeable only over a long period of time. While the effects of creep are not considered in this study, they should be considered in future research.

Structural steel

Steel is characterized as linear elastic by a modulus of elasticity (E_S), tensile strength, and thermal coefficient of expansion (α_S). Although structural steel is known to behave non-linearly when close to the yielding stress, most of the working stresses for steel in concrete pavement are well below yielding; the material is thus treated as linear elastic. An exception to the general working stresses are stresses at cracks where concrete distributes all the stress to the steel at the point of cracking. These steel stresses can become very large, with insufficient amounts of steel causing yielding or total failure. When yielding only occurs, large crack widths result, releasing stress in both concrete and steel but increasing the possibility of steel corrosion. Total failure results in loss of load transfer and increased distress development. The problem is minimized by designing the steel so that it is always below yielding stress.

Subbase and subgrade

Characterization of layers below the concrete slab is summarized by a modulus of subgrade reaction (k), where the subgrade support is characterized as an elastic foundation. The reaction force of the subgrade is directly proportional to the vertical deflection. This parameter is required only when the pavement is analyzed for vehicular loading, and stems from the Westergaard solution of a slab subjected to traffic loading. Stresses and displacements calculated according to Westergaard's equations have been shown to be less sensitive to the modulus of subgrade reaction; accurate estimations of the value are unnecessary (Ref 5).

Friction between the concrete slab and subbase is characterized as dependent on subbase type only and is described by a single point. This point is defined as the point of sliding, where the friction remains constant as the slab slides over the subbase. The assumptions inherent in this approach are based on work by Wimsatt and McCullough (Ref 16) and are explained in Chapter 2.

TEMPERATURE AND MOISTURE

Temperature and moisture vary in the three dimensions of space and in time. Pavement temperature is influenced by ambient air temperature, solar radiation, and thermal properties of pavement materials. Moisture variations occur when materials below the pavement surface are kept moist by trapped ground water. For practical purposes, moisture and temperature variations in the horizontal plane can be disregarded, as they are negligibly small for areas the size of one or two JCP slabs. Variations with depth, however, can be significant and can lead to warping and curling of concrete slabs. Models accurately predicting temperature variations have been

developed (Ref 22) and are available for use. The analysis in this report considers only variation of temperature and moisture with time. This is regarded as the overwhelming factor influencing design stresses and pavement behavior; a complete analysis, however, will need to include warping and curling.

GEOMETRY

For early-age analysis, the pavement is described as a one-dimensional slab. Although it has depth and unit width, no variations in strength, stress, or environmental conditions are taken into account in these directions. The slab is bordered by two joints at the ends, where no resistance to movement exists. An uncracked slab is, therefore, symmetrical about an axis at the center of the slab. When discontinuities such as cracks exist in the concrete, symmetry is assumed to remain. The first crack is assumed to occur exactly at the symmetry axis, and all further cracks at mirror positions each side of the symmetry axis. Figure 3.1 illustrates the concept of constant symmetry assumed in the slab. Slab-subbase interaction occurs at the surface of the concrete; all environmental forces acting on the pavement (including the friction force) are assumed to be uniaxial at the neutral axis. In other words, there are no resulting moments. For vehicular loading, Westergaard's assumptions, as described in the next section, apply.

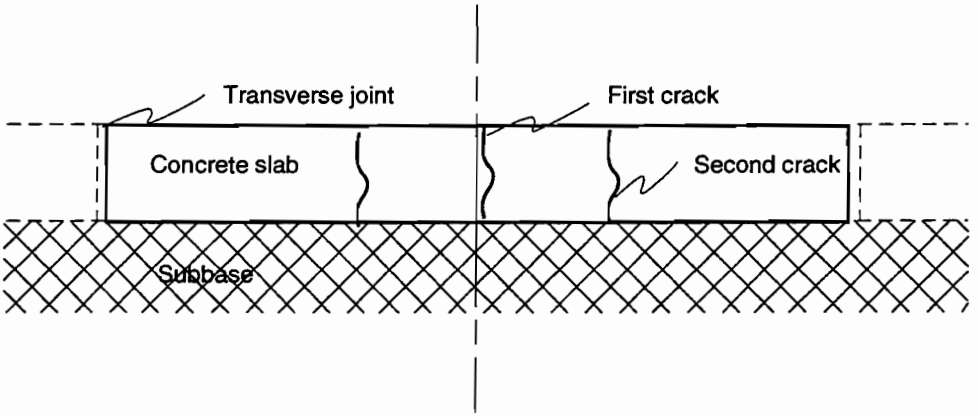

Figure 3.1 Assumed symmetry of JCP slabs

BOUNDARY CONDITIONS

Boundary conditions are necessary to solve the equilibrium equations resulting from environmental and traffic loading analysis. The traffic loading analysis boundary conditions are described in the assumptions set out below in the traffic loading section. For environmental analysis, boundary conditions change as cracks develop.

When no cracks exist, concrete and steel stress are assumed to be maximum at the axis of symmetry, where no displacement occurs. Full compatibility of strains between steel and concrete is assumed throughout the slab.

When the first crack develops, a condition exists, as explained in Chapter 5, where boundary conditions are necessary to solve a number of governing equations. These are as follows (a more complete description is provided in Chapter 5):

(1) Steel displacement is zero at the center of the crack.

(2) Concrete stress is zero at the crack.

(3) Bond stress exists only in the bond development zone.

(4) In the fully bonded zone, there is compatibility between concrete and steel.

(5) A point exists between the crack and the joint where concrete stress is at the maximum level and concrete and steel movement are zero (fixed point).

(6) The fixed point is not necessarily the point where full bond has been developed.

When the second and third (by symmetry) cracks form, the following is additionally assumed:

(1) The slabs between cracks act as CRCP slabs.

(2) The steel displacement at the second crack is zero.

Boundary conditions for the second and third cracks are acknowledged to be approximations, but are used because true conditions will not differ substantially from those assumed. Results, therefore, will be within acceptable ranges for engineering purposes.

VARIABILITY

The concept of variability must always be addressed when analyzing pavement structures. The scope of construction projects invariably results in variations in material parameters throughout the pavement. Assumptions for analysis include homogeneity of material properties throughout the pavement. This is, of course, not true for real-world situations, as is illustrated by the randomness of cracking in CRCP (Refs 3, 4). Variability for this analysis is taken into account by the variance of tensile strengths. This is the parameter shown to represent variability of concrete behavior best (Ref 4); the variance can be measured directly by statistical sampling of the concrete during construction. By using the variance of tensile strength, mechanistic crack spacing determination can be transformed into a probabilistic calculation.

If the tensile strength is known to vary, as shown in Figure 3.2, the distribution can be described by a mean and standard deviation. Dividing the standard deviation by the mean results in a coefficient of variance, which may be applied to tensile strength at any time during strength development. In other words, this assumes that the ratio between standard deviation and mean strength value remains constant throughout strength development. If a confidence level is attached to the mean and standard deviation, a strength value can be found above which strength will be at a percentage equal to the confidence level. A confidence level of 90 percent indicates that the strength in the field will be higher than the tensile strength used in analysis 90 percent of the time.

This translates to the following: 90 percent of the crack spacing will exceed the predicted crack spacing. The probability of a crack spacing less than the predicted value is therefore:

$$P = 1 - C \tag{3.1}$$

where:

P = probability of the crack spacing less than the predicted value from analysis, and

C = confidence level for concrete tensile strength.

In this manner, probabilities of crack spacing or stress levels can be calculated, with repetitive calculations of crack spacing at different confidence levels for tensile strength values resulting in a distribution as shown in Figure 3.3. Therefore, a distribution rather than a single value can be calculated for a distress parameter (crack spacing in this case). The two lines in the figure indicate that a different distribution will be achieved, by repetitive calculations, for each operating condition. For example, a greater pavement temperature differential will lead to a crack distribution moved toward the left, indicating larger crack spacing. Similar principles apply to tensile strength and to all other influencing parameters.

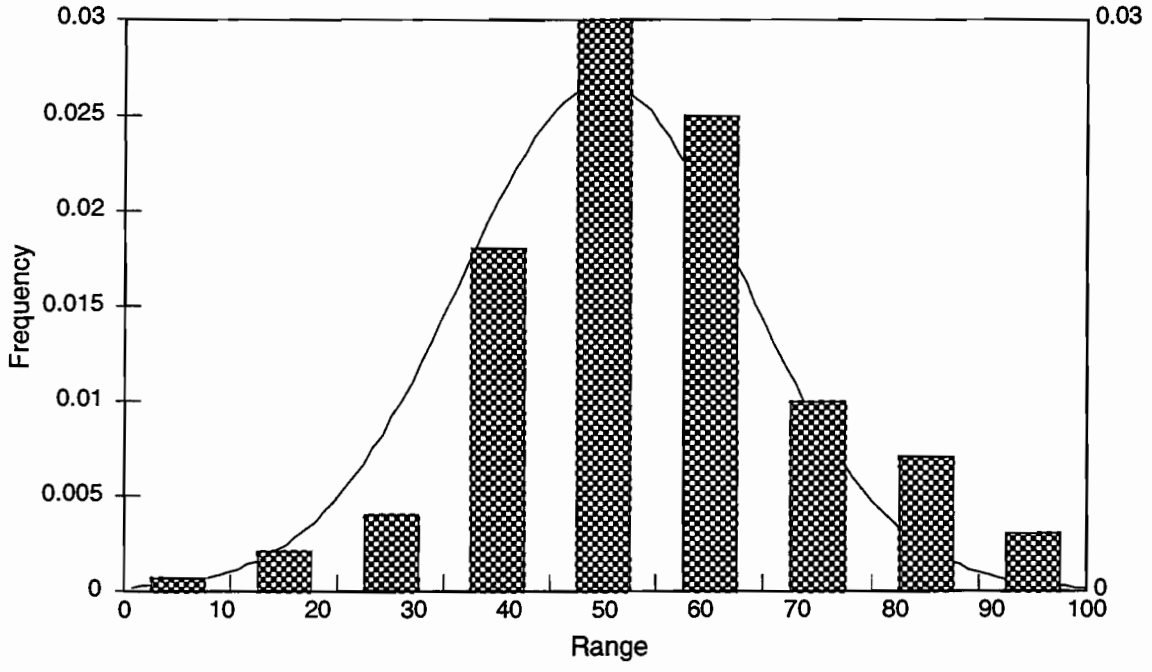

Figure 3.2 Example of tensile strength distribution for concrete

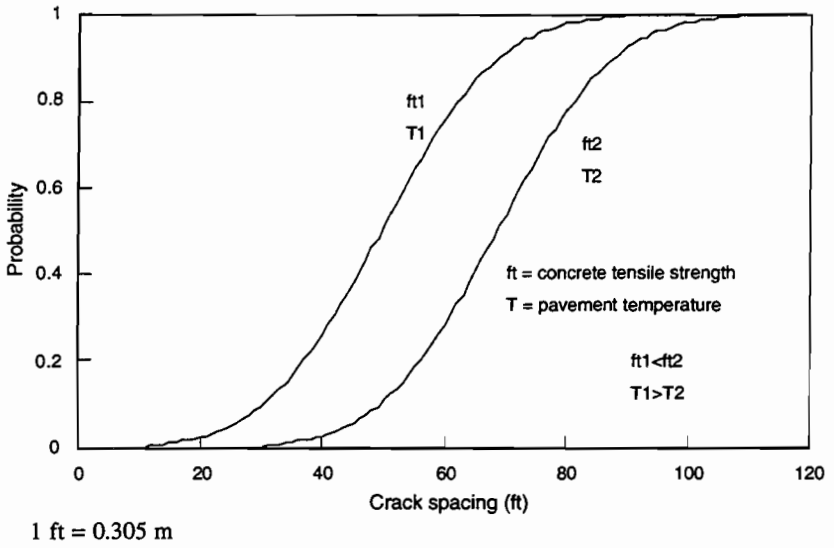

1 ft = 0.305 m

Figure 3.3 Theoretical crack spacing distribution as influenced by different parameters

TRAFFIC LOADING

Traffic is generally quite diverse in nature, making analysis of cyclic vehicular stresses rather complicated. The approach taken in this report is one of simplification. All loads are rendered equivalent to a standard 8000 kg (18000 lb) maximum axle load (ESALs). All calculations are subsequently performed using traffic expressed as ESALs.

The influence of traffic loads are investigated at mid-span of the slab and at the joints and cracks using Westergaard's equations. Stresses can subsequently be superimposed on those owing to environmental effects, and the associated distresses and pavement performance can be predicted. Westergaard's analysis of rigid pavement (Ref 5) is applied for all evaluations of traffic loading. Assumptions, some of which have already been discussed, are as follows:

(1) The concrete slab acts as a homogeneous, elastic solid in equilibrium.

(2) Reactions of the subgrade are vertical only and are proportional to the deflections of the slab.

(3) Thickness of the slab is uniform.

(4) Loads are distributed uniformly over a circular area for interior and corner load cases, and over a semi-circular area for the edge loading case and are static.

(5) The slab is infinite in all horizontal directions away from the load.

Load positions considered are interior, edge, and corner. Equations are summarized by Westergaard (Ref 5). Although this analysis method is simple and has a large number of assumptions, it provides a starting point from which more refined analyses procedures can be developed.

CHAPTER 4. EXISTING ANALYSIS AND DESIGN PROCEDURES

This chapter discusses analysis and design procedures relevant to JCP, concentrating in particular on research being conducted by the Center for Transportation Research (CTR) of The University of Texas at Austin. Existing procedures refer to analysis and design methods used and developed by CTR, by the Texas Department of Transportation (TxDOT), and by researchers nationwide. The locally developed methods use basic principles and strategies discussed in previous chapters.

MATERIAL CHARACTERIZATION

Project 1244 continues to work on the analysis, design, and specifications for PCC pavement using different coarse aggregates. Previous studies reported by Dossey and McCullough (Ref 11) have revealed significant variation in concrete properties using similar mix designs, but different coarse aggregates. While researchers have been aware of the influence of coarse aggregates on concrete properties for a considerable time (Ref 23), not until recently has the concrete industry been prompted to investigate such effects on the properties of high-strength concrete (Ref 24). The previous lack of interest was due to the marginal influence coarse aggregate has on relevant concrete properties in structural applications. Concrete pavement, on the other hand, is subjected to substantial environmental stresses. It is here that the properties, such as the thermal coefficient of expansion and the drying shrinkage, play a large role in determining critical stresses. Variation of these properties with coarse aggregate type warranted extensive investigation. Furthermore, performance indicators from the field, collected for a rigid pavement database maintained by CTR, showed significant variation when coupled with coarse aggregate type.

The above-mentioned facts and findings led to a three-phase research study under Project 1244. Phase I included only the two most commonly used coarse aggregates in Texas: limestone and siliceous river gravel (Ref 20). Standard mixes were used and relevant concrete properties were measured at set times during the early age of concrete development (28 days). Statistical analysis produced curves that could be fit to each property and for each type of aggregate. Phase II of the research (Ref 11) broadened the scope of aggregates to the eight most commonly used coarse aggregates in Texas. Additionally, the research was expanded to characterize concrete properties from the most prevalent chemical compounds constituting the coarse aggregate. Based on this research, concrete property development with age could be predicted by performing a simple inexpensive chemical test on an unknown aggregate type and assuming a basic concrete mix. These models are included in the program CHEM2 (Ref 25). It should be noted that these models predict concrete properties according to the most commonly used mix designs. Adjustment of mix designs will invariably produce different values for properties and should ultimately be laboratory tested to confirm or adjust the prediction models. The concrete property prediction models according to coarse aggregate type are included as an input guide for the user of the CRCP and JRCP analysis programs developed at the Center for Transportation Research (Ref

25). Provision has been made to correct for these inherent values for the properties when they seem wrong to the user or when they contradict laboratory testing.

Phase III approached the issue of blending known aggregates (limestone and siliceous river gravel) and the effect of that on the concrete properties of the same mix design. Findings summarized by Dumas et al. (Ref 21) show that concrete properties change almost exactly linearly when coarse aggregate mix proportions (by volume) change. For example, if limestone produces concrete with tensile strength of 2.76 MPa (400 psi), and siliceous river gravel 2.41 MPa (350 psi), a blend of half limestone and half river gravel will result in a tensile strength of 2.59 MPa (375 psi). These findings are incorporated in the CHEM2 prediction program.

The above-mentioned research has led to better characterization of time-dependent concrete properties. All other required inputs for material characteristics are constants or can be found in relevant references. Steel properties, in pavement applications, are an accepted constant and can be found in most structural steel handbooks. Slab-subbase friction is covered in Chapter 2; values are summarized in Table 2.1.

JRCP ANALYSIS PROGRAMS

There are several analysis programs based on the original JRCP-1 developed by Vallejo and McCullough in 1975 (Ref 2). JRCP-1 to JRCP-5 are updated or slightly modified versions of the original program. JRCP-1 was initially written as a FORTRAN-based program for the CDC mainframe computer at The University of Texas at Austin (Refs 2, 3). The nature of the FORTRAN language, together with the existing technology at the time, made the use of earlier versions of the program tedious. As technology developed, however, input and output have become more user friendly. Improvements to the JRCP program have led to the following versions:

(1) JRCP-2: Included determination of stresses and displacements as a result of minimum pavement temperature after the initial analysis period of 28 days.

(2) JRCP-3: Steel design and non-reinforced slab options removed; the option to force a crack included.

(3) JRCP-4: Algorithm to solve the uncracked slab situation (MODEL1) revised and terminal movement (joint width) included as output (Ref 26).

(4) JRCP-5: Normalized time-dependent concrete properties included (Ref 27).

Concurrently, Projects 422, 459, and 1169 at CTR produced findings and data related to JRCP. More accurate input to the analysis program was possible and included:

(1) Aggregate-dependent concrete properties (Ref 11)

(2) Subbase friction models (Ref 16)

Furthermore, desktop computer (PC-compatible) versions of the program were developed at the Center for Transportation Research. Rapid development of computer hardware made the

conversions possible; these computer versions included easy-to-use, menu-guided input and graphical representation of the output. These improvements have been retained for the improved version of JRCP described in this report.

Investigation of the use of the old JRCP analysis program for design procedures using different coarse aggregate types revealed a number of problems. These problems can be attributed to outdated analysis models, modifications to subroutines without corresponding changes to the rest of the program, or a combination of both. Research recently performed for the Federal Highway Administration (Ref 1) also indicated the following limitations of JRCP-4:

(1) The analysis period covers only the first 28 days of concrete life.

(2) Stresses due to wheel loading are not considered.

(3) Fatigue cracking from cyclic loading is not considered.

(4) Dimension of depth ignored in differential temperature and moisture analysis.

That JCP behavior is overwhelmingly governed by initial environmental conditions is still one of the relevant hypotheses investigated in any effort to model the performance of JCP; certainly cracking development, as a distress, is largely due to the environment. As a result of renewed interest in JCP, improved analysis based on existing procedures, with emphasis on early-age environmental analysis, were developed in this study. In addition, vehicular loading, fatigue, material variability, and distress prediction were incorporated in the model; a new approach to the problem resulted in a rewritten JRCP program called JRCP-6.

DESIGN AND PERFORMANCE PREDICTION MODELS

A comprehensive study of JCP (Ref 1) found the following available design and prediction programs and procedures:

(1) PREDICT, uses equations developed under the NCHRP 1-19 research study and developed at the University of Illinois.

(2) PEARDARP, a program developed at Purdue University used in conjunction with analysis program PMARP

(3) JCP-1, a design procedure based on theoretical studies and field surveys developed at the University of Illinois.

(4) DNPS86 a computerized version of the AASHTO design procedure.

(5) PCA design procedure based on theory, research experience, and in-service behavior.

(6) California Rigid Pavement Design Procedure, developed by California Department of Transportation for the design of PJCP.

(7) BERM, a program developed by Resource International based on the analysis of program RISK.

A previous study (Ref 1) concluded that none of the above-mentioned models or programs could adequately predict distresses and performance of evaluated sections. The evaluated sections covered a large portion of the country, including wet and dry regions, and freezing and non-freezing regions. Attempts were then made by the researchers to develop new models to fit the investigated sections. This clearly illustrates the predicament of the pavement design engineer. Exact theoretical modeling of pavement behavior is too complex to be performed within the resources of most practicing engineers. Therefore, the industry has had to fall back on quasi-mechanistic-empirical models, often having to extrapolate beyond the scope of the original investigated data. When results using these methods seem wrong, the approach is often to recalibrate models to include new data. The strategy in this report concentrated on design procedures or distress predictions based on data compiled in Texas, narrowing the design factorial sufficiently to summarize the data, while providing an approximate prediction based on theory and on local service history. Extrapolating beyond these parameters yields inaccurate predictions.

CTR JCP DATABASE

Project 1342 is updating and improving the rigid pavement database for the Texas Department of Transportation. Continuous monitoring of test section performance, coupled with design and traffic information, provides an invaluable tool on which to base empirical predictions. A comprehensive condition survey of the test sections is currently being completed. Unfortunately, a large number of JCP sections have been overlaid or reconstructed, while new sections do not have a long service history. As a result, limited information exists on JCP in Texas. Distress prediction from these data is limited in scope, but recommendations for future work, when more data are available, can be provided.

CHAPTER 5. IMPROVED EARLY-AGE MODELING

Jointed concrete pavement (JCP) can be analyzed by incorporating environmental and vehicular effects in the analysis of pavement behavior, as was discussed in previous chapters. These effects may be broken down into temperature and moisture effects for the environment, and into the effects of different vehicle weights, tire pressures, and traffic loading positions. Furthermore, the effects of these loading conditions can be investigated for different components of the slab — for example, internal stresses in the concrete slab or interactions at the transverse joints. For the most part, this chapter investigates the modeling of the early-age environmental effects on the slab, cracks, and joints. The convention defined for joints in Chapter 2 is adopted in this chapter. All references to cracks imply forced cracks or transverse contraction joints (i.e., controlled cracks).

EARLY-AGE BEHAVIOR

Early-age behavior refers to the concrete pavement's behavior within the first 28 days of pouring. It is assumed that the pavement will not be subjected to loading other than environmental loading during this time. The modeling procedures described here are not, however, restricted to this period in time and may be used to analyze environmental effects on the pavement at any time.

Geometric models

The concept of modeling a concrete pavement subjected to temperature differentials and concrete drying shrinkage is adapted from work performed by McCullough et al. (Ref 3) in 1974. These ideas were applied to jointed concrete pavements by Vallejo and McCullough (Ref 2) in 1975. In these analyses, tensile stress was found to control behavior; in other words, when tensile stress exceeds tensile strength, the slab cracks. While various improvements to these methods have since been made, the basic geometric models remain the same. The conventions explained in Figure 5.1 remain applicable for all modeling performed in Chapter 5 and used in JRCP-6. The Cartesian coordinate system shown in the figure sets the x coordinate of the one-dimensional model, along the longitudinal axis. Displacements or movements of the slab, as well as forces acting on free bodies in the direction of the positive x axis, are considered positive. Tension is also considered a positive stress in this convention.

Consider a slab of jointed concrete pavement, like the one illustrated in Figure 5.1. A slab of concrete contracts as a result of concrete drying shrinkage and a temperature difference lower than the setting temperature. Restraint from friction between the slab and subbase and the bonded reinforcing steel result in stress build up, as shown in Figures 5.1 and 5.2. The free ends at the transverse joints move towards the center of the slab, where concrete and steel stresses are maximum and movement is zero. The system may be modeled as a symmetric half slab based on the following basic assumptions:

(1) Steel and concrete are linearly elastic.

(2) Concrete and steel are fully bonded and no relative movement exists.

(3) Temperature variations and drying shrinkage are uniformly distributed throughout the slab in all three directions.

(4) No frictional effects at transverse and longitudinal joints are considered.

(5) Materials are homogeneous and isotropic.

These assumptions reduce the problem to a simple one-dimensional linear elastic problem, which can be solved using equilibrium, compatibility, and constitutive equations.

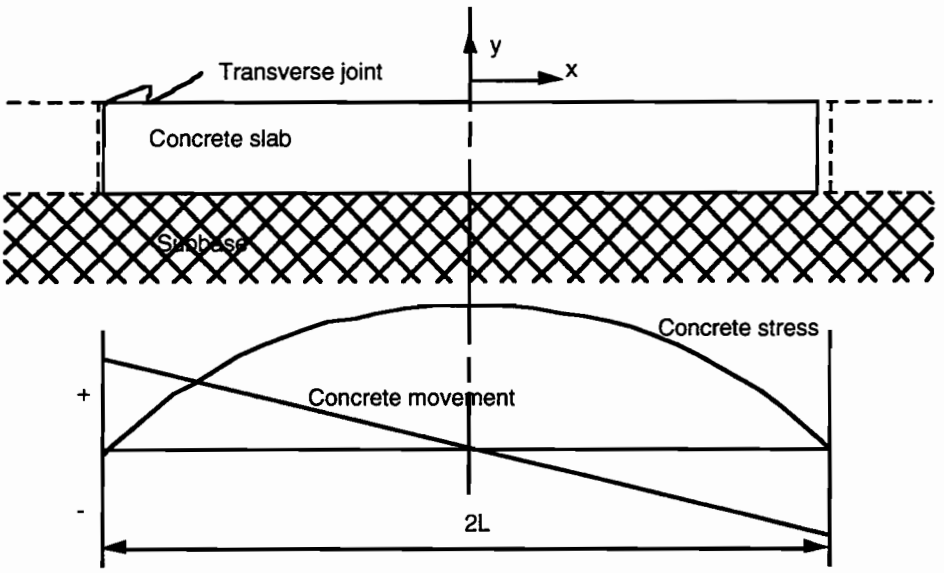

Figure 5.1 Uncracked jointed concrete pavement (JCP)

Consider the free body diagram presented in Figure 5.2. The origin of the x-axis is at mid-slab, and a cross-section equilibrium is achieved at distance x. Equilibrium of forces in the x direction results in the following:

$$\sum F_x = 0 \qquad \int_x^L F_f \, dt - F_{cx} - F_{sx} = 0 \tag{5.1}$$

where:

Ff = friction force per unit length,

Fcx = force in the concrete at position x, and

Fsx = force in the steel at position x.

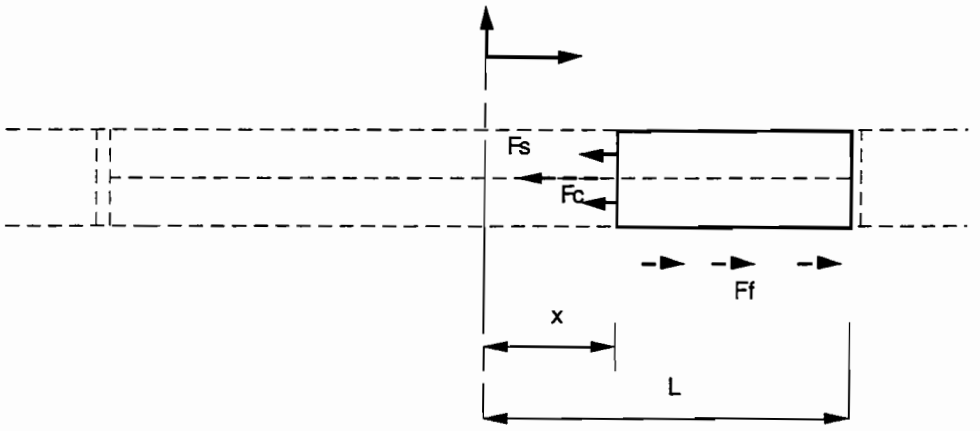

Figure 5.2 Free body diagram of uncracked JCP

Transforming the equation into stresses per unit width results in:

$$\frac{\int_x^L F_f \, dt}{D} - \sigma_{cx} - p\sigma_{sx} = 0 \tag{5.2}$$

where:

D = concrete thickness,

p = As/Ac (where As is the area steel and Ac is the area concrete for the cross section), and

σ = stress in the steel and concrete respectively at position x.

Compatibility of displacements along the x-axis is considered next. Displacements are a sum of strains over the length of the slab. Factors that contribute to concrete strain include stress in the longitudinal direction, drying shrinkage, and temperature variation. Similarly, strain in the steel is a result of stress in the steel and temperature variation.

$$\frac{du_{cx}}{dx} = \frac{\sigma_{cx}}{E_c} - \alpha_c \Delta T - Z \tag{5.3}$$

$$\frac{du_{sx}}{dx} = \frac{\sigma_{sx}}{E_s} - \alpha_s \Delta T \tag{5.4}$$

where:

u_{cx} = displacement of the concrete at position x,

u_{sx} = displacement of the steel at position x,

Ec = modulus of elasticity of concrete,

Es = modulus of elasticity of steel,

α_c = thermal coefficient of expansion of concrete,

α_s = thermal coefficient of expansion of steel,

ΔT = temperature change (positive if temperature decreases from setting temperature), and

Z = drying shrinkage of concrete.

Because displacements of steel and concrete are equal in fully bonded areas, strains are also equal. Equating Equations 5.3 and 5.4 yields Equation 5.5:

$$\sigma_{cx} = \frac{\sigma_{sx}}{n} + E_c([\alpha_c - \alpha_s]\Delta T + Z) \tag{5.5}$$

where:

n = Es/Ec

Differentiating Equations 5.2 and 5.5 with respect to x leads to:

$$\frac{F_f}{D} + \frac{d\sigma_{cx}}{dx} + p\frac{d\sigma_{sx}}{dx} = 0 \tag{5.6}$$

$$\frac{d\sigma_{cx}}{dx} = \frac{1}{n}\frac{d\sigma_{sx}}{dx} \tag{5.7}$$

From 5.6 and 5.7, the rate of change in concrete and steel stresses can be found:

$$\frac{d\sigma_{cx}}{dx} = \frac{-F_f}{nD(p + \frac{1}{n})} \tag{5.8}$$

Constitutive equations for concrete and steel material behavior and characterization of the friction force complete the necessary assumptions required to solve the system. Constitutive equations assuming linear elasticity have inherently been assumed up to now; this assumption

continues for the following equilibrium discussions. Friction force, based on work performed by Wimsatt and McCullough (Ref 16), is assumed to follow the model shown in Figure 5.3.

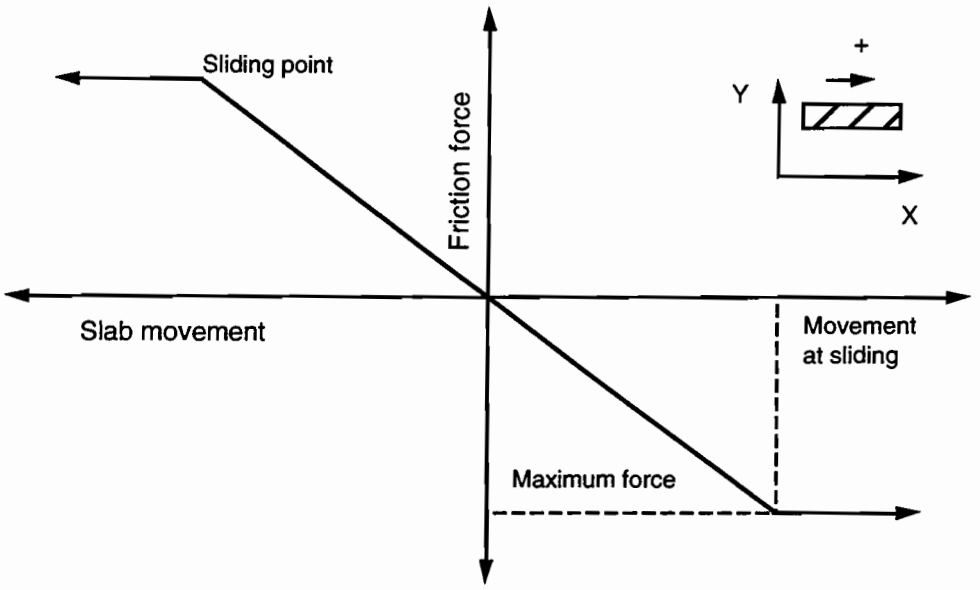

Figure 5.3 Slab-subbase friction model

$$\text{Fricmu} = \frac{F_u}{Y_u} \tag{5.10}$$

where:

Fricmu = modulus of friction,

Fu = maximum friction force after which sliding occurs and the friction force remains constant at this value, and

Yu = movement at which sliding commences.

Stresses, strains and displacements can now be calculated for the system depicted in Figure 5.1. Because the equations are, however, not explicit, the solution requires the iterative method discussed in later paragraphs.

When concrete stress exceeds concrete strength, the slab cracks, changing the boundary conditions; as a result, the equations above do not all apply to the entire slab. For reasons argued in later paragraphs, the first crack is assumed to occur at the middle of the slab in the x direction.

A new situation then develops, which is illustrated in Figure 5.4. It should be noted that displacements shown in Figure 5.4 are relative to the origin of the x and y axes, which, owing to the established sign convention defined previously, causes negative symmetry. Figure 5.4 represents a typical situation where there is reinforcement present and the concrete is contracting. In the case of plain jointed concrete pavement (PJCP), the equations described above simply apply to a shorter slab, and load transfer at the crack occurs through aggregate interlock only. However, reinforcing steel complicates the situation considerably, as will be explained.

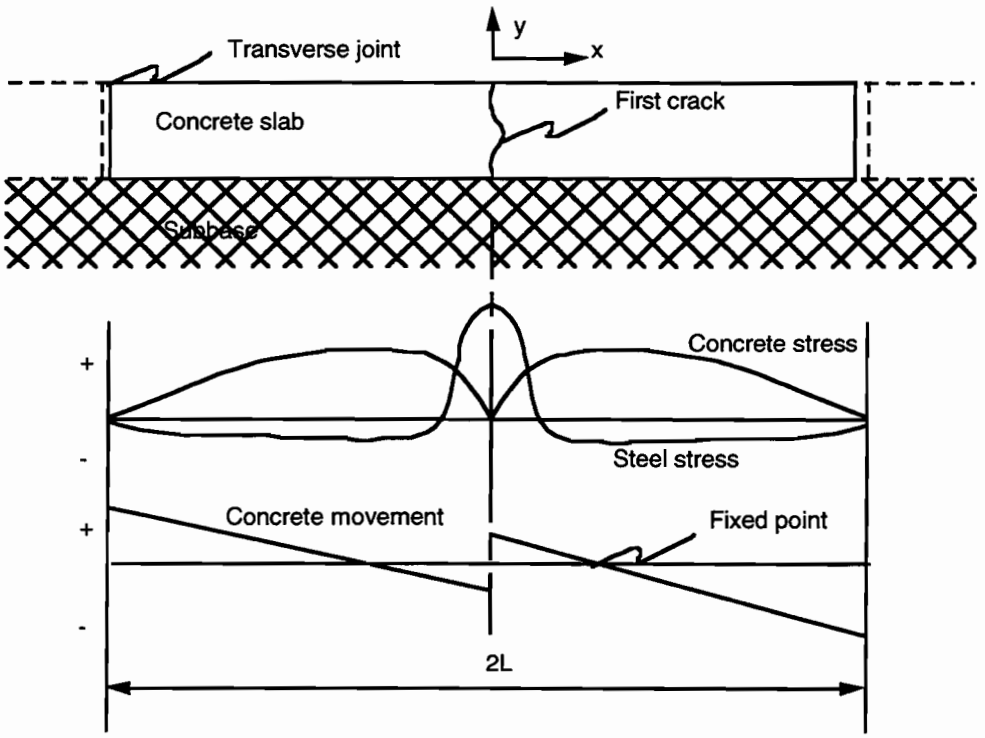

Figure 5.4 One-crack situation for jointed reinforced concrete pavement (JRCP)

A slab that has cracked once remains symmetrical; accordingly, modeling simplified to half a slab is valid. At the crack, concrete stress is relieved and transferred to the steel. Moving toward the free end of the slab from the crack, the steel stress is transferred from the steel to the concrete, as the concrete tends to slip over the reinforcement. The mechanism is called transfer of stress by bond stress. From the opposite end of the slab (the free end or jointed end), concrete behaves as it did when the slab was uncracked, and stress increases towards the cracked point. Somewhere in the half slab, concrete movement is zero and concrete stress reaches a maximum, satisfying the compatibility and equilibrium principles. From Figure 5.4 it can be noted that the half slab is now divided into two lengths (L1 and L2). The intersection point is the point where movements are zero and concrete stress is maximum. This may be regarded as a fixed point for

sections of slab on either side. All equations that apply to the uncracked slab also apply to the section of the cracked slab defined by L1. The section of the cracked slab L2 is divided into a fully bonded length (a) and bond development length (b). For the fully bonded length, the same principles apply as for the uncracked slab, but for the bond development zone new relationships apply because in this case there is relative movement between concrete and steel.

In previous solutions to the cracked reinforced slab problem, the methods assumed that transfer of stress from steel to concrete is constant in the non-bonded zone (where concrete slips over reinforcement). Recent investigations in structural engineering have, however, proved this assumption to be untrue. Through pull-out tests, bond stress was found to be a function of the relative movement between concrete and steel. Extensive research was performed in this area by Won et al. (Ref 4), who developed a mechanistic solution to the continuously reinforced pavement problem. This solution, also used to model the cracked JCP situation, is considered an innovation to cracked JCP slab modeling. Concrete stresses in the cracked slab largely depend on the stress transferred between steel and concrete at the crack; it is therefore important to accurately model the bond stress at the crack. Consider the free body diagram in Figure 5.5 where, as with the uncracked slab, equilibrium at any point x results in Equation 5.11.

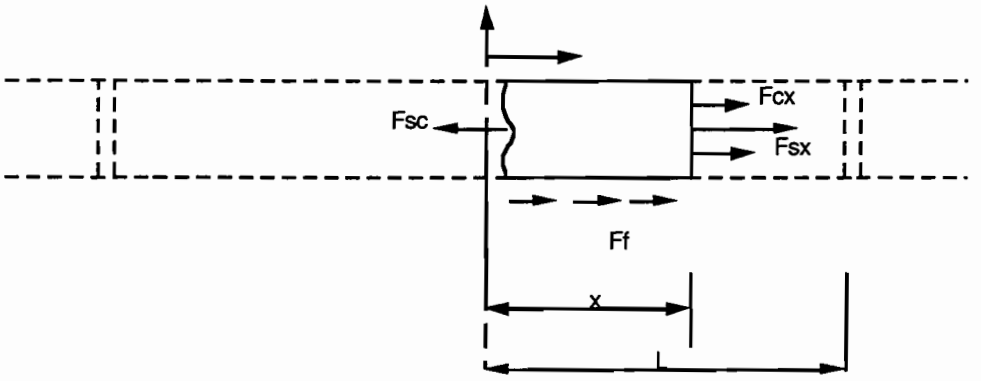

Figure 5.5 Free body diagram for cracked JRCP

$$F_{cx} + F_{sx} - F_{sc} - \int_0^x F_f \, dt = 0 \qquad (5.11)$$

where:

Fsc = force in the steel at the crack.

As before, transforming forces to stresses per unit width results in:

$$\sigma_{cx} + p\sigma_{sx} - p\sigma_{sc} - \frac{\int_0^x F_f\,dt}{D} = 0 \tag{5.12}$$

When considering compatibility, Equations 5.3 and 5.4 hold for the cracked situation in the fully bonded and bond development zones. Equation 5.5, however, is valid only for the fully bonded zone. In Figure 5.6, the bond development length (b) represents the length over which full bond is developed between steel and concrete. Inside this length, a segment dx is considered in a free body diagram. Equilibrium for the steel and concrete:

$$F_\alpha + dF_\alpha + f_b(x)\pi\phi\,dx + F_f dx - F_\alpha = 0 \tag{5.13}$$

$$F_{sx} + dF_{sx} - f_b(x)\pi\phi\,dx - F_{sx} = 0 \tag{5.14}$$

where:

fb(x) = bond stress distribution function, and

ϕ = diameter of the steel reinforcement.

Transforming these to stress variations results in:

$$\frac{d\sigma_\alpha}{dx} = -\frac{4f_b(x)p}{\phi} - \frac{F_f}{D} \tag{5.15}$$

$$\frac{d\sigma_{sx}}{dx} = \frac{4f_b(x)}{\phi} \tag{5.16}$$

As before, the constitutive equations for concrete and steel materials are assumed to be linear, with the friction force handled in the same way as represented in Figure 5.3. Three extra variables or functions are unknown: bond development length, bond stress distribution function, and the steel stress at the crack. Won et al. (Ref 4) provide three equations to solve the problem; and although the derivation is not included in this section, the equations are presented below.

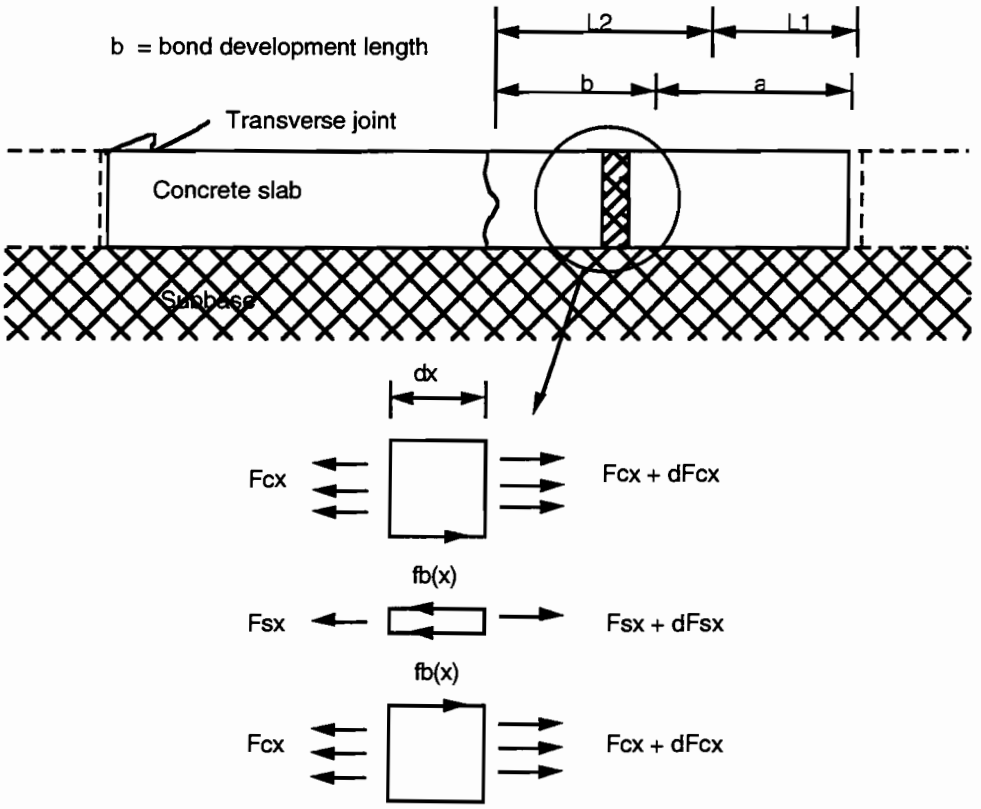

Figure 5.6 Free body diagram of the bond development zone

$$f_b(x) = 2AK\left(\cosh\left[\frac{cx}{b}\right] + \cos\left[\frac{\pi x}{2b}\right]\{\cosh[c] - 1\} - \cosh[c]\right) - \frac{\beta b}{\alpha c} e^{\left(\frac{-\alpha}{b}\right)}$$
$$+ \frac{b}{\alpha}\left(\frac{c}{\alpha Kb} - \frac{b}{c}e^{-c} - L\right)\cos\left(\frac{\pi x}{2b}\right) - \frac{\beta}{\alpha}(x + a) + \frac{\beta b}{\alpha c}e^{-c} + \frac{\beta L}{\alpha} \qquad (5.17)$$

where:

$$2A = \frac{\frac{b}{c}\left(\left[\frac{\sigma_{sc}}{E_s} + \{\alpha_c - \alpha_s\}\Delta T + Z\right] - \frac{\beta}{\alpha K}\left[1 + c - \frac{2c}{\pi}\right]e^{-c} - \beta\left[bL + \frac{2c}{\pi aK} - \frac{2bL}{\pi} - \frac{1}{\alpha K}\right]\right)}{\sinh(c) - c\cosh(c) - \frac{2c}{p} + \frac{2c}{p}\cosh(c)}$$

K = bond stiffness which is the bond stress per unit slip (set at 30,000 psi/in or 5.25 MPa/m),

$c = \sqrt{\alpha Kb}$,

α = $\frac{4(1+np)}{\phi E_s}$,

a = fully bonded length,

b = bond development length,

L = length of slab from the cracked end to the point of zero displacement,

x = coordinate on the slab (origin at the point where full bond is achieved, b from the cracked end),

β = $\frac{\Theta}{E_c D}$, and

θ = slope of the subbase frictional stress distribution (assumed to be a straight line, 0 at the point of zero movement and a maximum at the crack).

Equation 5.17 is derived from a function proposed by Yang and Chen (Ref 26) and solved for the specific boundary conditions by Won et al. (Ref 4).

$$\frac{4}{\phi}\int_{-a}^{b}\int_{x}^{b} f_b(t)dtdx = \sigma_{sc}L - E_s\alpha_s\Delta TL \tag{5.18}$$

where:

L = length of slab from the cracked end to the point of zero displacement

Equation 5.18 is derived from the steel boundary conditions from Equation 5.16.

$$b = \frac{\phi K_p}{4}\left(\sigma_{sc}\left[1-\frac{1}{C1}\right]+\left[\frac{C2}{C1}-\frac{\int_{-a}^{b}F_f dx}{pDC1}+\frac{\int_{-a}^{0}F_f dx}{D\{p+\frac{1}{n}\}}\right]\right) \tag{5.19}$$

where:

Kp = a constant determined from a pull-out test (set at 0.0028),

C1 = $1+\frac{1}{np}$, and

C2 = $\frac{E_c}{p}([\alpha_c-\alpha_s]\Delta T+Z)$.

Equation 5.19 is derived from an equation proposed by Somayaji and Shah (Ref 27) for the relationship between transfer load and bond development length.

While the system of equations is defined, the equations are implicit and various iterations need to be performed to determine the bond development length, the friction force, and, finally, the point of fixivity. The solution method is explained in the following paragraphs.

If the cracked model calculates concrete stresses that are larger than the concrete strength, the slab will crack again. Through symmetry, cracks will occur at the same distance on either side of the first crack owing to homogeneous tensile strengths. The resulting slab is modeled as represented in Figure 5.7. The slab is divided into a "CRCP" section of length L2, and a free end slab of combined length L3 and L4, restricted by crack 2 on the inside. The free-end section (L3 and L4) is modeled in the same way as the single crack slab. Inherent in this statement is the assumption that steel displacement is zero at the second crack. This is, of course, not always true. However, movements are considered small enough to be disregarded in the modeling process, and the system is modeled as a "shorter" single crack slab. Furthermore, the "CRCP" slab (L2) is modeled as a CRCP slab — in other words, assuming a point of fixivity at the center of slab length L2. The equations discussed above all apply to the "CRCP" case, with the same restrictions for the bond development zones.

Any further cracking that may occur is not considered, since it is not envisaged that JRCP would be designed to crack more than three times. Similar trends and assumptions may be applied for these cases, with the number of CRCP slabs simply increasing and the free end slab decreasing in length.

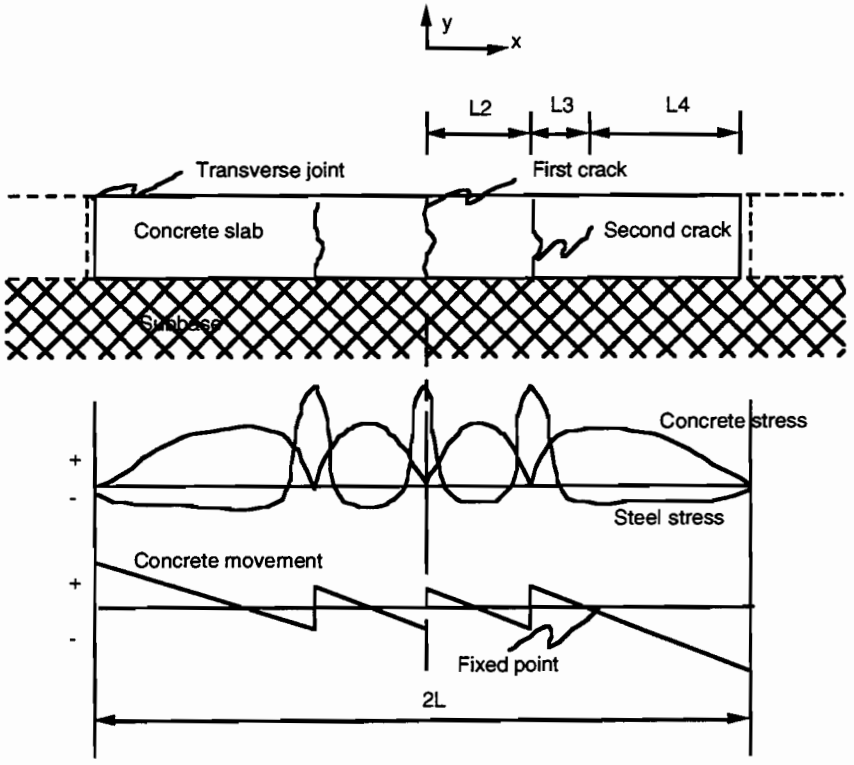

Figure 5.7 Three-crack situation for JRCP

Solution methods

The implicit nature of the governing equations for JCP requires an iterative solution method, as was discussed above. The simplest case, a no-crack situation as shown in Figure 5.1, will be discussed first. An iteration algorithm is shown in Figure 5.8. This algorithm, applicable to the free-ended side of any cracked slab, is called MODEL1, after the JRCP-6 subroutine. The solution consists basically of the same method that has been used by Vallejo and McCullough (Ref 2) and other researchers; however, the non-zero friction start-off is added to hasten convergence.

First, the problem is defined by material characteristics, slab geometry, and reinforcement details. Then a friction force function is assigned by assuming linear movement from the fixed point to the free end. Once the friction function is set, concrete stress and movement functions can be computed as follows. Concrete stress is computed by substituting Equation 5.5 into Equation 5.2, leading to Equation 5.20:

$$\sigma_{cx} = \frac{\frac{\int_x^L F_f dt}{D} - pE_s([\alpha_c - \alpha_s]\Delta T + Z)}{1 - pn} \tag{5.20}$$

Concrete movement is computed by integrating Equation 5.3 between zero, the fixed point in Figure 5.2, and the point at which the movement calculation is required, leading to:

$$u_{cx} = \frac{1}{E_c}\int_0^x \sigma_{cx} dt - (\alpha_c \Delta T + Z)x \tag{5.21}$$

Once concrete movement is known, new friction forces can be assigned to each segment using the following:

$$F_{fx} = Fricmu * u_{cx} \tag{5.22}$$

where:

$$0 < Ffx < Fu$$

The process is repeated until convergence is achieved, usually within ten iterations.

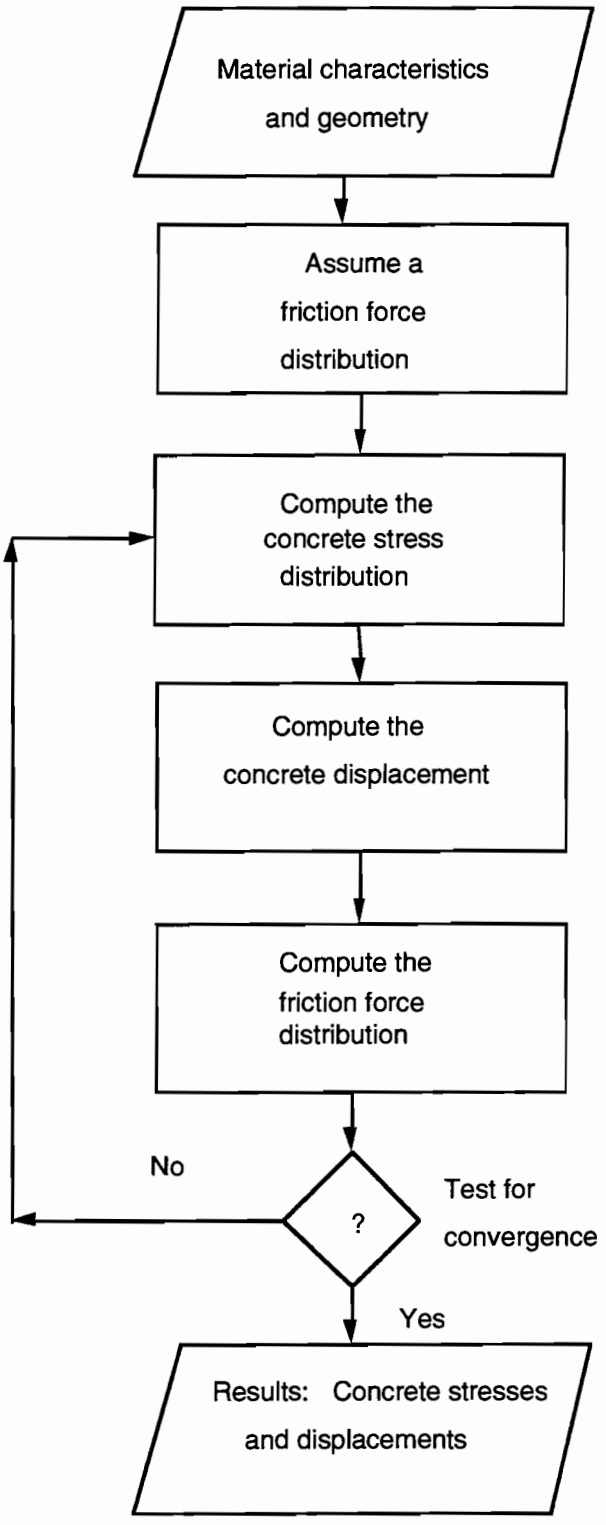

Figure 5.8 Free-ended slab solution algorithm (MODEL1)

A cracked slab poses a more complex problem. First, the governing equations are based on the assumption that there is a fixed point where concrete stress is maximum, concrete is fully bonded to steel reinforcement, and slab movement is zero. The slab toward the transverse joint side of the fixed point reacts exactly as an uncracked slab, with the half slab length equal to the length from the transverse joint to the fixed point. This portion of the slab can be analyzed using the uncracked slab algorithm MODEL1. The assumptions for the fixed point are carried over from the CRCP situation, where there is an infinite number of slabs of equal length on either side of the slab considered. When these conditions exist, the fixed point is located at the center of the slab. In the cracked JRCP situation, the unknown fixed point position must be found by iteration until all governing equations are satisfied. On the other hand, when a CRCP type slab exists, as is the case when more than one crack occurs in a JRCP slab, an approximation is made that the fixed point is once again at the center of the slab. Here, the condition of zero movement is most probably not met, though the assumption should nevertheless provide practical answers sufficiently close to the true solution for engineering purposes.

Second, three variables are added when the reinforced slab cracks. As explained in the previous section, bond length, bond stress function, and steel stress at the crack have to be found before the equilibrium function can be solved. The equations derived for these three variables (5.17, 5.18, and 5.19) are based on a number of assumptions:

(1) The bond stress distribution function is based on experimental results.

(2) Subbase friction is linearly distributed with the value zero at the fixed point.

(3) At the fixed point, there is no slip, full compatibility and no bond stress.

(4) At the crack, there is no concrete stress and no bond stress.

(5) Steel displacements at cracks and fixed points are zero.

(6) The fixed point position is known.

The solution algorithm for the cracked slab situation is presented in Figure 5.9. Equations used in the algorithm are derived from governing relationships presented in the section above. Consider Figures 5.5 or 5.6 ,where the x-axis origin is at the crack. It is assumed that the fixed point position is at length L2 from the origin.

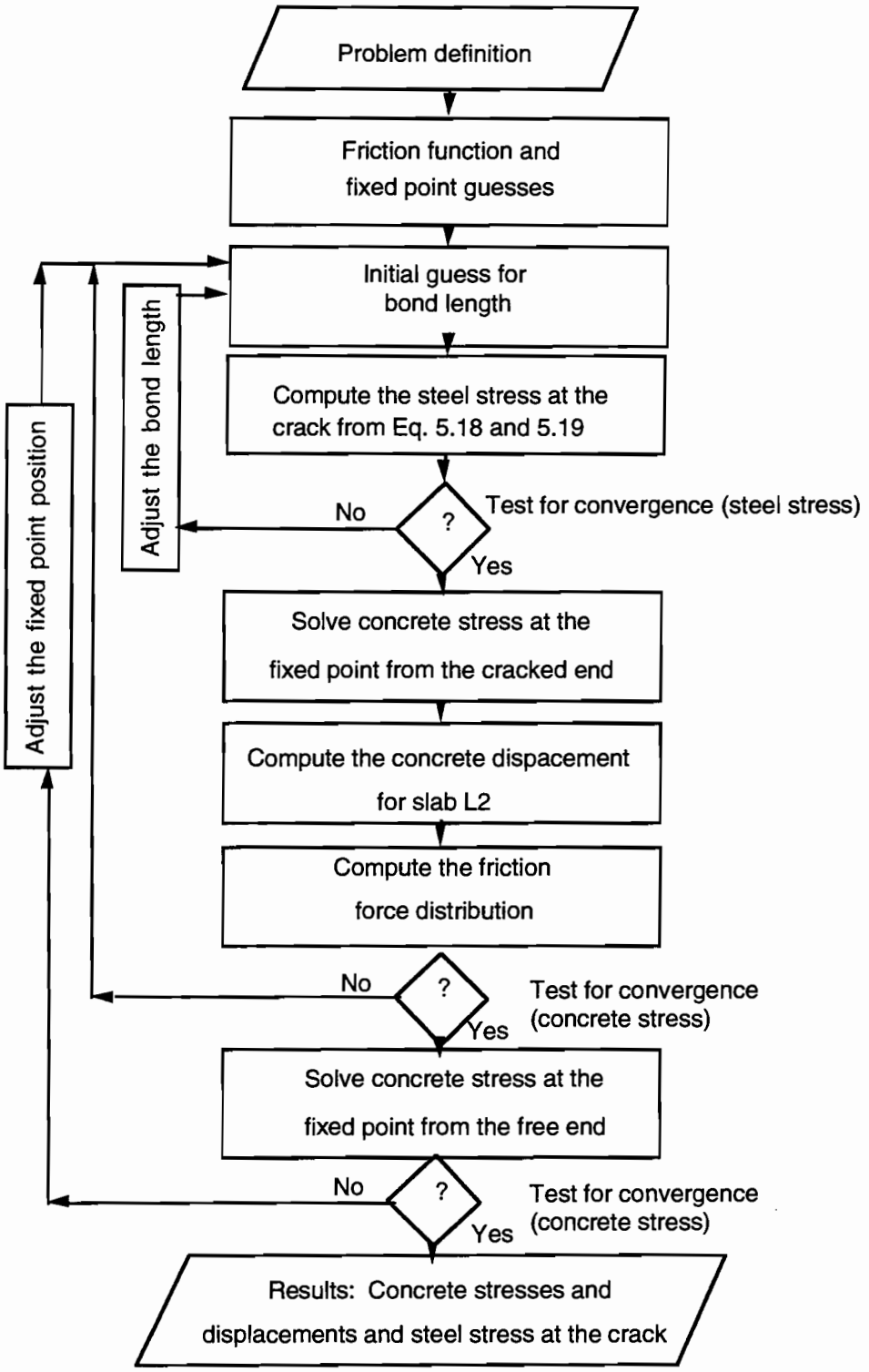

Figure 5.9 Cracked JRCP solution algorithm (including MODEL2)

Concrete stress in the bond development zone is computed by integrating Equation 5.15 between the crack and position x:

$$\sigma_{cx} = \frac{4p}{\phi}\int_0^x f_b(t)dt + \frac{1}{D}\int_0^x F_f\,dt \tag{5.23}$$

Concrete stress in the fully bonded zone is calculated by integrating Equation 5.8 between the bond length (b) and the position x:

$$\sigma_{cx} = \sigma_{cb} + \frac{\int_b^x F_f\,dt}{nD(p + \frac{1}{n})} \tag{5.24}$$

where:

σcb = concrete stress at the bond development length from Equation 5.23.

Concrete movement is calculated as before using Equation 5.21. Friction forces are adjusted, as in Equation 5.22.

Investigation of the solution algorithm in Figure 5.9 shows that there are three loops to solve the system. The first loop converges on the correct bond development length and steel stress at the crack for the given boundary conditions (friction force and fixed point position). The second loop adjusts the friction forces based on the calculated concrete movement; the third loop converges to the correct fixed position. The first two loops investigate only the section of slab from the assumed fixed point to the crack; it is called MODEL2 after the equivalent subroutine in JRCP-6. The final loop involves the use of the non-cracked solution algorithm to solve the portion of free moving slab of length L1 (MODEL1). This is a cumbersome, time-consuming process if undertaken without the use of a computer program.

For cases where the slab has cracked more than once, all the required equations have been set up, up to this point. The portion of the slab from the free end (transverse joint) to the first encountered crack is handled exactly as explained above for the case where there is only one crack. Solutions for all further sections of slab, between successive cracks, are somewhat simpler than the free-ended slab, because the fixed point is assumed to occur at the midpoint between cracks. The outer loop in Figure 5.9 is therefore eliminated and a solution is achieved more rapidly.

The assumption that cracks occur at points of highest stress is based on the assumption of a homogeneous concrete material. Although this is not exactly true in the field, it is argued that the cracks have the highest probability of occurring at or in proximity of the point of highest stress. The variation in crack position that might occur has negligible effect on subsequent solutions, as is illustrated in Table 5.1 below. An arbitrary length of uncracked slab is assumed to crack at three different positions: at midway and at 5 percent and 10 percent of the total length away from

midway. Comparisons are made between relevant calculated values. Variation is seen to be acceptable.

Table 5.1 Variable crack position effect on maximum concrete stress and joint and crack width

Cracks at:	L	0.95L	0.90L
Concrete stress	100%	94%	89%
Joint width	100%	96%	92%
Crack width	100%	94%	88%

JRCP-6

The solution methods described above, and summarized in Figures 5.8 and 5.9, are used in an improved version of the JRCP program. Appendix A contains input and output for the program for specific examples. These examples do not include the traffic loading analysis and distress prediction screens in JRCP-6, but will be updated after calibration is complete. The development of the traffic loading and distress prediction models are discussed in Chapter 6.

Chapter 7 discusses input and output drivers and runs through JRCP examples. Furthermore a brief sensitivity analysis of relevant variables for solution of the free-ended uncracked slab (MODEL1) and the "CRCP" case where the point of fixivity is set (MODEL2) is added to the chapter to provide information on important variables Also, comprehensive field data from a PJCP section are used to validate a part of the calculation procedure.

The JRCP-6 flow diagram is presented in Figure 5.10. First, the problem is defined by reading the input data for the pavement geometry, material properties, and iteration control parameters. Concrete properties are entered as time-dependent values for the first 28-day period; ultimate values for tensile strength, modulus of elasticity, and drying shrinkage are included at this time. Minimum concrete temperatures are entered for each day up to and including day 28. Yearly maximum and minimum pavement temperatures complete the required inputs for the environmental analysis.

The program then progresses through the first 28 days using current time-dependent properties, calculated in subroutine FORWAR, to calculate concrete stress, which is compared to the concrete strength. Depending on the current state of cracking, the program advances to the next state, if concrete stress exceeds concrete strength. No further calculations are performed if the slab cracks more than three times. There are, therefore, three possible scenarios of analysis: a no-crack state, a one-crack state, and a three-crack state. Each of these states of cracking requires different solution methods, as described in the sections above. The subroutine solving an uncracked slab, described in Figure 5.8, is called MODEL1, while the subroutine solving the inner two loops of

Figure 5.9 is called MODEL2. The outer and third loop of Figure 5.9 is solved in the main program of JRCP-6. The main program, therefore, successively calls FORWAR, MODEL1, and/or MODEL2 to check daily maximum concrete stress, or if cracks occur, eventually leading to the end of the 28-day stabilized crack spacing.

The pavement is now in the final state for analysis of environmental effects on maximum and minimum steel and concrete stresses, maximum and minimum joint widths, and maximum and minimum crack widths (if any develop). If during the final stage of analysis, the slab undergoes further cracking owing to the environment, analysis is repeated for the next state of cracking, provided no more than three cracks exist. Results provide data to design joints (mainly dowels and joint sealant), design required steel reinforcement, and analyze joints and interior regions of the slab for vehicular loading by simple Westergaard analysis.

Once the analysis of the subsets of behavior is complete, superimposition of stresses can be used to determine maximum interior slab stresses and bearing stresses of dowels at transverse joints. Results provided from these analyses can now be used to predict distress development in the future, according to time or traffic (as input by the user).

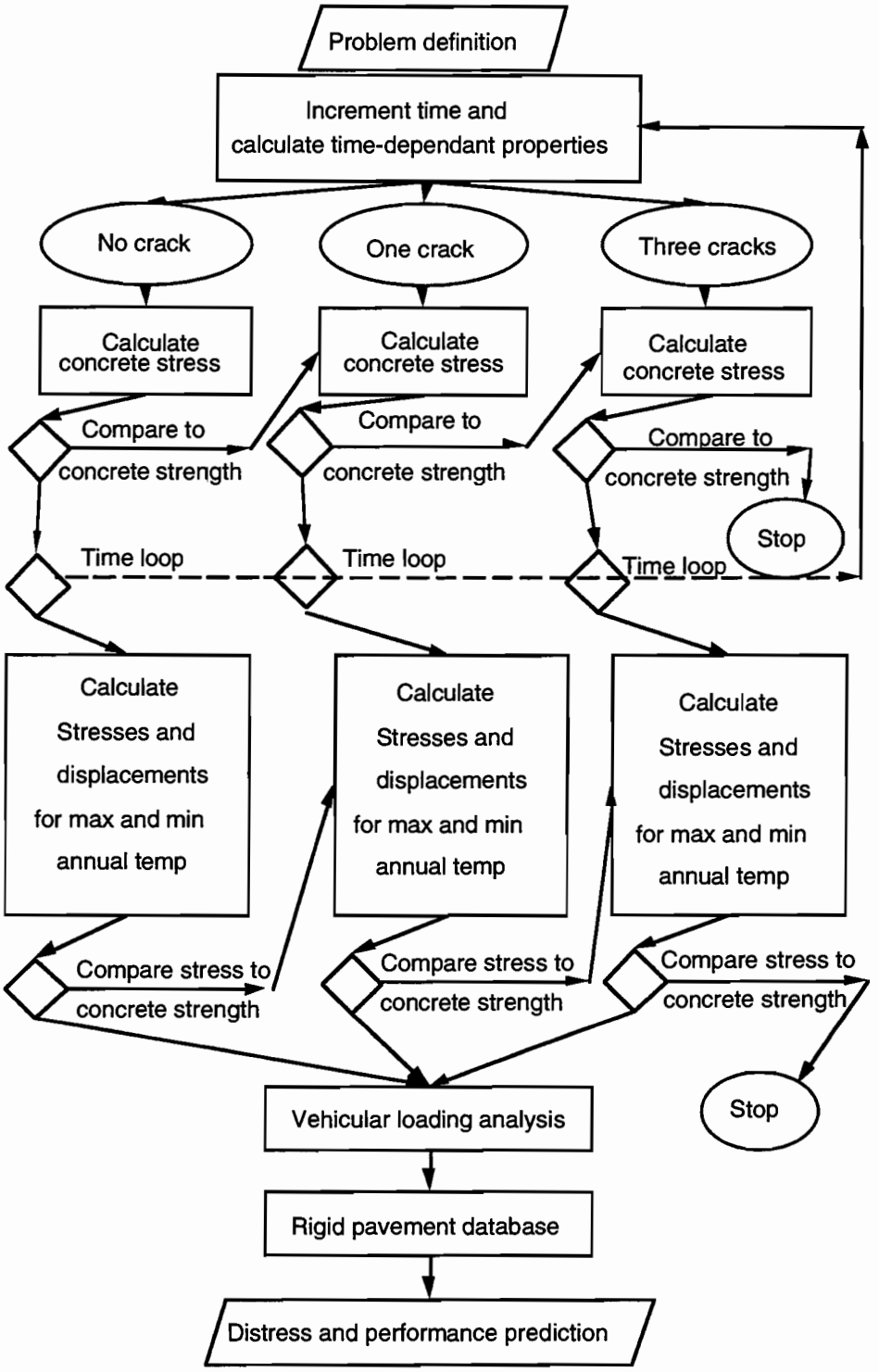

Figure 5.10 JRCP-6 solution algorithm

CHAPTER 6. VEHICULAR LOADING AND DISTRESS PREDICTION

This chapter discusses vehicular loading and its application in JRCP-6. In addition, distress surveys, drawn from the CTR rigid pavement database, are summarized in graphical form; a prediction method of transverse cracking and corner breaks is also discussed and included in the JRCP-6 program. While this work is at present incomplete and requires calibration, it is included as a starting point for future work.

TRAFFIC LOADING

The analysis of environmental effects on a pavement, described in Chapter 5, produces crack spacing, stress, and displacement results. These are not the absolute values, since the pavement is additionally subjected to vehicular loading. Traffic loading causes localized stresses in the slab in the general area of the wheel load. These stresses contribute to deterioration of the pavement through fatigue, which is manifested as distress. Current analysis of traffic loading ranges from three-dimensional, non-linear, dynamic finite element analysis to Westergaard's linear elastic, static analysis. This study uses Westergaard's analysis for evaluation of concrete slab stresses, and uses Friberg's method to calculate stresses surrounding dowel bars at the transverse joints. Both these analyses are covered in more detail in Chapters 3 and 8.

The JRCP-6 traffic loading module uses Westergaard analysis of the interior and edge loading conditions, as described in Chapter 3. These distresses are combined with environmental stresses by the superposition principle. As a first estimate, the average environmental tensile stress in the concrete slab is added to the traffic-loading induced stress to calculate the stress ratio at which the pavement operates. Stress ratio, fatigue principles, and the application thereof in JRCP-6 are explained in the paragraphs concerned with transverse cracking and corner breaks in this chapter.

DISTRESS PREDICTION

Performance of a pavement, as defined by riding quality, has been shown to be dependent on levels of physical distresses (Ref 28). The riding quality value is directly proportional to the longitudinal profile (or smoothness) of the pavement surface. Distresses such as cracking, spalling, and faulting contribute to riding quality deterioration with time. When a designer is able to predict development of distresses over time or cumulative traffic, an improved design is possible. The most prevalent distresses, as found by extensive condition surveys done on JCP in Texas, are the following (in order of occurrence frequency):

(1) Transverse cracks
(2) Spalling
(3) Corner breaks
(4) D-cracking

The subject of distress prediction is a topical one in pavement analysis circles, mainly because of the complexity of the problem and the consequent inability to develop accurate, field-proven models. Researchers are forced to fall back to regression models based on simplified analyses of large-scale field results. Models often use local condition survey databases and/or AASHO Road Test data. All of these empirical type distress predictions have very limited scope of application, which are only applicable to the conditions and design data as represented by the various surveyed sections. In light of the discussion above, this study investigates development of distress models applicable to pavements in Texas. Thus, transverse cracks, spalling, faulting, corner breaks, and D-cracking are reviewed.

Transverse cracking

Theory and model development: Crack spacing, represented by the average value for a section of pavement, decreases with increasing cumulative traffic, as illustrated in Figure 6.1 (Ref 3). The figure implies that after an initial crack spacing is reached during the curing period, the mean crack spacing decreases asymptotic to the final crack spacing owing to the additional influence of traffic and continued environmental effects. There are two mechanisms by which the additional cracks develop: instant cracking owing to stresses developed during a low pavement temperature period after curing (possibly combined with a vehicular load), and fatigue of concrete subjected to the combined stresses owing to traffic and environmental effects. Modeling fatigue behavior is not a simple problem, because stresses vary significantly for every passing vehicle, while environmental effects have daily and seasonal cycles. Attempts have been made to solve the problem by using Miner's principle (Ref 29), as expressed by Equation 6.1.

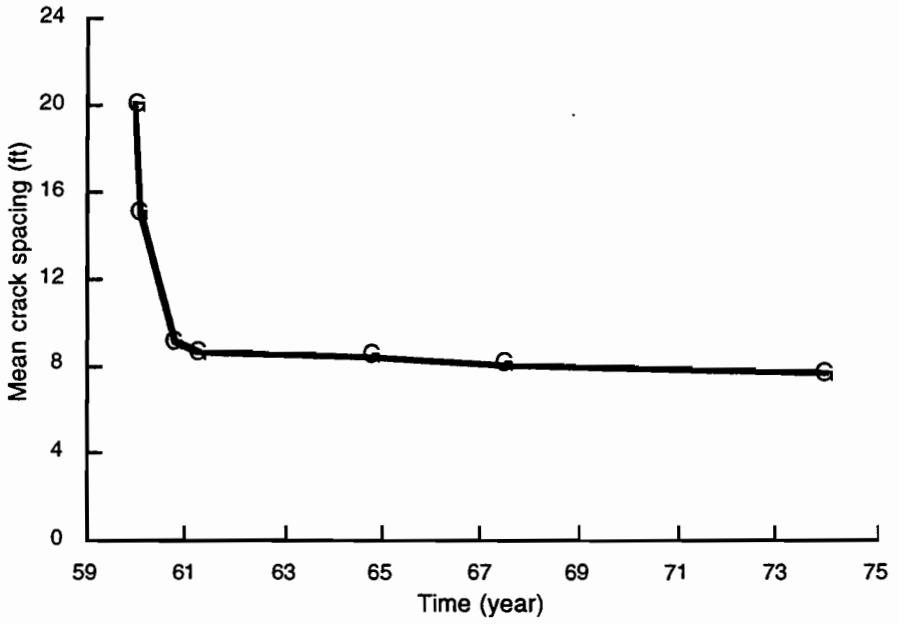

1 ft = 0.305 m

Figure 6.1 Decreasing mean crack spacing over time for CRCP (Ref 3)

$$CI = \sum_i \sum_j \sum_k \frac{n_{ijk}}{N_{ijk}} \tag{6.1}$$

where:

CI = cracking index (pavement cracks when CI=1),
i = counter for the seasonal variance,
j = counter for the time of day,
k = counter for the load type,
n = number of applied loads, and
N = allowable total loads before cracking.

A cumulative cracking index is calculated for the entire design period, with designs adjusted until the value is less than one. This study proposes a simple approach: all vehicle loads are considered stationary and are expressed as 8,000 kg (18,000 lbs) equivalent single axle loads (ESALs) by load equivalency factors. Concrete stress caused by environmental effects is taken as the average stress between that calculated for the minimum and maximum temperatures. Vehicular stress for the interior loading condition is calculated using Westergaard's equations and then superimposed on environmental stress. The fatigue equation developed by the American Concrete Institute (ACI) and reported by Yoder and Witczak (Ref 6) determines the load repetitions before failure (Eq. 6.2):

$$SR = \frac{\sigma}{f} \tag{6.2}$$

where:

SR = stress ratio (applications before failure found in a published table of stress ratios versus maximum applied loads before cracking),
σ = applied tensile stress (vehicular and environmental), and
f = concrete tensile strength.

Allowable repetitions are found in a table (Ref 6) that lists repetitions versus stress ratios. The stress ratio is influenced by the applied stress and concrete tensile strength only, as is apparent from Equation 6.1. Applied stress remains constant when ESALs are used to calculate the stress from traffic loading. In a study of in-service pavement fatigue in Texas (Ref 30), fatigue curves or S-N curves were developed by indirect tensile testing of cores taken directly from constructed pavements. Relations varied slightly from site to site. A conservative relation between fatigue life and stress-strength ratio found by the Crumley and Kennedy is selected for use in the following discussion and incorporated in JRCP-6 (Eq. 6.3):

$$\text{Log } N_f = -0.092\ SR + 9.98 \qquad (6.3)$$

where:

N_f = Repetitions to failure.

It is stressed that this is a rough estimate based on one study only. Factors such as the effect of magnitude of variation in stress on the relationship, the existence of a fatigue limit and the sequence of loading, for example, have been ignored. The equation is included to provide a starting point for future improvements.

In order to simulate gradual cracking over time, as represented in Figure 6.1, the variance of tensile strength may be used. Equating confidence levels of tensile strength values to percent of slabs cracked, a distribution of cracked slabs versus load applications can be derived. For example: if a high confidence level represents a tensile strength for which most test values will be greater than (a small value), this will result in a high stress ratio and a lower number of allowable applications. In this way, a distribution of cracks, as is represented in Figure 6.2, can be derived.

To illustrate the concept, suppose 18 m (60 ft) JRCP slabs are analyzed. If the environmental analysis predicts a mean crack spacing of 9 m (30 ft) and every slab cracks once, there will be 10 cracks in a 180-m (600-ft) section. If the stress ratio predicts 50 percent cracks after 500,000 ESALs, it means that half of the 9-m (30-ft) slabs will be cracked, translating to twenty 4.5-m (15-ft) slabs and ten 9-m (30-ft) slabs. The mean crack spacing will, therefore, be 6 m (20 ft). Crack spacing development with time is now possible. The described methodology is incorporated in the JRCP-6 transverse crack prediction module.

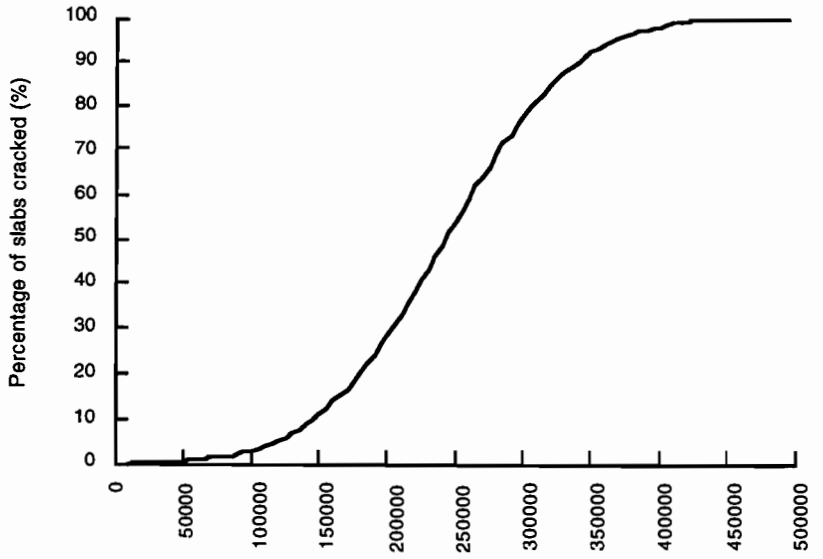

Figure 6.2 Transverse crack development by stochastic and fatigue principles

Database information: Investigation of transverse crack data retrieved from the rigid pavement database revealed the following:

(1) Average JRCP slabs ranging from 4.5 m (15 ft) to 18 m (60 ft) in length have one to four cracks each (Figure 6.3). These cracks are believed to mostly originate from initial cracking, with additional cracking resulting from concrete fatigue.

(2) PJCP sections (all 4.5-m, or 15-ft slabs) have less than 0.5 cracks per slab (Figure 6.4). The cracking is attributed to progressive failure caused by load repetitions.

(3) Cracking is more pronounced in undoweled slabs (Figure 6.5).

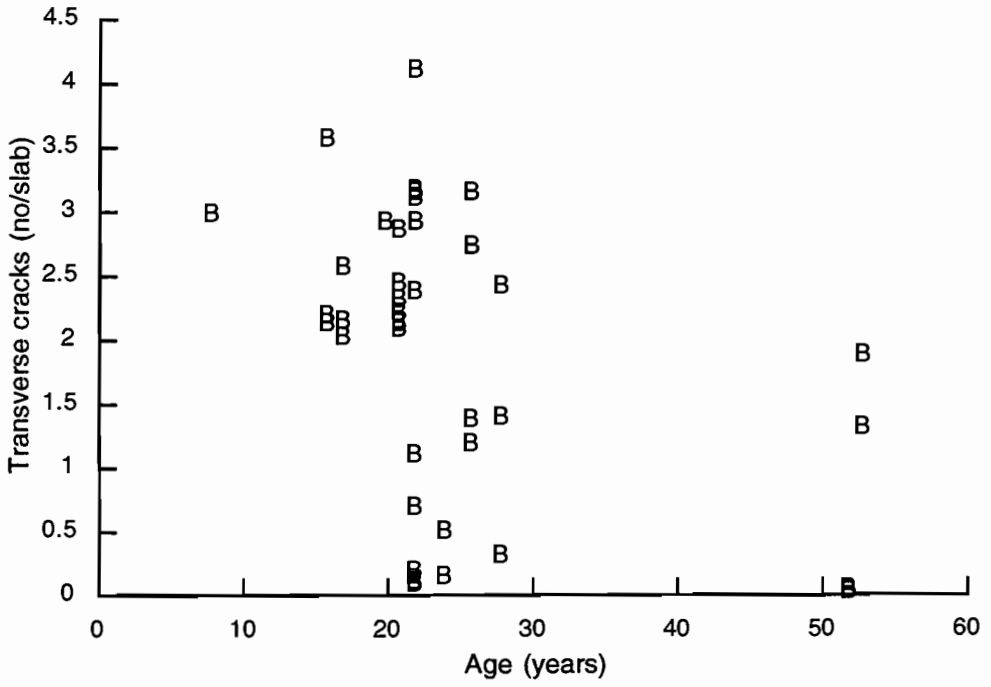

Figure 6.3 Number of transverse cracks per slab in JRCP

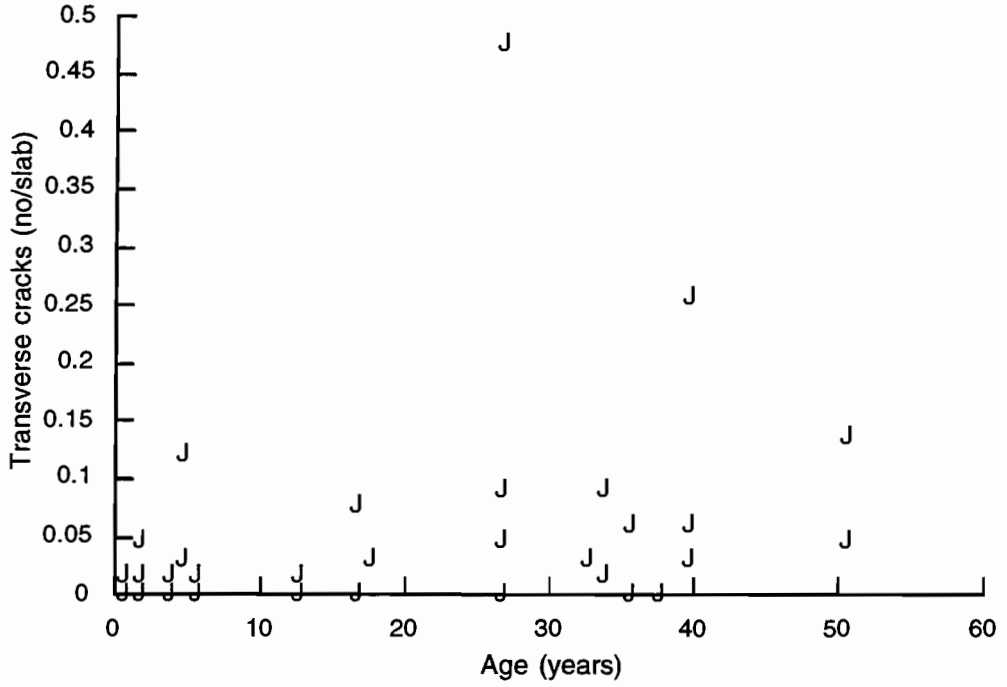

Figure 6.4 Number of transverse cracks per slab in PJCP

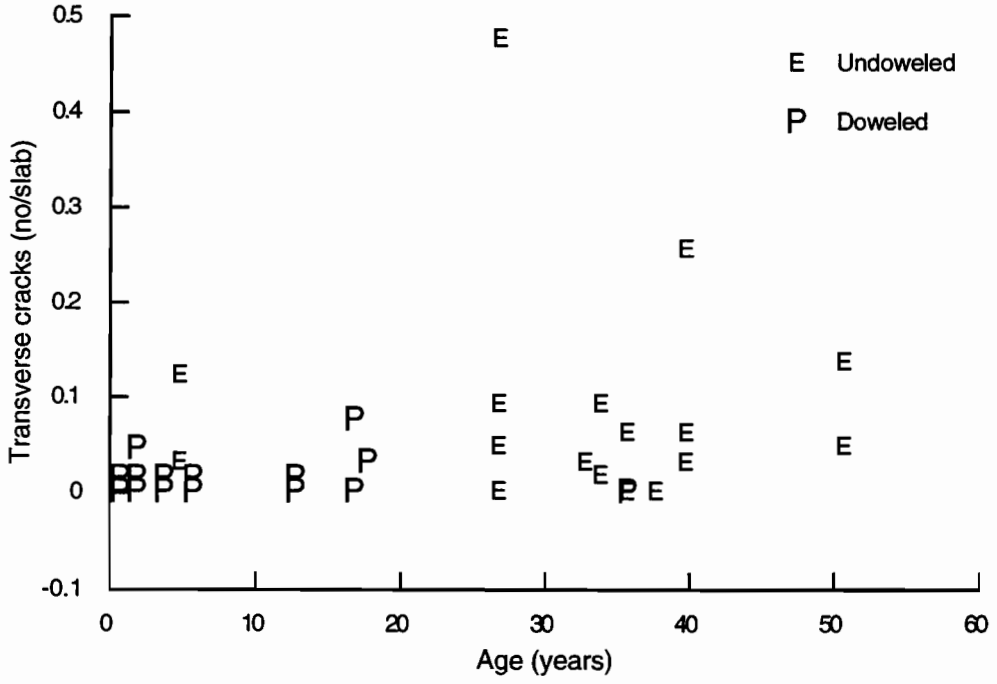

Figure 6.5 Transverse cracking in PJCP per load transfer mechanism

Spalling

Spalling, as was discussed in Chapter 2, is initiated by horizontal delaminations 25 to 50 mm (1 to 2 in) below the surface of the slab (Ref 14). These delaminations, which occur during cracking, develop into spalling under the influences of traffic loading and environmental effects.

Predicting spalling distress, according to Senadheera et al. (Ref 14), is, therefore, a two-step process: (1) predict if delaminations will occur and then (2) predict development of delaminations into spalls over time. At the time of this study, models to predict spalling according to this theory have not yet been completed, though they may be viable for future use as they are developed for Texas conditions. The rigid pavement database was used to make the following preliminary observations about spalling in JCP:

(1) Spalling is more pronounced in sections where siliceous river gravel was used as coarse aggregate for the concrete, as opposed to limestone (Figure 6.6).

(2) Spalling is more common in hot, dry areas of the state (Figure 6.7).

(3) A large number of sections do not show any spalling after up to 50 years of service.

(4) Climatic conditions lead to horizontal plane cracking (delaminations).

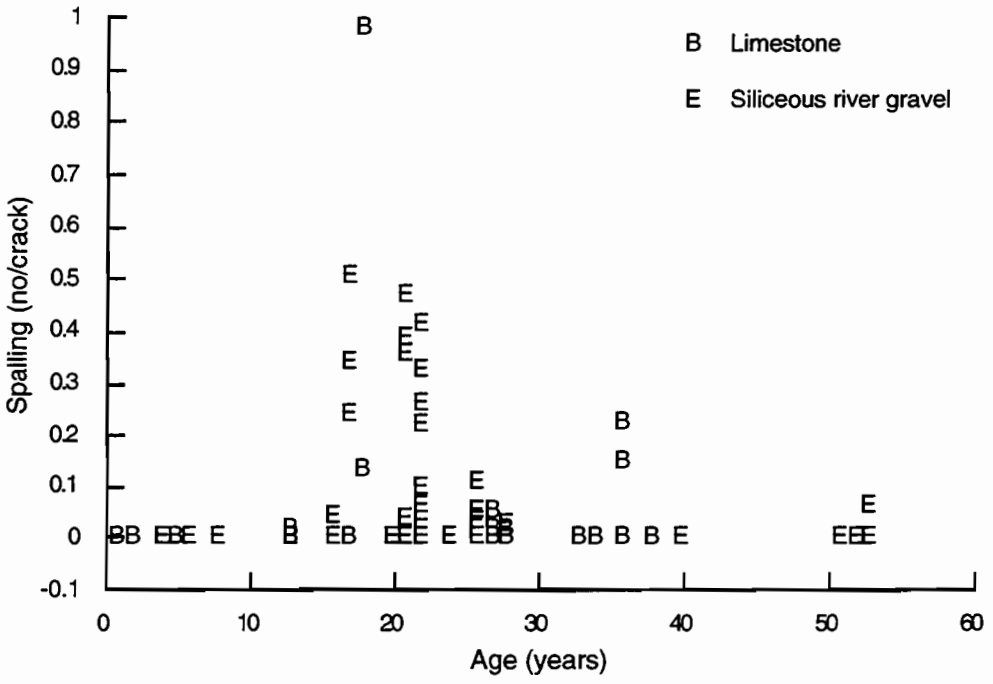

Figure 6.6 Spalling in JCP by coarse aggregate type

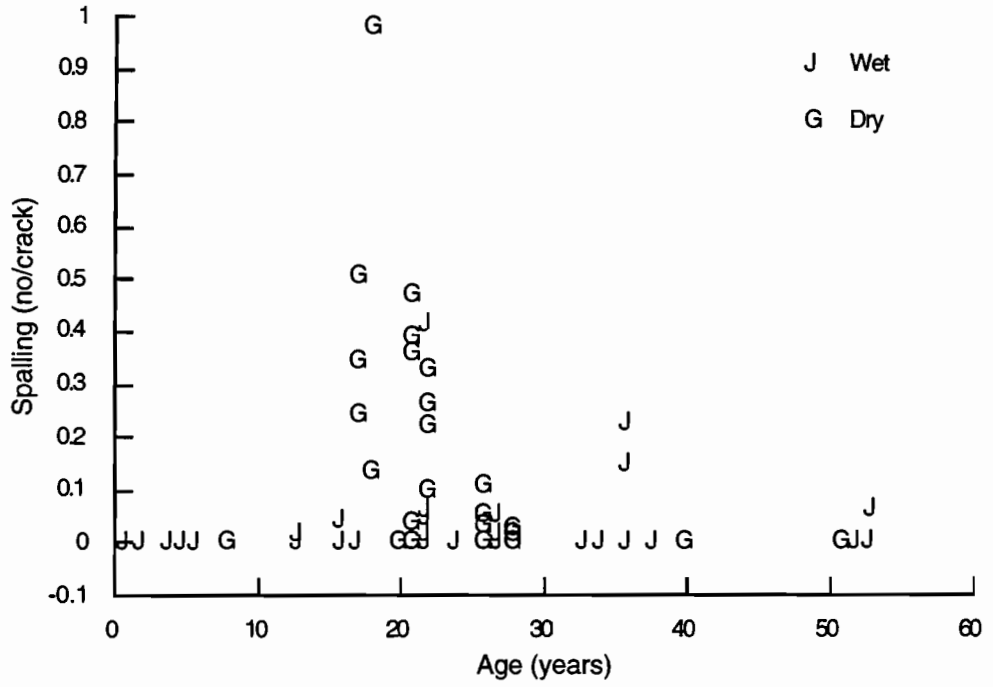

Figure 6.7 Spalling in JCP by climatic region

Faulting

Although faulting is not a common distress type in Texas (since most pavements have doweled transverse joints), it is included as a distress because it is difficult and expensive to repair when it does occur. Condition survey data may be used to develop a regression model in the future. The high occurrence of faulting in JRCP sections surveyed is mostly a result of cement-treated bases (CTB). The large slab-subbase friction caused by this type of layer increases stress in the steel at the cracks, compromising load transfer and resulting in faulting development. These results, shown in Figure 6.8, illustrate the importance of calculating steel stress at cracks. If the steel stress at the crack and crack widths, which controls water ingression and oxidation of reinforcing, are controlled, faulting can be avoided at cracks in JRCP.

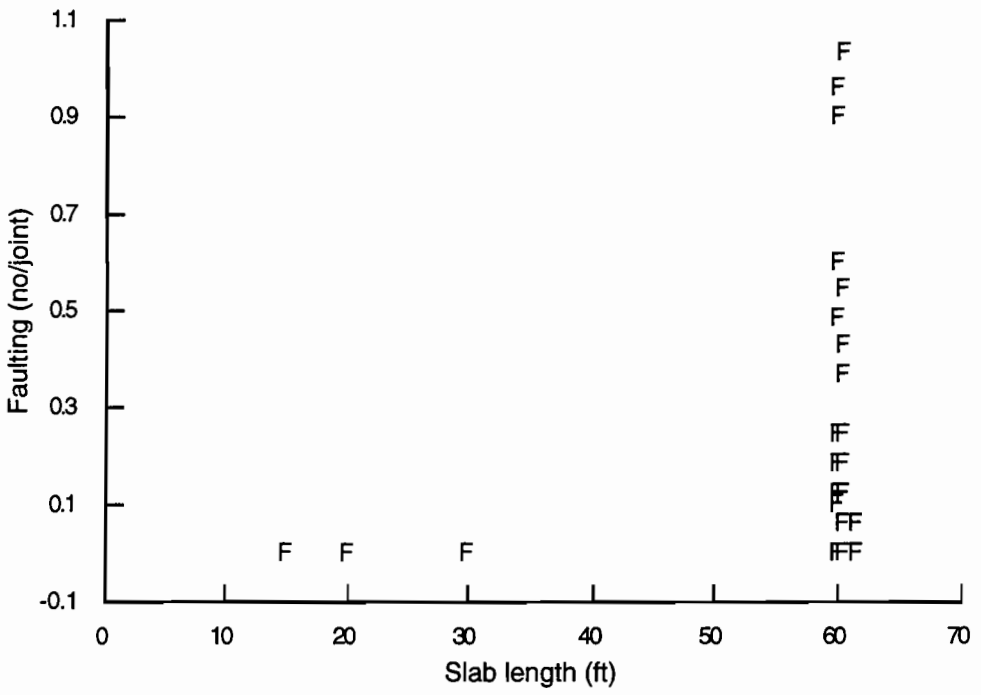

1 ft = 0.305 m

Figure 6.8 Faulting in JRCP

Corner breaks

Similar to transverse cracking after the curing period, corner break distress prediction is based on fatigue principles. The stress leading to cracking is, however, not as dependent on environmental stresses, as calculated by the methods described in Chapter 5, since environmental stresses at the edge of the pavement are low. For this study, the environmental stresses are ignored and only vehicular loading is taken into account for distress prediction of corner breaks. Stress ratios are calculated using the edge loading condition, and relevant strength as determined for transverse cracking. The result is a progressive increase of corner breaks as load applications increase, coupled with the normal distribution of tensile strengths. The following is concluded from the rigid pavement database:

(1) Available data suggest that corner breaks are more prevalent in undoweled pavements (Figure 6.9).

(2) Corner breaks occur more often in JRCP than in PJCP (Figure 6.10).

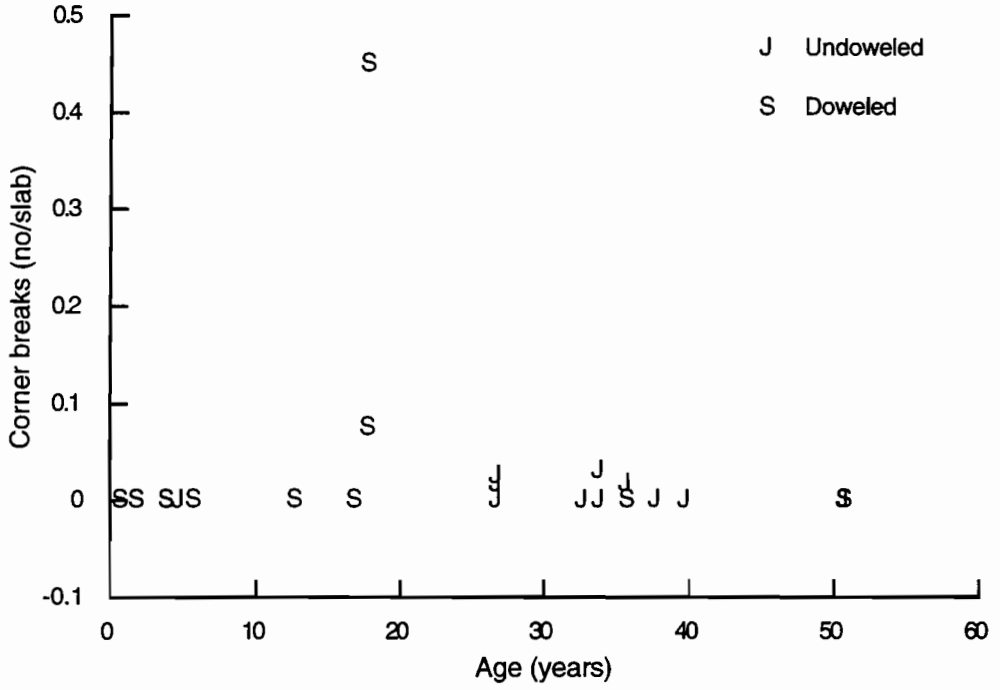

Figure 6.9 Corner breaks in PJCP by load transfer type

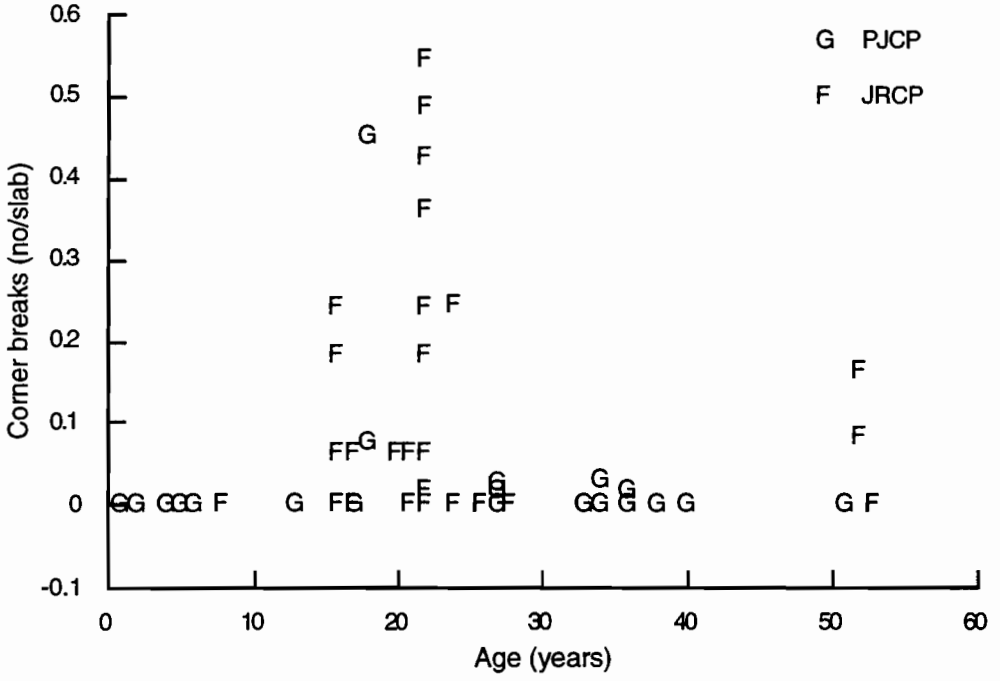

Figure 6.10 Corner breaks in JCP

D-cracking

D-cracking distress is not predicted, as it can be prevented by coarse aggregate specifications. However, a few comments on the database information:

(1) There is no clear distinction between frequency of occurrence in limestone and siliceous river gravel sections.

(2) JRCP sections show more D-cracking that PJCP (Figure 6.11). Dwiggens et al. (Ref 13), however, conclude that D-cracking does not seriously affect JRCP performance.

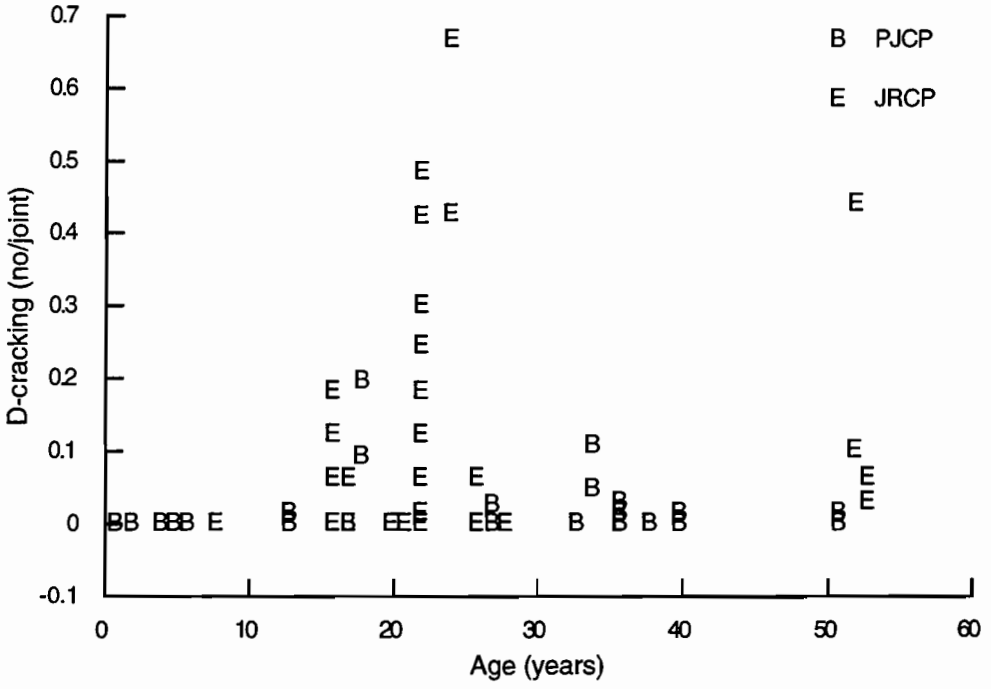

Figure 6.11 D-cracking in JCP

Summary

A database that is limited in scope has been used to derive the conclusions above. However, a starting point for improved modeling and discussion of future improvements has been provided. Cracking and corner break models based on mechanistic and stochastic procedures are proposed and should be further calibrated. Spalling models based on thorough investigation, theoretical analysis, and distress data for the Texas conditions are referred to and will be available for use in the near future. Faulting prediction will be unnecessary if proper design and analysis techniques prevent loss of load transfer at joints and cracks. Finally, D-cracking can be prevented by specifications restricting the use of detrimental aggregate.

CHAPTER 7. JRCP-6: APPLICATIONS AND SENSITIVITY ANALYSIS

This chapter discusses JRCP-6 program applications, including input and output options. A sensitivity analysis of the subroutines MODEL1 and MODEL2 are included to give the user an indication of expected results. Also included are examples in which the slab cracks according to the three possible scenarios (no crack, one crack, and three cracks). Finally, JCP field data are calibrated to verify stresses computed for the uncracked case.

Hardware required to run JRCP-6 include a IBM PC-compatible computer, an 80386 processor, a processor speed of 20 MHz, and a numeric co-processor. Microsoft DOS version 5.0 with a color video graphics adapter (VGA) is recommended.

APPLICATIONS

The JRCP-6 program was written to analyze jointed reinforced concrete pavements. It is the opinion of the authors that JRCP should not crack at more than three points per slab during early age. For this reason, the program does not analyze a pavement if it detects more than three cracks caused by environmental effects. In such situations, the user will be forced to change the geometry, tensile strength of the concrete, or steel parameters to make full analysis possible. The example problems and sensitivity analyses reported in this chapter provide the inexperienced user with acceptable input parameter ranges.

An additional application, which is less obvious to the user, is for plain jointed concrete pavement (PJCP). This type of pavement, which has no reinforcement, can be analyzed by JRCP-6 by setting the steel percentage to zero. Analysis will only be successful if the slab does not crack. When a crack occurs, the program analyzes the interaction between concrete and steel at the crack; an error will result if no steel is present. Analysis of concrete stresses and displacements can still, however, be performed if the user ensures no cracking by setting the tensile strength at an unusually high level. The user can then manually check calculated stresses against true tensile stresses in order to reach an optimum slab length. Joint spacing can be established that will ensure no further environmental cracking for the conditions analyzed. This is the approach taken in the calibration section reported later in this chapter. During analysis of JCP, the program uses only the MODEL1 subroutine to calculate stresses and displacements.

INPUT AND OUTPUT

User friendly input screens guide the user through the required input variables required to analyze JRCP. The software for these input drivers was developed at the Center for Transportation Research. A screen-by-screen explanation of input requirements is given below; examples of actual screens are provided in Appendix B.

Input screen 1: Introduction

An introductory screen identifies the program as JRCP version 6. No user input is required.

Input screen 2: Problem number and description

The first user input screen identifies the problem for future file reference (and for use with hard copies of the input and output). A problem number and short description are requested.

Input screen 3: Steel properties

(1) Percent reinforcement: the amount of reinforcement present in the slab expressed as a percentage of the cross sectional area of the concrete slab.

(2) Type of reinforcement: a distinction is made between tied, deformed reinforcement and welded mesh. The distinction is required because welded mesh reacts differently when a concrete slab cracks. It is assumed that tied transverse reinforcement provides no resistance to concrete sliding across the steel in the bond development zone. Welded steel mesh, however, is assumed to provide total load transfer at the first encountered transverse steel bar. The solution algorithm for the bond development length, therefore, checks for the mesh input flag and sets the bond development length equal to the mesh spacing, if mesh is used as reinforcement.

(3) Mesh spacing: This field becomes active only if mesh reinforcement is specified in the previous input field.

(4) Bar diameter: the diameter of a single longitudinal reinforcement bar.

(5) Elastic modulus: Young's elastic modulus for the longitudinal reinforcement.

(6) Thermal coefficient: the thermal coefficient of expansion and contraction for the steel.

Input screen 4: Concrete properties

(1) Pavement thickness.

(2) Thermal coefficient: thermal coefficient of expansion and contraction for the concrete.

(3) Slab length: the total length of the uncracked slab from transverse joint to transverse joint.

(4) Confidence level for tensile strength: the level of confidence the user requires for the calculated crack spacing. If the user judges the tensile strengths input in the fields below to be accurate, a confidence level of 50 percent will result in the mean value being used for stress versus strength checks. If the user wants to be certain cracking will not occur at spacing less than that calculated by the program, a high confidence level (e.g., 99 percent) should be input. This feature allows the user to set the level of certainty for the crack prediction. Typically, a high level will be chosen for cases where cracking will be critical (PJCP, for example).

(5) Tensile strength coefficient of variance: the standard deviation expected or known for the tensile strength of the concrete divided by the mean value for the same population. These values are taken from the 28-day test results and allows for a stochastic element to be introduced into the calculations, as explained in Chapter 3.

(6) Aggregate type: the eight most commonly used aggregates for concrete pavements in Texas are listed. The user may also select "other" for blends of aggregates or non-listed aggregates. The aggregate type selected is used in a calculation model for time-dependent properties. The shape of the curve for properties versus time is therefore set by the aggregate type selected, and the user is allowed to change 28 day values. However, by selecting "other," the user is allowed to override the shape and magnitude and inputs values for 1-, 3-, 7-, and 28-day properties.

(7) Time-dependent concrete properties: tensile strength, compressive strength, elastic modulus, and drying shrinkage are given by selecting the aggregate type; these can be overridden in the highlighted fields.

Input screen 5: Environmental factors

(1) Concrete setting temperature: the concrete temperature at which solidification or setting takes place. This is the stage at which, after hydration has commenced, the concrete slab is first able to resist internal and external forces.

(2) Initial analysis period: sets the number of days the environmental analysis runs, starting at day one. For each of these days, the program checks stress against strength and allows cracking to occur when stresses exceed strengths. Reducing the number of analysis days cuts down running time. This is recommended where constant ambient temperatures are expected for the entire 28 days, as cracking is most likely to occur during the first few days.

Note: the initial analysis period does not need to be specified in terms of days. The user can change the time units to suit the application; however, caution must be used for the time-dependent concrete properties that need to be changed to the same units of time. For example, if a sawing analysis is performed, the user wants to know when to saw the joints in order to prevent uncontrolled cracking and still ensure workable, stiff concrete. This type of analysis will cover the first 48 hours, but the concrete properties will have to be input for the same time period.

(3) Annual maximum and minimum ambient temperature: the yearly minimum and maximum ambient temperatures expected for the area in which the pavement is located.

(4) Daily minimum ambient temperatures before full strength: the daily minimum ambient temperature starting at day one after construction and extending for the period input in field (2) above. The ambient temperature is converted to mean pavement temperature by a simple algorithm developed from field data (Ref 8).

Input screen 6: Parameters for linear slab-base friction relationship

(1) Maximum friction force: the maximum friction force achieved during sliding, as explained in Chapter 2 and as listed in Table 2.1.

(2) Movement at sliding: the point on the force-versus-movement curve where the maximum friction is reached; these are listed for different subbase materials in Table 2.1.

Input screen 7: Traffic loading parameters

(1) Equivalent single axle wheel load: the load used to calculate traffic-induced stresses; also, all applications to various levels of failure are expressed as multiples of these loads.

(2) Tire pressure: the tire pressure is used to calculate the loaded area.

(3) Modulus of subgrade support (k): defines the elastic support provided to the slab by the subbase and subgrade.

Input screen 8: Iteration and tolerance control

(1) Maximum iterations allowed: a parameter from which all unlimited iterations are controlled to prevent infinite loops. A value of 10 is recommended.

(2) Relative closure tolerance: a parameter that controls all convergence checks during iterations. A value of 5 percent is recommended.

Note: these two parameters control the accuracy and subsequently the computation time. When error messages indicate convergence was not achieved, accuracy might need to be reduced in order to achieve results.

(3) Force crack? an option to force the one-crack situation. Useful when crack initiators are used or a crack is expected as a result of factors outside the scope of the program.

Input screen 9: Execution options

This is a control screen that allows the user to start the analysis for the data set in memory, recheck or edit data, save the input file, or exit the program. At any time during the input phase the user can page through previous screens using the page-up or page-down keys. Control to move between fields is provided by the arrow keys or the tab button. The space bar is used to select fields where more than one option is available. A user menu to save or recall current input files is accessible at any time by pressing the F1 key. Output screens provide a graphically enhanced summary of the program output. The following are found on respective output screens:

Output screen 1

In the top left corner of the screen is a problem number and legend for the graph on the right. In the bottom left side of the screen is a summary of the problem definition. The graph on the right is a plot of concrete stress and strength development versus time during the initial analysis period. Dates when the slabs crack can be read off the graph by locating points where the stress

curve intersects the strength curve. When the first crack occurs, stress is transferred to the steel and concrete stress is reduced to a lower value; the graph will show a discontinuity at this point. If three cracks occur, there are effectively four slabs to analyze between transverse joints. Two of these are eliminated from the analysis procedure as a result of to symmetry. The remaining "CRCP" slab and "free ended" slab continue to develop separate stresses; they are both represented in the graph.

Output screen 2

Once again the top left corner identifies the problem and contains a legend for the graph on the right. Below that is a field containing transverse joint widths for the maximum and minimum annual temperature conditions. These maximum and minimum values can be used for transverse joint design. In the bottom left corner is a summary of variables at the cracks. Crack widths and steel stresses at the cracks are presented. The user can toggle between first ("CRCP slab") and second (free slab) cracks in the three crack case by using the F2 key. The graph on the right illustrates concrete stress versus distance from the transverse joint to the center of the original slab. Only half the slab is shown, because symmetry applies to all three cracking cases.

Output screen 3

This screen shows distress prediction information provided as a function of load applications. The user can convert these applications to time if the distribution and growth rate of traffic is known for the design period and is converted to equivalent single axle wheel loads used as input in screen 7 of the input module.

SENSITIVITY ANALYSIS

A sensitivity analysis of the respective environmental analysis models — MODEL1 and MODEL2 — was completed during development of the program. These sensitivity analyses illustrate the effect that various input parameters have on the pavement behavior and act as logic tests for the respective models. The user is reminded that these models form part of the total analysis program and do not represent outputs for the JRCP situation as a whole. Results from this analysis are restricted to the assumptions and application restrictions of the respective models, as explained in Chapter 2. Restrictive boundary conditions are presented in Figures 7.1 and 7.2.

Each sensitivity analysis is based around a base case scenario. For this scenario, input parameters are selected to represent a typical practical situation. Input variables are then assigned with high and low values representing the ranges found in practical applications. Multiple analyses are then completed by changing only one variable at a time. Relevant output parameters are summarized, respectively, in Tables 7.1 and 7.2.

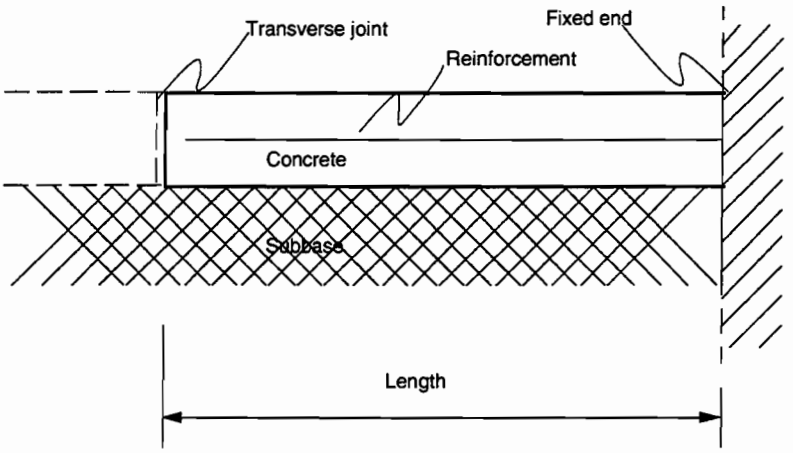

Figure 7.1 MODEL1 geometric model

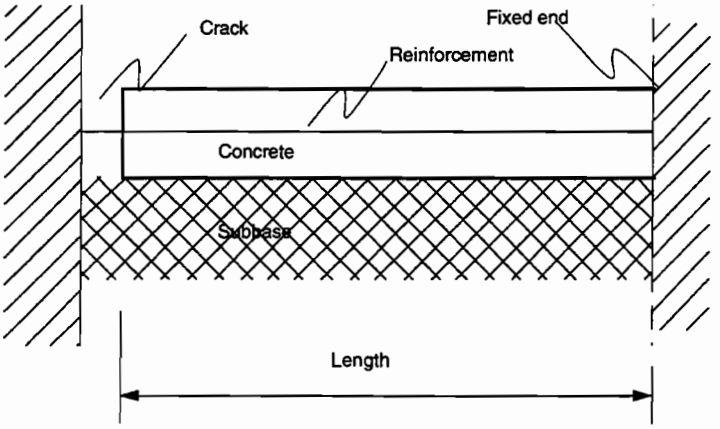

Figure 7.2 MODEL2 geometric model

MODEL1

Relevant input parameters for the base case are as follows:

(1) Percent steel reinforcement: deformed bars 0.1 percent
(2) Bar diameter: 12 mm (0.5 in.)
(3) Elastic modulus: 200 GPa (29,000,000 psi)
(4) Steel thermal coefficient: 2.8 micro strain/°C (5 micro strain/°F)
(5) Pavement thickness: 250 mm (10 in.)
(6) Concrete thermal coefficient: 2.8 micro strain/°C (5 micro strain/°F)
(7) Slab length: 23 m (75 ft)
(8) Aggregate type: Limestone
(9) Time-dependent concrete properties: default for limestone

(10) Temperature differential: 36°C (20 °F)

(11) Maximum friction force: 21 kPa (3 psi)

(12) Movement at sliding: 0.5 mm (0.02 in.)

Results indicate that concrete stress is most sensitive to slab thickness, slab length, and slab-subbase friction. Joint width is controlled mostly by slab length, temperature differential and thermal coefficient, and drying shrinkage of concrete. It is interesting to note that sliding of the slab is featured prominently in the few cases considered; for example, in the case of thermal coefficient and temperature results, joint widths increase significantly while concrete stress remains almost constant.

MODEL2

Relevant input parameters for the base case are as above for the MODEL1 sensitivity analysis, except for the following: Slab length: 6 m (20 ft), and concrete thermal coefficient: 3.3 micro strain/°C (6 micro strain/°F).

Table 7.1 Sensitivity analysis for MODEL1

Variable	Values	Maximum concrete stress (psi)*	Joint width (in)**
Base case	**as above**	132	0.25
Reinforcement (%)	**0.0**	127	0.25
	0.3	141	0.25
Slab thickness (in)**	**5**	256	0.23
	15	90	0.26
PCC thermal coefficient	**3**	129	0.22
(micro strain/∞F)#	**8**	135	0.30
Slab length (ft)##	**15**	23	0.05
	75	267	0.47
Drying shrinkage	**100**	123	0.16
(micro strain)	**400**	142	0.43
Temperature (∞F)#	**10**	129	0.21
	50	135	0.39
Maximum friction,	**1, 0.02**	48	0.26
movement at sliding	**2, 0.02**	83	0.26
(psi, in)*, **	**6, 0.04**	234	0.24
	2, 0.003	95	0.26
	6, 0.01	267	0.23

* 1 psi = 6.9 kPa
** 1 in = 25.4 mm
# 1 °F = 1.8°C + 32
1 ft = 0.305 m

Table 7.2 Sensitivity analysis for MODEL2

Variable	Values	Steel stress at crack (psi)*	Maximum concrete stress (psi)*	Crack width (in)**
Base case	**as above**	58300	72	0.036
Slab length (ft)##	**10**	39500	48	0.019
	60	105500	155	0.103
Thickness (in)**	**8**	58300	74	0.036
	15	58300	70	0.036
Friction (psi)*	**1**	58400	67	0.037
	5	58200	78	0.036
Concrete (micro strain/∞F)#	**3**	57100	72	0.036
	8	60000	72	0.036
Dry. shrinkage (micro strain)	**500**	76000	103	0.072
	800	88100	126	0.107
Steel diameter (in)**	**0.25**	84400	98	0.036
	1.00	39600	54	0.037
Steel content (%)	**0.3**	55800	189	0.033
	0.6	52100	341	0.029
Temp. diff. (∞F)#	**10**	52000	64	0.029
	30	64000	80	0.043

* 1 psi = 6.9 kPa
** 1 in = 25.4 mm
# 1 °F = 1.8°C + 32
1 ft = 0.305 m

Table 7.2 reveals that steel stress at the crack, maximum concrete stress, and crack width are sensitive to the slab length. The algorithm for finding the fixed point for cracked cases of JRCP is, therefore, important in determining final solutions. Also, of practical importance, is the effect of steel diameter. Increasing steel diameters without increasing steel content effectively reduces steel stress at the crack and maximum concrete stress without influencing crack widths. On the other hand, maximum concrete stress is sensitive to steel content. Steel, therefore, plays a significant role in determining design parameters in cracked JRCP. Crack widths are largely influenced by drying shrinkage and temperature differentials, while these parameters do no seem to have an effect on steel or concrete stress. The crack width can, therefore, be controlled in design by reducing shrinkage and setting temperatures.

EXAMPLE PROBLEMS

Three examples representing three of the possible outcomes for the JRCP situation in terms of environmentally induced transverse cracking are presented below. Input and output are summarized in Appendix A.

CALIBRATION

Construction data and design data for a plain jointed concrete pavement are used to verify the early-age analysis part of the program. The project was constructed in Ticuman, Mexico, near Mexico City. It was designed by Transtec consulting engineers from Austin, Texas, and was constructed by Interstate Highway Construction (USA). The project is atypical in that no transverse joints were sawn. The pavement was, therefore, left to crack by its own internal mechanisms. A distribution of slab lengths, consequently, resulted at an early age and can be used to calibrate a part of JRCP-6. An extensive set of concrete property test data and ambient temperature on site data for the period directly after construction make this project ideal for a calibration exercise.

Design data

A 175 mm (7 in) thick PJCP 6.5 m (21.3 ft) wide was constructed on an existing asphalt concrete pavement; no transverse joints were sawn. Complete sets of data are available for concrete poured in the period 9/23/1993 through 10/2/1993. Curing temperatures and minimum and maximum ambient temperatures were recorded daily; these are summarized in Figure 7.3.

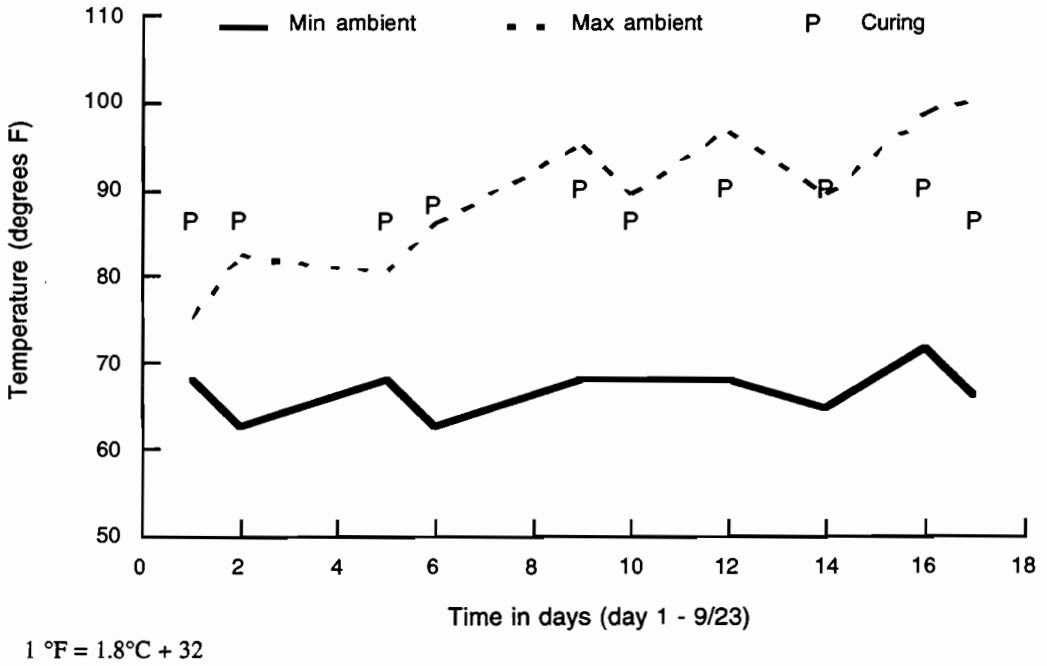

Figure 7.3 Daily ambient and curing temperatures

Material characteristics

The cement-rich concrete mix used contained coarse aggregate from crushed igneous rock from the region. Compressive and flexural strengths were measured at 1, 3, 7, 14 and 28 days (Table 7.3).

Tensile strength can be derived from flexural strength by a conversion factor of 0.8 to 0.9. JRCP-6 was used to select a coarse aggregate type that best suited the available data (granite). Values for elastic modulus and drying shrinkage for the concrete were assumed from the granite database. Table 7.4 summarizes assumed values.

A thermal coefficient of expansion of 3.9 micro strain/°C (7 micro strain/°F) was assumed for the concrete. Asphalt subbase friction values of 20 to 28 kPa (3 to 4 psi) at 0.5 mm (0.02 in.) movement were selected from Table 2.1.

Table 7.3 Average values for concrete characteristics measured for concrete pours between 9/23/1993 and 10/2/1993

Day	Compressive strength (psi)*	Flexural strength (psi)*
1	1579	341
3	3102	398
7	-	526
14	3955	-
28	4695	683

* 1 psi = 6.9 kPa

Table 7.4 Derived and assumed values for concrete properties

Day	Tensile strength (psi)*	Elastic modulus (millions psi)*	Drying shrink. (micro strain)
1	273-303	2.3	27
3	318-354	3.3	73
7	421-468	3.5	146
28	546-608	3.5	299

* 1 psi = 6.9 kPa

Setting temperature and time of concrete placement were not recorded. Curing temperature was assumed to be the temperature of the concrete at placement. If hydration, therefore, occurs after the recording of temperature, setting temperature was estimated to be between 31 to 42°C (87 and 107°F).

Crack spacing distribution

A crack survey was completed on 10/8/1993, six to fifteen days after the respective concrete pours. The average minimum ambient temperature during that period was 19°C (66°F). Crack spacing distribution for the concrete poured in the period analyzed is shown in Figure 7.4.

The mean crack spacing was 18 m (58 ft), with a variance of 343 m (757 ft). It is interesting to note that the distribution is skewed towards the large crack spacing.

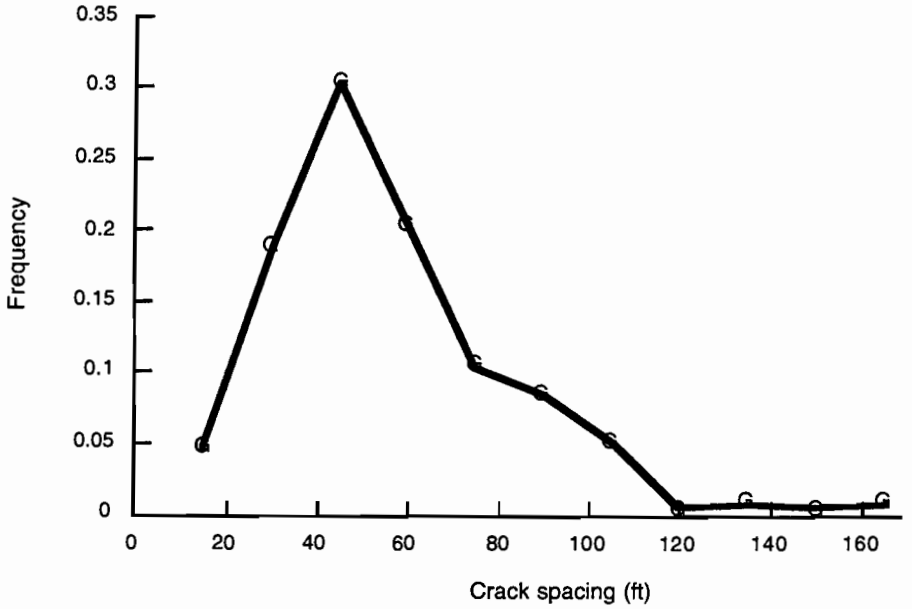

1 ft = 0.305 m

Figure 7.4 Crack spacing distribution

Modeling results

A slab length of twice the mean crack spacing was analyzed to compare to tensile strength values. If values were equal, the program's ability to predict mean crack spacing would be validated. Setting temperature and friction variables were used in a mini-factorial analysis for an initial analysis period of 15 days. Results are summarized in Table 7.5.

Table 7.5 Analysis results

Variable	Value of variable	Concrete stress (psi)*
Setting temperature	87	237-280
(¤F)#	97	261-284
	107	273-286
Friction (psi*, in)**	3, 0.02	237-280
	4, 0.02	335-376

* 1 psi = 6.9 kPa
** 1 in = 25.4 mm
# 1 °F = 1.8°C + 32

It can be seen that concrete stress predictions are close to tensile strength values, and that cracking will most probably occur during the first several days. The following theory could therefore be postulated: A slab length equal to the total concrete pour length originally existed. As the PCC temperature dropped, stresses developed to the point where strength was exceeded and the slab cracked. The process continued in all resulting slab lengths greater than the mean crack spacing. Once sections of cracked slab length were smaller than the mean crack spacing, stresses would no longer exceed strengths and the slabs would remain uncracked. A slab with a length equal to 40 m (125 ft) would therefore crack, resulting in two 20 m (62 ft) slabs, while a slab with a length of 30 m (90 ft) would remain uncracked. When material variability is added to the scenario, the distribution of cracks could be explained.

Summary

JRCP-6 effectively modeled a PJCP on asphalt subbase. While it is an encouraging result, it offers no proof that the program models all situations correctly. Calibrations need to be performed for different designs and environmental conditions. Most urgent is a calibration of a JRCP case where cracking is expected within the curing period.

CHAPTER 8. DESIGN

INTRODUCTION

Design models are restricted by the quasi-mechanistic-empirical methodology used for their development. These restrictions include the scope of gathered field data used in their development. Designers should extrapolate beyond these margins using extreme caution. This report does not include the development of a design model, but provides an analysis model as a tool for development and discusses the methodology to be used in this process. Design is essentially the reverse process of analysis. When analyzing pavements, all inputs concerning the geometry, reinforcement, subbase type, and joint spacing are given. The user requires output in the form of stresses and displacements for the given pavement, which represent the pavement response to a set of environmental and traffic conditions. Reversing the process consists of limiting inputs for the pavement in terms of stresses, displacements and distresses, while the user requires the geometry, reinforcement, and joint spacing as output for this given set of conditions.

Repetitive analyses, covering an input factorial that includes most possible ranges for investigation, will lead to a database of information concerning analytical response of JCP. When this information is statistically analyzed and connected to condition surveys and to time or traffic histories of pavement distresses, models covering design and distress prediction can be developed. Design models are, therefore, based on mechanistic and empirical techniques and can be continuously calibrated as new information becomes available.

THICKNESS

The thickness of concrete pavements is largely determined by vehicular loading conditions, limiting load associated distresses, and load transferring devices. Where load magnitudes are high, pavements tend to be thicker, as is seen in airport runways and aprons, while efficient load transfer at cracks (as found in CRCP) eliminates critical corner and edge loading conditions, allowing thinner slabs to be constructed. Furthermore, boundary conditions, such as tied concrete shoulders, increase load carrying capacity, reducing required slab thickness.

Although theoretical analyses may predict required thicknesses accurately, design is restricted to construction tolerances. Therefore, thicknesses typically vary in increments of 25 mm (1 in.), simplifying design by rounding to the conservative thickness. Typical thicknesses for concrete pavements are as follows:

(1) Airport pavements (JCP) 380 to 500 mm (15 to 20 in.)

(2) JCP without dowels 250 to 380 mm (10 to 15 in.)

(3) JCP with dowels 250 to 300 mm (10 to 12 in.)

(4) JRCP with dowels 200 to 300 mm (8 to 12 in.)

(5) CRCP 150 to 250 mm (6 to 10 in.)

These thicknesses have been proven to be successful by full-scale projects and are seldom departed from. The designer usually has an idea, based on experience, of what thickness will be required, and will use a design program simply to confirm and refine initial estimates.

REINFORCEMENT

Designing reinforcement for concrete pavements is a trade off process between crack spacing and load transfer at cracks. High percentage steel results in small crack widths and good load transfer but also causes small crack spacing. Steel, therefore, controls behavior at cracks by providing an additional load transfer mechanism and keeping cracks tight, but also increases the possibilities of distresses by developing higher environmental stresses in the concrete slab and increasing the amount of cracks in the pavement. Furthermore, because of total transfer of stress from the concrete to steel when the pavement cracks, high stresses are built up in the steel. It is, in fact, quite possible that steel may yield or fracture at the crack owing to extreme stresses, reducing load transfer to aggregate interlock only, and enhancing probabilities for faulting and pumping. Steel may also be rendered useless to the pavement when corrosion of reinforcing occurs at cracks. Water and deicing materials can infiltrate cracks when crack widths are large, which in turn accelerates oxidation. This unwanted process is curbed by reducing crack widths. Reinforcement design of concrete pavements involves the following aspects:

(1) Crack spacing
(2) Crack widths
(3) Axial tensile stress in steel at the cracks
(4) Load transfer
(5) Bearing stress on the concrete

Typical ranges for the amount of steel reinforcement for JRCP is 0.1 to 0.3 percent by cross sectional area.

JOINTS

Joints to be designed for JCP include transverse expansion and contraction joints and longitudinal joints. Transverse expansion joints are to be designed to allow free contraction and expansion of the slab without allowing water to infiltrate the lower pavement structure. Transverse contraction joints (controlled cracks) relieve stress build up in the concrete; however, the joints can allow water ingression into the pavement. When these joints are not sealed, the widths need to be small enough to prevent excess infiltration. Water in the pavement leads to corrosion of the reinforcement, weakening of the subgrade, and increased probabilities for pumping. Longitudinal joints are only necessary when full lane widths cannot be paved, and joints tie slabs together in the transverse direction to act as one homogeneous, wide slab. The design objectives for longitudinal joints are, therefore, to achieve total load transfer and to keep the joint as tightly closed as possible. Applicable to both transverse and longitudinal joints is the concept of load transfer. Efficient load

transfer at joints reduces the probabilities for faulting and pumping and reduces stress concentrations. Design of all joints, therefore, should fulfill two primary objectives: efficient load transfer and minimum water ingression.

Load transfer

Concrete pavement behavior in transverse and longitudinal directions should be considered equivalent. Contraction and stress build up in the transverse direction is often neglected, but can be handled in exactly the same manner as the longitudinal directions. If transverse reinforcing is simply allowed to run through the longitudinal joint instead of using tie bars, a section of pavement with length equal to the total roadway width and crack spacing at lane widths may be analyzed. In this way, correct steel percentages can be used to achieve small joint widths and tensile stresses below yielding point.

Alternatively, a simple equation suggested by Yoder and Witczak (Ref 6) can be used as a quick method to safely determine required load transferring steel at cracks or longitudinal joints:

$$A_s = \frac{WLf}{2f_s} \tag{8.1}$$

where:

As = required steel per foot width,

W = weight of slab (lb./sq. ft),

L = length of the slab,

f = coefficient of resistance (assumed to be 1.5), and

fs = allowable steel stress.

Transverse or contraction joints in JCP allow the free end of the slab to contract and expand as the pavement temperature decreases or increases. These movements prevent large stress build ups in the pavement and are essential for typical JCP behavior. Large joint widths (18 mm or 0.75 in.) can be encountered as the slab is subjected to varying ambient temperatures.

Without any load transferring device, vehicular loading will cause rapid development of pumping and faulting at transverse joints. Dowel bars are therefore encouraged for all new designs. However, for a joint to operate successfully, joint lockup by misalignment or bonding of dowels to concrete must be prevented. Proper construction techniques and quality control measures are required to achieve well-performing transverse joints.

The design of dowel bar thickness and spacing is based on stress analyses by Timoshenko (Ref 31), adopted by Friberg (Ref 32) for design purposes, and reported by Yoder and Witczak (Ref 6). It is somewhat a trial-and-error method, as dowel bar size and spacing are assumed and resulting maximum bearing stress is compared with the allowable bearing stress. The bearing stress of a dowel bar in concrete according to Friberg (Ref 32) is:

$$\sigma_b = \frac{KP}{4\beta^3 EI}(2+\beta z) \tag{8.2}$$

where:

$$\beta = \sqrt[4]{\frac{Kb}{4EI}} \tag{8.3}$$

K = modulus of dowel support ranges between 81 to 407 GPa/m (300,000 and 1,500,000 pci),

b = diameter of dowel,

E = modulus of elasticity of the dowel,

I = moment of inertia of the dowel,

P = transferred load,

z = joint width, and

σ = bearing stress.

Allowable bearing stress (Ref 6) recommended by ACI Committee 325 can be determined by:

$$f_b = (\frac{4-b}{3})f_c \tag{8.4}$$

where:

fb = allowable bearing stress (psi),

b = dowel diameter, and

fc = compressive strength of concrete.

Dowel design is now possible once the transferred load at each dowel bar is known for every type of vehicle, lateral distribution, and wheel and axle configuration. A wide range of possibilities exist. This report follows the suggestions of Westergaard, as set out by Yoder and Witczak (Ref 6). Maximum load is assumed to be carried by the dowel directly below the load, decreasing linearly to zero at distance 1.8l from the load where:

$$l = \sqrt[4]{\frac{Eh^3}{12(1-\mu^2)k}} \tag{8.5}$$

where:

l = radius of relative stiffness,

E = modulus of elasticity of the concrete slab,

h = thickness of the concrete slab,

μ = Poisson's ratio for concrete, and

k = modulus of subgrade reaction.

Furthermore, the total transferred load by dowel action equals 45 percent of the total load. A single dowel bar may carry transferred load from more than one wheel group if the dowel bar is within 1.8l for more than one load.

Joint width

This section discusses design criteria for joint widths. Separate criteria exist for sealed and unsealed joints. Typically in JCP, only transverse expansion joints are sealed, as shown in Figure 2.8. Expansion joints are usually doweled, and thus slab movement in the longitudinal direction is free. Large movement occurs at transverse expansion joints; therefore, to prevent excessive water ingression, the joints are sealed by a weathering resistant and elastic material, such as neoprene or silicon. Transverse contraction joints (controlled cracks) and longitudinal joints are not typically sealed, for movement is restricted at these joints by reinforcement. However, it is also desired to prevent penetration of water at these joints; if the crack width sought to prevent infiltration is not practical, the joints can be sealed.

Sealed joints: The restriction here is the ability of the sealing material to seal the joint for the range of movement to be expected during field service. The range of movement for transverse expansion or contraction, as well as for longitudinal joints, may be calculated using JRCP-6. A range of 1 to 15 mm (0.1 to 0.6 in) is to be expected. The effect of joint width on dowel design is negligible, as confirmed by Equation 8.2.

Unsealed joints: Two criteria for CRCP crack widths are specified by McCullough et al. (Ref 33). Allowable crack widths are specified based on prevention of spalling and steel and subgrade erosion.

Horizontal stresses in the PCC, which can cause spalling, are proportional to crack widths. Therefore, by limiting crack widths, spalling may be prevented. A study of various CRCP pavements (Ref 33) revealed that, by limiting crack widths to 0.6 mm (0.024 in.), spalling can be controlled. Also, a study of water percolation (Ref 33) found that crack widths of 0.3 mm (0.01 in.) will prevent water ingression, while crack widths of greater than 0.8 mm (0.03 in.) resulted in high enough permeability to allow heavy corrosion of reinforcing and subgrade erosion.

However, to design for such criteria is impractical, as it will result in large amounts of steel and excessive cracking. Fortunately, the conditions of large crack widths do not occur constantly and probability of large crack widths coinciding with precipitation is small. The solution is to use weather data for the region to be designed for, and calculate a design case for each criterion at a confidence level dependent on the designer or controlling agency. Maximum allowable crack width calculated for a selected occurrence probability, for the spalling criterion, is an ultimate value that has to be satisfied, while sealing the joint may be an alternative if the water ingression criterion is not achieved.

JRCP-6 DESIGN APPLICATION

Below is an example of the use of JRCP-6 as an design tool. The example provides a methodology to develop a design algorithm by generating multiple sets of results through multiple runs of JRCP-6.

Input

Standard environmental conditions are selected as input for all analysis runs used in this example. The concrete properties were selected as default values in the input driver for PCC made using limestone as coarse aggregate. It is assumed that a thickness of 250 mm (10 in.) is required to conform to vehicular loading requirements. Furthermore, the following criteria are set for design decision:

(1) One contraction joint per slab
(2) Maximum slab length
(3) Crack width less than 1 mm (0.04 in.)
(4) Steel stress less than 415 MPa (60 000 psi)

The input factorial is summarized in Table 8.1. The output is connected to input by a case number.

Table 8.1 Design input by case number

	Case Number					
Steel diameter (in)*	**0.5**			**0.75**		
Steel content (%)	**0.1**	**0.2**	**0.3**	**0.1**	**0.2**	**0.3**
Slab length (ft)**						
40	1	5	9	13	17	21
60	2	6	10	14	18	22
80	3	7	11	15	19	23
100	4	8	12	16	20	24

* 1 in = 25.4 mm

** 1 psi = 6.9 kPa

Results

Results of the analysis runs are summarized in Table 8.2. Listed are the number of cracks per slab after the initial environmental analysis, as well as joint width (transverse expansion joint), crack width (transverse contraction joint), steel stress at the crack, and maximum concrete stress. The ranges given are for the minimum and maximum temperature cases after the initial analysis period. When the design criteria are applied to the table of results, case numbers 7, 19, and 20 are

possible solutions. Case 7, a slab length of 24.4 m (80 ft) and reinforcing of 0.2 percent and 12 mm (0.5 in.) diameter, meets all criteria except for the maximum steel stress at the crack. To ensure that the steel does not yield, a shorter slab length might be selected. Case 19 and 20, a slab length of 24.4 to 30.5 m (80 to 100 ft) and reinforcing of 0.2 percent and 19 mm (0.75 in.) diameter, also meets the criteria but has crack widths larger than the maximum allowable. It would, therefore, seem that the optimum solution to the problem would be a slab length of 22.9 m (75 ft) and reinforcing of 0.2 percent and 12 mm (0.5 in) diameter.

Table 8.2 Design factorial results

Case number	Cracks per slab	Joint width (mils)*	Crack width (mils)*	Steel stress (psi)**	Concrete stress (psi)**
1	0	49 - 197			46 -72
2	0	70 - 292			81 - 110
3	1	66 - 312	28 - 75	56 - 90	76 - 120
4	3	62 - 297	20 - 65	53 - 85	70 - 111
5	0	49 - 197			48 - 76
6	0	69 - 291			85 - 122
7	1	75 - 347	16 - 38	41 - 62	92 - 136
8	>3				
9	0	49 - 196			51 - 78
10	0	69 - 291			85 - 122
11	>3				
12	>3				
13	0	49 - 197			46 - 72
14	0	70 - 292			81 - 110
15	1	63 - 299	31 - 90	48 - 80	70 - 114
16	1	74 - 362	39 - 119	55 - 94	88 - 140
17	0	49 - 197			48 - 76
18	0	69 - 291			85 - 122
19	1	72 - 343	19 - 43	37 - 54	84 - 136
20	3	73 - 351	15 - 43	38 - 54	84 - 132
21	0	49 - 196			51 - 78
22	0	69 - 291			86 - 120
23	>3				
24	>3				

* 1 mils = 0.0254 mm

** 1 psi = 6.9 kPa

CHAPTER 9. SUMMARY, CONCLUSIONS AND RECOMMENDATIONS

SUMMARY

An overview of jointed concrete pavement concepts, behavior, analysis, and design has been presented. The reaction of the pavement to concrete drying shrinkage and changing pavement temperature over time was identified as of considerable importance for the analysis of JCP in the long term. Review of existing analysis techniques for modeling early-age behavior of concrete pavements to the environment led to modification of existing JRCP analysis methods developed at the Center for Transportation Research. A new version of the program, JRCP-6, has been written as part of this study. Analysis algorithms for the uncracked JRCP slab have been carried over from previous versions, and minor modifications have been made to the numerical solution techniques. Algorithms for the cracked slab have been changed significantly by using steel-concrete interactions at the crack, which were originally developed for CRCP. These models are considered an improvement on all previously existing analysis strategies. The development and inclusion of vehicular loading and distress prediction models were initiated. Although these are simplistic in nature, a starting point has been provided, from which future improvements can be made. Mechanistic design procedures are usually based on successful analysis models; consequently, development of a design program has been proposed using the improved analysis program developed in this research.

CONCLUSIONS

Investigation of behavior prediction of jointed concrete pavement leads to the realization that the behavior of jointed concrete pavement is highly complex. The reaction of the pavement to different loading conditions can be described by a large number of parameters, each dependent on a set of variables. The systems approach of dividing the problem into subsets leads to a manageable complexity, but even for these subsets, many assumptions and simplifications need to be made in order to achieve results for the analysis process. Application of this strategy led to the results described in previous chapters, of which the development of the JRCP-6 analysis program is most significant.

The JRCP-6 analysis program can successfully be used to predict stresses and displacement for JRCP and PJCP subjected to temperature fluctuations and concrete drying shrinkage. These calculations may be used in long-term behavior prediction and to develop design strategies. Results derived from sensitivity analyses, calibration, and general application of JRCP-6 lead to the following secondary conclusions regarding analysis of JCP subjected to environmental effects:

(1) Computed parameters change logically with varying input parameters. Concrete stress is most sensitive to slab thickness, slab length, steel content, and slab-subbase friction. Joint and crack widths are most sensitive to temperature differentials, drying shrinkage, and slab length.

(2) Considerable sliding between the concrete slab and underlying subbase occurs for all temperature ranges and drying shrinkage values.

(3) Cracking most often occurs during the first day or two after construction, within reasonable temperature distributions.

(4) Positions of maximum concrete stress after the first crack has developed are predominantly closer to the center of the slab.

(5) Steel stresses at the crack can vary significantly with varying slab length, steel diameter, and steel percentage. These need to be checked for possible failure in tension of reinforcing at cracks.

(6) Slab-subbase friction plays a dominant role in uncracked JRCP, but the effect is reduced in relative importance in cracked pavements by steel-concrete interactions at the crack.

(7) Variance of tensile strength can successfully be used to take material variability into account for analysis purposes.

Predicting distresses by mechanistic-empirical methods has had limited success in the past. It is concluded that distress predictions are to be limited to applications within the development space of the model. Prediction models are generally based on performance data and should be applied only to analyses and design within similar environmental conditions. In this light, preliminary investigation of JCP data from the Texas database can be used, in conjunction with mechanistic analysis procedures, to develop prediction models that are specific to Texas. This report and the JRCP-6 program include distress prediction for transverse cracking and corner breaks. These models have been developed on the basis of the Westergaard vehicular load analysis, variance of tensile strengths representing all variance in a pavement system, and portland cement concrete fatigue studies on in-service pavements in Texas.

RECOMMENDATIONS

An analysis program for jointed concrete pavement is provided to compute stresses and displacements for a PCC pavement slab. The program can be used for analysis, design, and sensitivity studies of input parameters for PJCP and JRCP. Calibrations of transverse crack and corner break prediction and joint and crack movement should be performed for future verification or for improving the presented models. Furthermore, additional distress prediction models, such as spalling and faulting, should be incorporated to broaden the scope of the existing analysis model.

In the long term, JCP analysis strategies should integrate multi-dimensional geometry, dynamic vehicular loading, and non-linear material behavior and interactions. This will provide the user with a more accurate simulation of JCP field behavior. These goals are achievable using technology currently available and are seen as recommendations for future research.

REFERENCES

1. Smith, K. D., D. G. Peshkin, M. I. Darter, and A. L. Mueller, "Performance of Jointed Concrete Pavements," Volumes I–V, Federal Highway Administration Report FHWA-RD-89-138, Washington, D.C., November 1990.
2. Rivero-Vallejo, F., and B. F. McCullough, "Drying Shrinkage and Temperature Drop Stresses in Jointed Reinforced Concrete Pavement," Research Report 177-1, Center for Highway Research, The University of Texas at Austin, August 1975.
3. McCullough, B. F., A. A. Ayyash, W. R. Hudson, and J. P. Randall, "Design of Continuously Reinforced Concrete Pavements for Highways," NCHRP 1-15, Center for Highway Research, The University of Texas at Austin, August 1975.
4. Won, M., K. Hankins, and B. F. McCullough, "Mechanistic Analysis of Continuously Reinforced Concrete Pavements Considering Material Characteristics, Variability and Fatigue," Research Report 1169-2, Center for Transportation Research, The University of Texas at Austin, March 1991.
5. Westergaard, H. M., "Computation of Stresses in Concrete Roads," *Proceedings,* Highway Research Board, Fifth Annual Meeting, December 1925.
6. Yoder, E. J., and M. W. Witczak, *Principles of Pavement Design,* 2nd edition, John Wiley & Sons, Inc., 1975.
7. Mindess, S., and J. F. Young, *Concrete,* Prentice Hall, Englewood Cliffs, New Jersey, 1981.
8. Suh, Y. C., B. F. McCullough, and K. Hankins, "Development and Application of Randomness Index for Continuously Reinforced Concrete Pavement," Research Report 1244-3, Center for Transportation Research, The University of Texas at Austin, March 1992.
9. "Standard Specifications for Construction of Highways, Streets and Bridges," Texas Department of Transportation, March 1993.
10. Lu, J., H. Castedo, and B. F. McCullough, "Normalization of Models 1 and 2 for Tensile Strength, Modulus of Elasticity and Drying Shrinkage Made with Texas Coarse Aggregates," Center for Transportation Research, The University of Texas at Austin, February 1989.
11. Dossey, T. and B. F. McCullough, "Characterization of Concrete Properties with Age," Research Report 1244-2, Center for Transportation Research, The University of Texas at Austin, March 1992.
12. Jimenez, M. A. O., B. F. McCullough, and K. Hankins, "Monitoring of Siliceous River Gravel and Limestone Continuously Reinforced Concrete Pavement Test Sections in Houston 2 Years after Placement, and Development of a Crack Width Model for CRCP-7 Program," Research Report 1244-4, Center for Transportation Research, The University of Texas at Austin, March 1992.
13. Dwiggens, M. E., M. I. Darter, J. P. Hall, and J. B. DuBose, "Pavement Performance Analysis of the Illinois Interstate Highway System," *Proceedings,* Fourth

International Conference on Concrete Pavement Design and Rehabilitation, Purdue University, West Lafayette, April 1989.

14. Senadheera, S., and D. Zollinger, "Spalling Model," Research Report 1244-11, Texas Transportation Institute, Texas A&M University, College Station, Tx, August 1994.

15. McCullough, B. F., J. C. Ma, and C. S. Noble, "Limiting Criteria for the Design of CRCP," Research Report 177-17, Center for Transportation Research, The University of Texas at Austin, August 1979.

16. Wimsatt, A. W., B. F. McCullough, and N. H. Burns, "Methods of Analyzing Influencing Frictional Effects of Subbases," Research Report 458-2F, Center for Transportation Research, The University of Texas at Austin, November 1987.

17. Ioannides, A. M., and R. A. Salsilli-Murua, "Interlayer and Subgrade Friction: A Brief Review of the State-of-the-Art," A Report Prepared for the Federal Highway Administration, Pavement Division DTFH61-85-C-00103, Washington, D.C., December 1988.

18. Wu, W., and B. F. McCullough, "Terminal Movement in Continuously Reinforced Concrete Pavements," Research Report 1169-4, Center for Transportation Research, The University of Texas at Austin, January 1992.

19. Annual Book of ASTM Standards, 1980, 1985, 1991, Section 4, Construction, Vol. 04.02, Concrete and Mineral Aggregates.

20. Green, W. J., R. L. Carrasquillo, and B. F. McCullough, "Coarse Aggregate for PCC - Pilot Study Evaluation," Research Report 422-1, Center for Transportation Research, The University of Texas at Austin, September 1987.

21. Dumas, A., T. Dossey, and B. F. McCullough, "Effects of Aggregate Blends on the Properties of Portland Cement Concrete Pavements," Research Report 1244-8, Center for Transportation Research, The University of Texas at Austin, August 1994.

22. Solaimanain, M., and T. W. Kennedy, "Predicting Maximum Pavement Surface Temperature Using Maximum Air Temperature and Hourly Solar Radiation," Transportation Research Record 1417, Transportation Research Board, Washington D.C., January 1993.

23. Neville, A. M., *Properties of Concrete,* 3rd edition, Pitman, Great Britain, 1981.

24. Baalbaki, W., B. Benmokrane, O. Chaalal, and P. C. A'tcin, "Influence of Coarse Aggregate on Elastic Properties of High Performance Concrete," *ACI Materials Journal,* Vol. 88, No. 5, 1991.

25. Kunt, M. M., and B. F. McCullough, "Improved Design and Construction Procedures for Concrete Pavements Based on Mechanistic Modeling Techniques," Research Report 1169-5F, Center for Transportation Research, The University of Texas at Austin, June 1992.

26. Yang, S., and J. Chen, "Bond Slip and Crack Width Calculations of Tension Members," Title No. 85-S39, *ACI Structural Journal,* July-August 1988.

27. Somayaji, S., and S. P. Shah, "Bond Stress Relationship and Cracking Response of Tension Members," *Proceedings, ACI Journal,* Title No. 78-20, May-June 1981.

28. "The AASHO Road Test," Report 5, Pavement Research, Highway Research Board, Special Report 61E, 1962.

29. Miner, M. A., "Cumulative Damage in Fatigue," Transactions, American Society of Mechanical Engineers, Vol. 66, 1945.

30. Crumley, J. A., and T. W. Kennedy, "Fatigue and Repeated-Load Elastic Characteristics of Portland Cement Concrete" Research Report 183-9, Center for Highway Research, The University of Texas at Austin, June 1977.

31. Timoshenko, S., and J. M. Lessels, *Applied Elasticity,* Westinghouse Technical Night School Press, Pittsburgh, Pennsylvania, 1925.

32. Friberg, B. F., "Design of Dowels in Transverse Joints of Concrete Pavements," *Transactions,* ASCE Vol. 105, 1940.

33. McCullough, B. F., J. C. Ma, and C. S. Noble, "Limiting Criteria for the Design of CRCP" Research Report 177-17, Center for Transportation Research, The University of Texas at Austin, August 1979.

APPENDIX A:

JRCP-6 EXAMPLE PROBLEMS

Common JRCP-6 Input Screens for All Examples

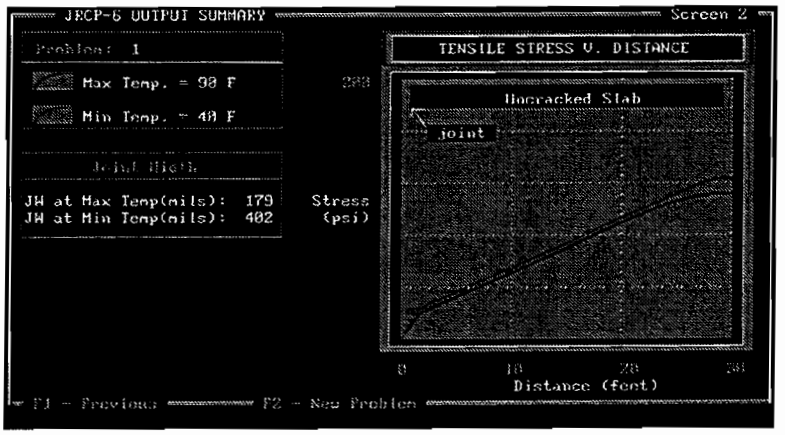

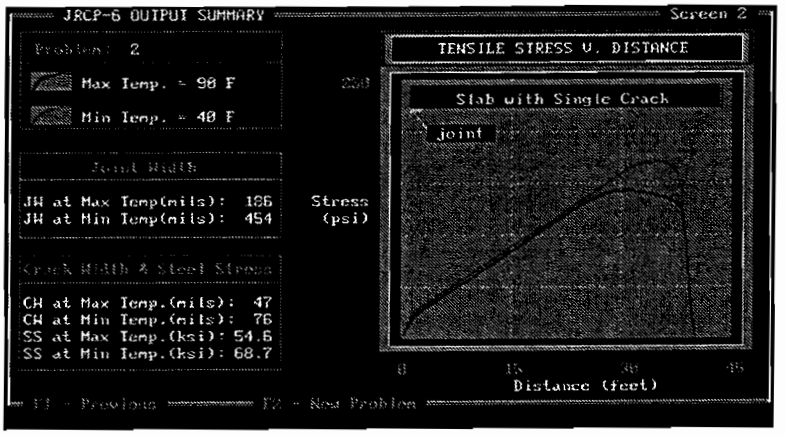

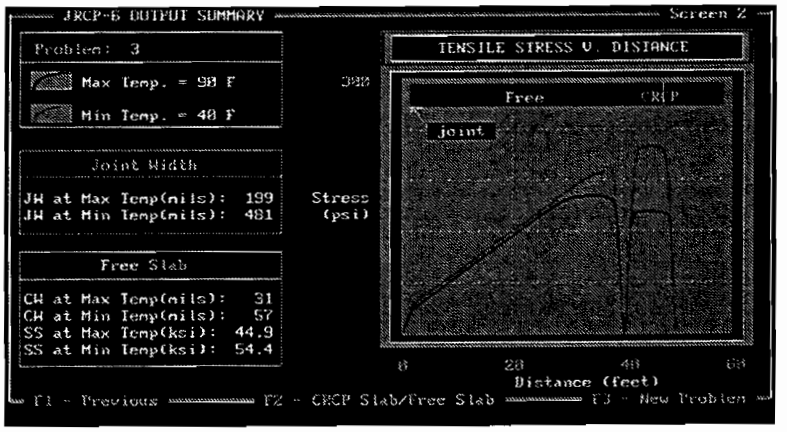

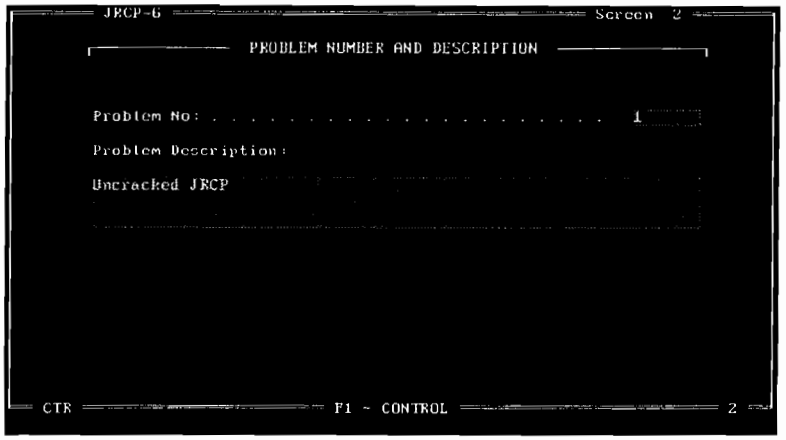
JRCP-6
Screen 2
PROBLEM NUMBER AND DESCRIPTION
Problem No: 1
Problem Description:
Uncracked JRCP
CTR
F1 - CONTROL
2

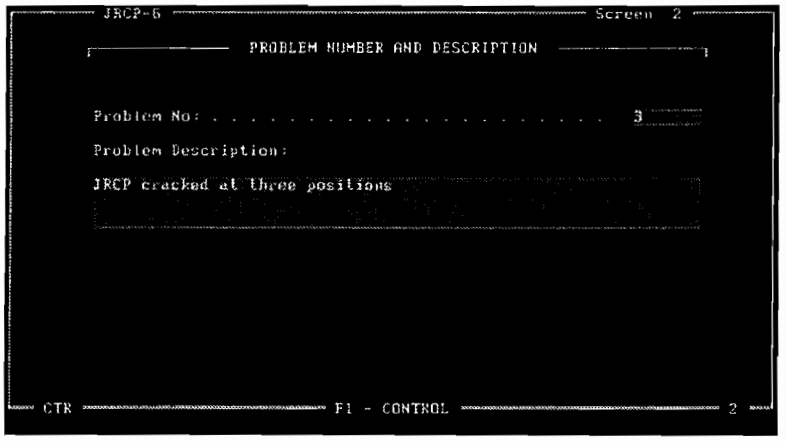
JRCP-6
Screen 2
PROBLEM NUMBER AND DESCRIPTION
Problem No: 3
Problem Description:
JRCP cracked at three positions
CTR
F1 - CONTROL
2

EXAMPLE 1

An example of JRCP-6 where no cracking is expected as a result of environmental effects during the first year

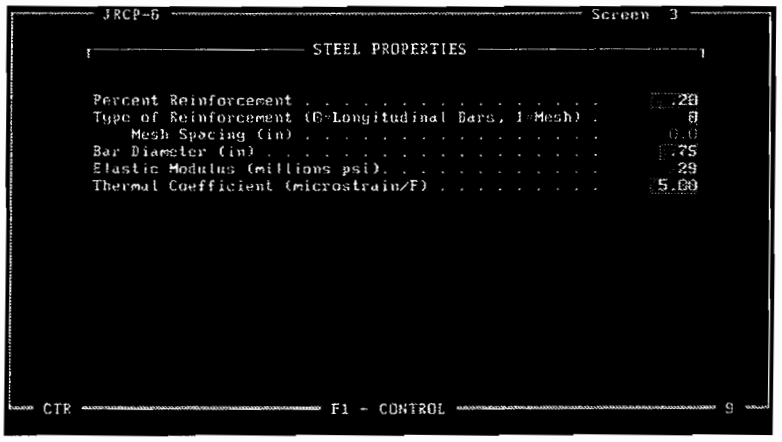

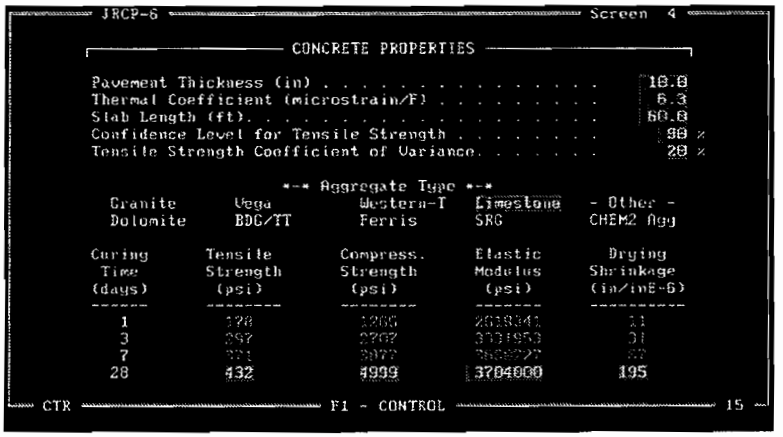

EXAMPLE 2

An example of JRCP-6 where each slab is expected to crack once as result of environmental effects during the first year

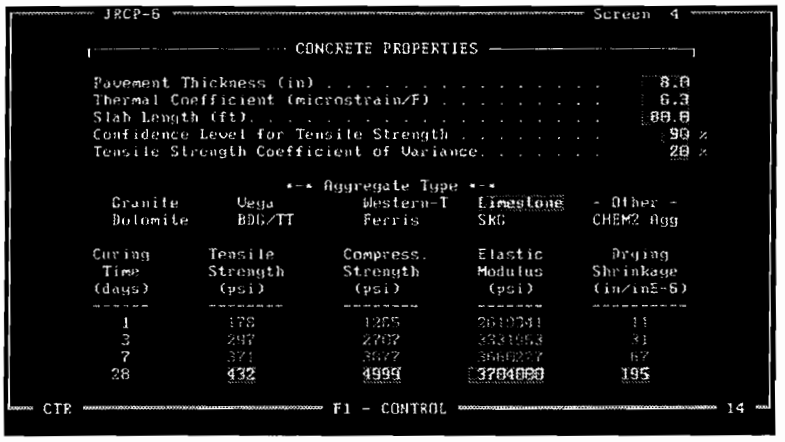

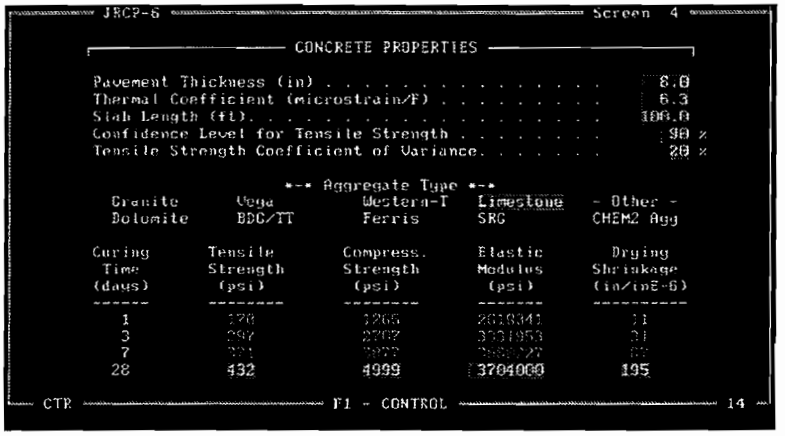

EXAMPLE 3

An example of JRCP-6 where each slab is expected to crack three times as result of environmental effects during the first year